



LANXESS
Energizing Chemistry

Additives solutions for Polyurethane

APAC Lanxess Virtual Day 2020

PLA AT team – Alex Zhang, Hongjie Zhou
Shanghai, 2020.09.16

PUBLIC

Lanxess BU PLA: Polyurethane Additives Portfolio



Disflamoll®/Levagard®/PHT4-Diol™/ Reofos®

Stabaxol®

Addolink®

Addovate®

Addocat®

Flame Retardants



Hydrolysis Stabilizers



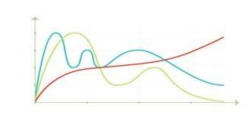
Crosslinkers



Emulsifiers & Foam Stabilizers



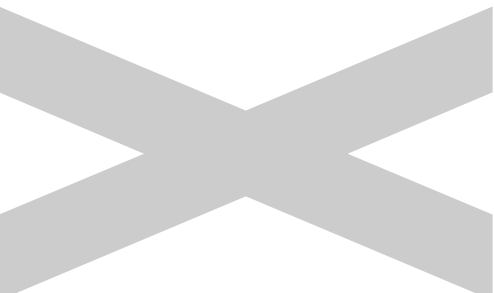
Catalysts



PUBLIC

Disflamoll® / Levagard®

Flame retardants for flexible PU foam



Flame retardants for flexible PU foam

LANXESS
Energizing Chemistry

Disflamoll® 51092

- Butylated triphenyl phosphate
- Phosphorus content: 8,5 %
- Viscosity: 100 mPa·s (20°C/68°F)



Emerald Innovation™ NH-1

- Phosphate ester blend
- Phosphorus content: 7,9 %
- Viscosity: 82 mPa·s (23°C/73°F)



Levagard® TP LXS 51114

- Phosphorus compound
- Phosphorus content: 9,0 %
- Viscosity: 6.500 mPa·s (23°C/73°F)



Flame retardants for flexible PU foam

LANXESS
Energizing Chemistry

Levagard® 2000

- Oligomeric alkyl phosphate ester
- Phosphorus content: 16,4 %
- Viscosity: 100 - 120 mPa·s (23°C/73°F)



Levagard® 3000

- Oligomeric alkyl phosphate ester
- Phosphorus content: 12,8 %
- Viscosity: 100 - 160 mPa·s (23°C/73°F)



Levagard® 3001

- Blend of phosphorus compounds
- Phosphorus content: 14,7 %
- Viscosity: 623 mPa·s (23°C/73°F)
-



Polyether foam Test formulation



Components	Amount [php]
Polyether polyol (OHZ 56)	100
Water	3,0
Amine catalyst	0,08
Tin catalyst	0,16
Stabilizer	1,0
Phosphorus flame retardant	6
TDI 80	40,9
Index	107

Polyether foam

- All foams were prepared on lab scale according to a standard procedure
- Flame retardant dosage was **6** php in all foams

Polyether foam

Foam properties

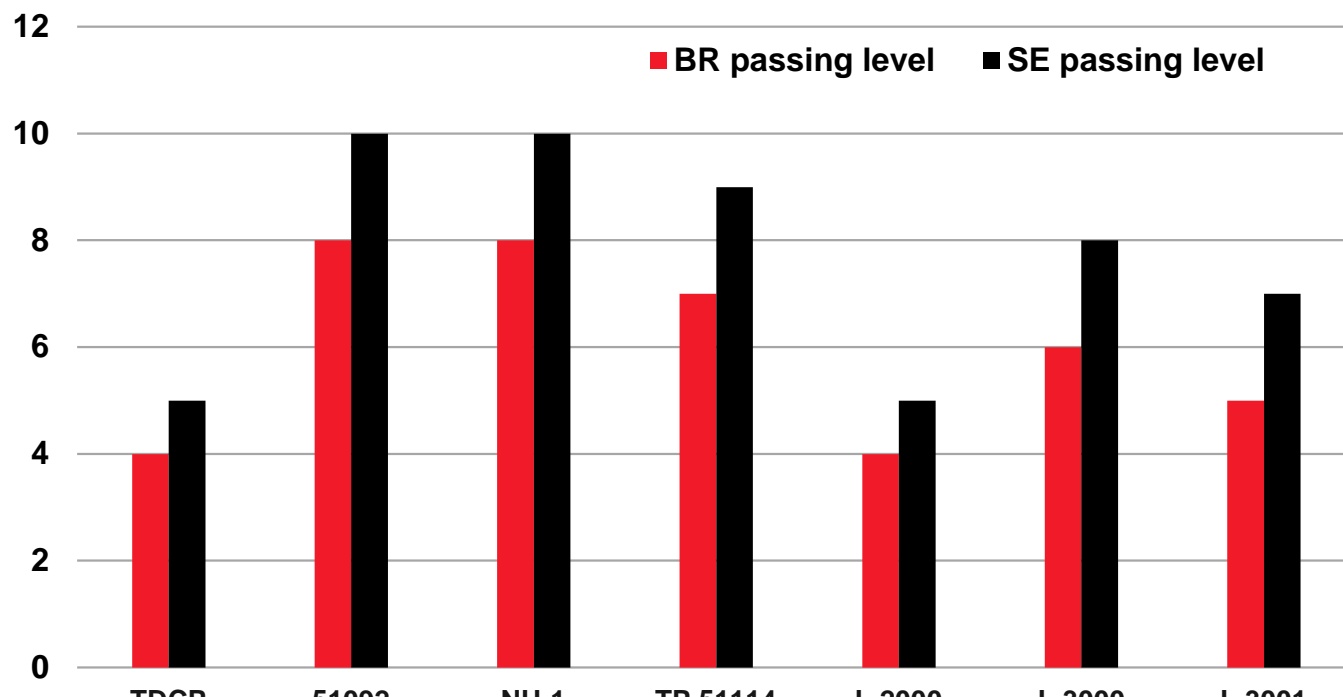


Properties	Units	without FR	TDCP	D 51092	NH-1	TP 51114	L 2000	L 3000	L 3001
Density	kg/m ³ (pcf)	33.2 (2.1)	33.8 (2.1)	33.5 (2.1)	33.3 (2.1)	33.1 (2.1)	33.3 (2.1)	33.2 (2.1)	33.7 (2.1)
Cream time	s	13	15	14	13	15	14	14	13
Rise time	s	150	160	155	150	152	152	155	150
Air flow	mm w.c.	180	185	170	150	200	190	170	160
CLD 40%	kPa (psi)	4.0 (0.58)	3.4 (0.49)	3.3 (0.48)	3.5 (0.51)	3.4 (0.49)	3.2 (0.46)	3.4 (0.49)	3.8 (0.55)
Compression set (22h, 50%, 70°C)	%	6.1	6.8	6.3	6.7	6.6	8.1	4.3	3.5

Polyether foam Efficiency – FMVSS 302

LANXESS
Energizing Chemistry

Passing level [php]



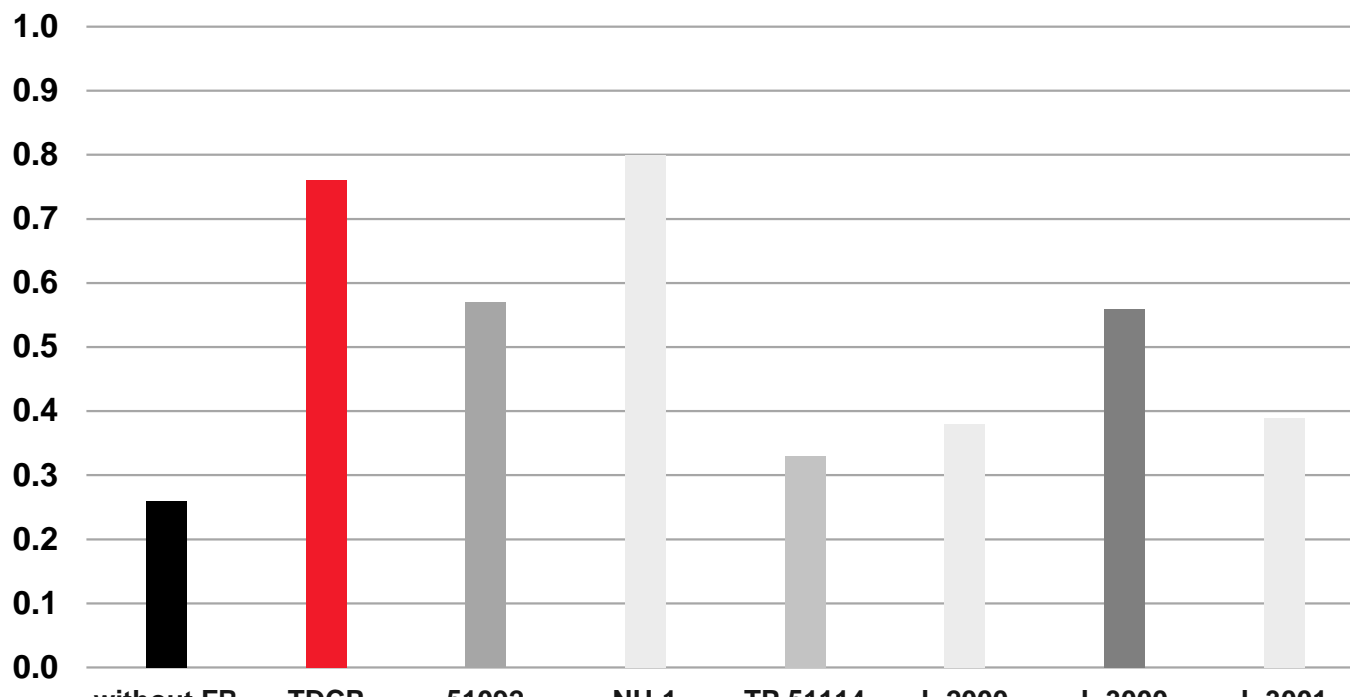
FMVSS 302

- Passing level to achieve BR and SE classification was determined

Polyether foam Fogging B

LANXESS
Energizing Chemistry

Fogging B [mg]



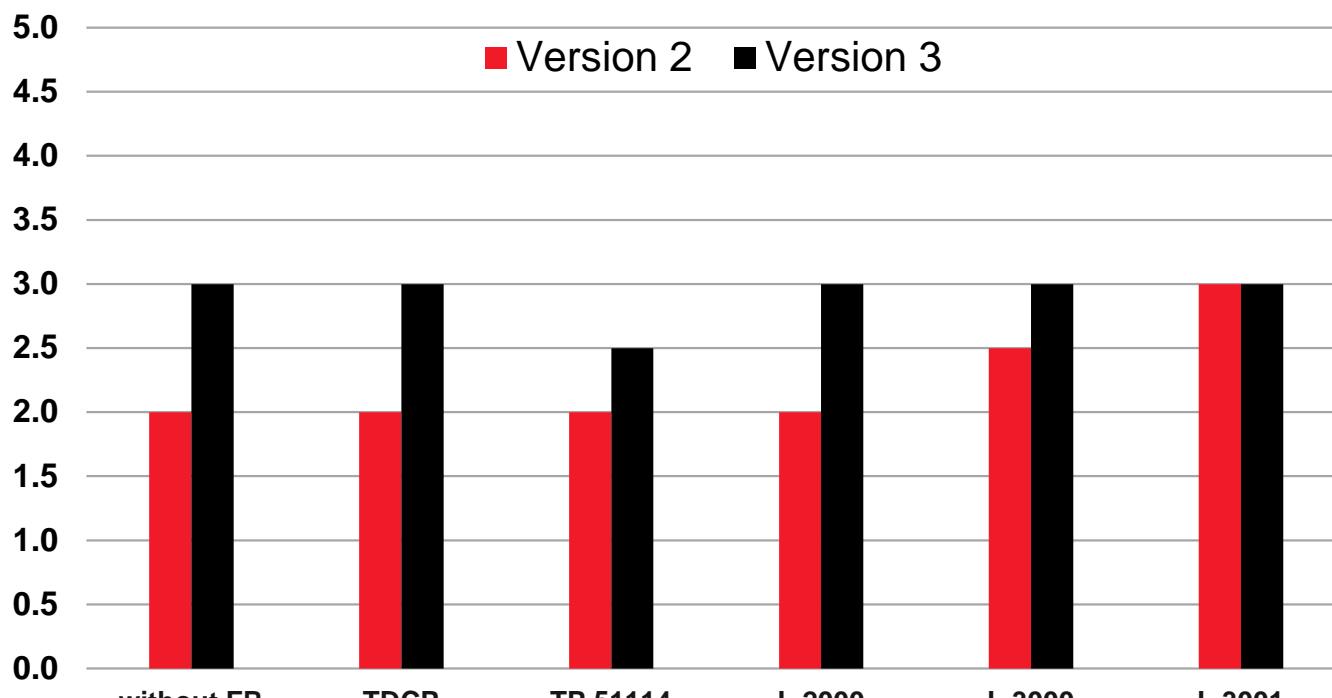
Fogging B (DIN 75201)

- Fogging of foams containing 6 php flame retardant
- Fogging B after 16 hours at 100°C/212°F was determined gravimetrically

Polyether foam Odor – VDA 270

LANXESS
Energizing Chemistry

Odor rating

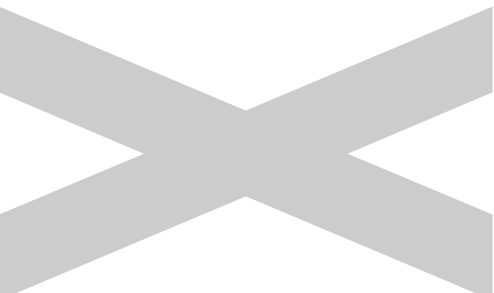


VDA 270

- Foams contain 6 php flame retardants
 - VDA 270
 - Version 2:
24 hours at 40°C
 - Version 3:
2 hours at 80°C
- All foams pass the requirements of automotive industry

Levagard® / Disflamoll® / PHT4-Diol™

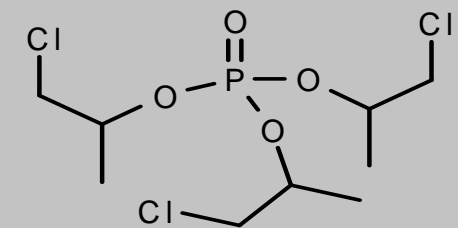
Flame retardants for rigid PU foam



Flame retardants for rigid PU foam

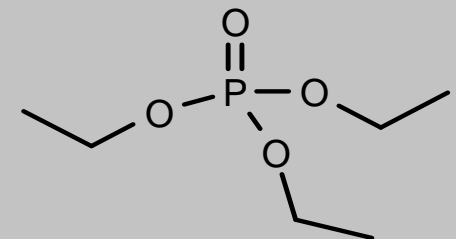
Levagard® PP

- Tris(2-chlor-isopropyl) phosphate (TCPP)
- Phosphorus content: 9,5 %
- Chlorine content: 32,5 %
- Viscosity: 85 mPas (20°C/68°F)



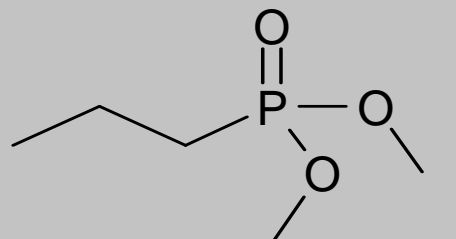
Levagard® TEP-Z

- Triethyl phosphate (TEP)
- Phosphorus content: 17,0 %
- Viscosity: 2 mPas (20°C/68°F)



Levagard® DMPP

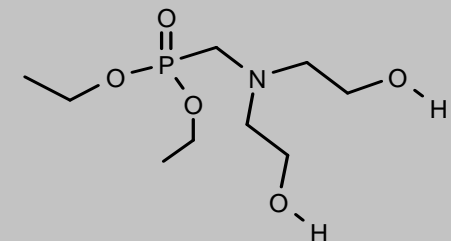
- Dimethyl propyl phosphonate
- Phosphorus content: 20,3 %
- Viscosity: 2 mPas (20°C/68°F)



Flame retardants for rigid PU foam

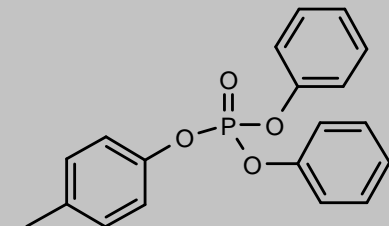
Levagard® 4090 N

- N,N-bis-(2-hydroxylethyl) aminomethane phosphonic acid diethyl ester
- Phosphorus content: 12,1 %
- OH number: 400 – 500 mg KOH/g



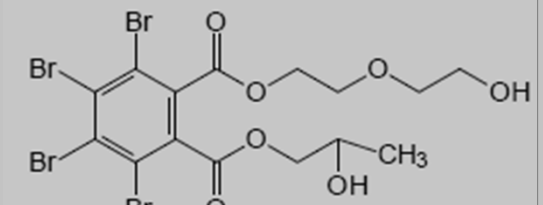
Disflamoll® DPK

- Cresyl diphenyl phosphate
- Phosphorus content: 9,1 %
- Viscosity: 46 mPas (20°C/68°F)



PHT4-Diol™

- Tetrabromophthalate diol
- Bromine content: 46 %
- Viscosity: 90.000 mPas (25°C/77°F)



Flame retardants for rigid PU foam

New developments



Levagard® 2000

- Oligomeric alkyl phosphate ester
- Phosphorus content: 16,4 %
- Viscosity: 100 - 120 mPa·s (23°C/73°F)
- Density: 1,23 g/cm³ (23°C/73°F)
- Miscible with water

Levagard® 2100

- Organic phosphonate
- Phosphorus content: 18,4 %
- Viscosity: 25 - 40 mPa·s (23°C/73°F)
- Density: 1,18 g/cm³ (23°C/73°F)
- OH number: 300 - 330 mg KOH/g
- Miscible with water

Rigid PIR foam Test formulation



Components	Amount [php]	Amount [%]	PIR formulation
Aromatic polyester polyol (OHZ 240)	100	27,8	<ul style="list-style-type: none">All foams were prepared on lab scale according to a standard procedure
Catalyst 1 (PMDETA)	0,25	0,1	<ul style="list-style-type: none">Amount of isocyanate was adjusted when a reactive flame retardant was used (index constant)
Catalyst 2 (K-Acetate)	0,35	0,1	
Catalyst 3 (K-Octoate)	1,9	0,5	
Stabilizer	2,5	0,7	
Water	0,5	0,1	
n-Pentane	24,3	6,8	
Phosphorus flame retardant	25	7,0	
Isocyanate (polymeric MDI)	205	56,9	
Index	300		

PIR foam

Foam properties (25 php FR)

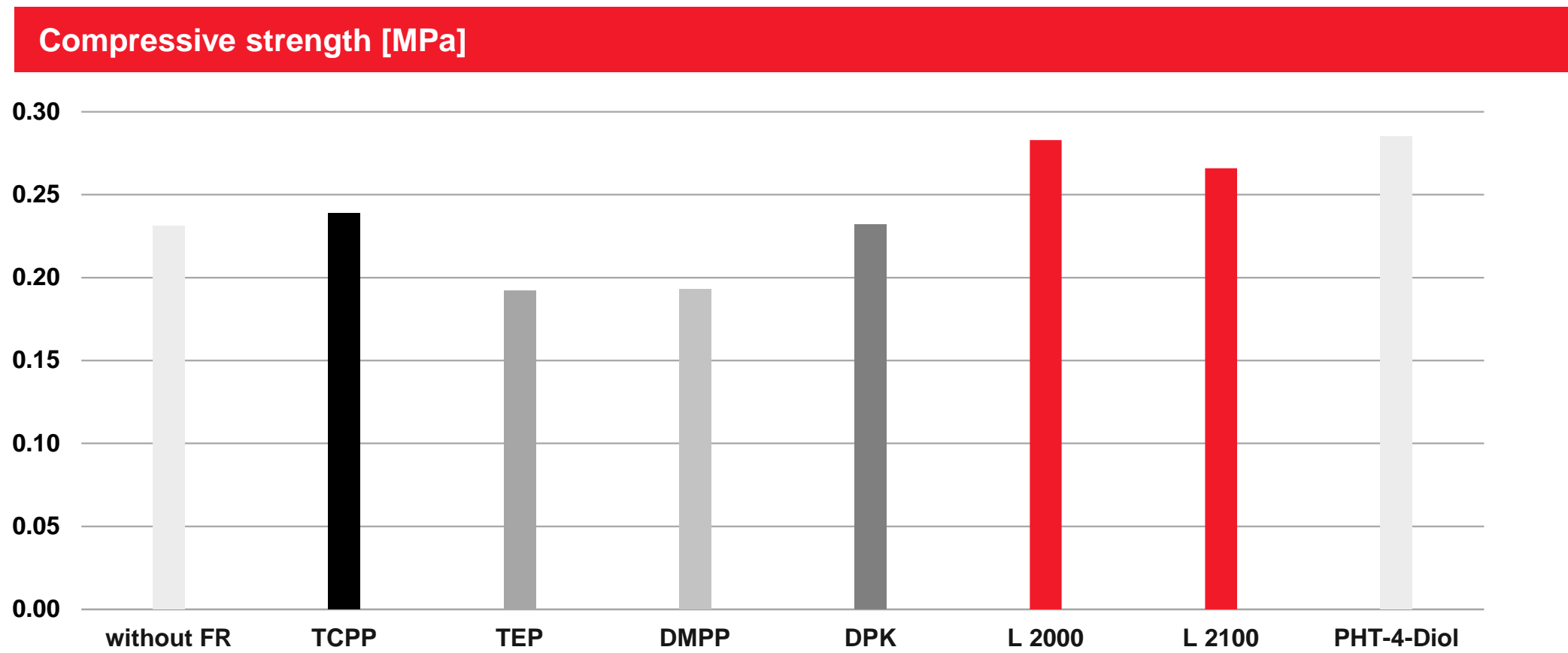


Properties	Units	no FR	TCPP	TEP	L 2000	L 2100
Density	kg/cm ³ (pcf)	26.5 (1.65)	29.1 (1.82)	27.3 (1.70)	28.2 (1.76)	31.4 (1.96)
Cream time	s	15	15	13	15	12
Gel time	s	55	50	45	48	40
Open cell content	Vol-%	8.8	4.6	11.6	7.8	7.5
Thermal conductivity	mW/K m	21.8	21.9	20.8	21.4	20.9

PIR foam

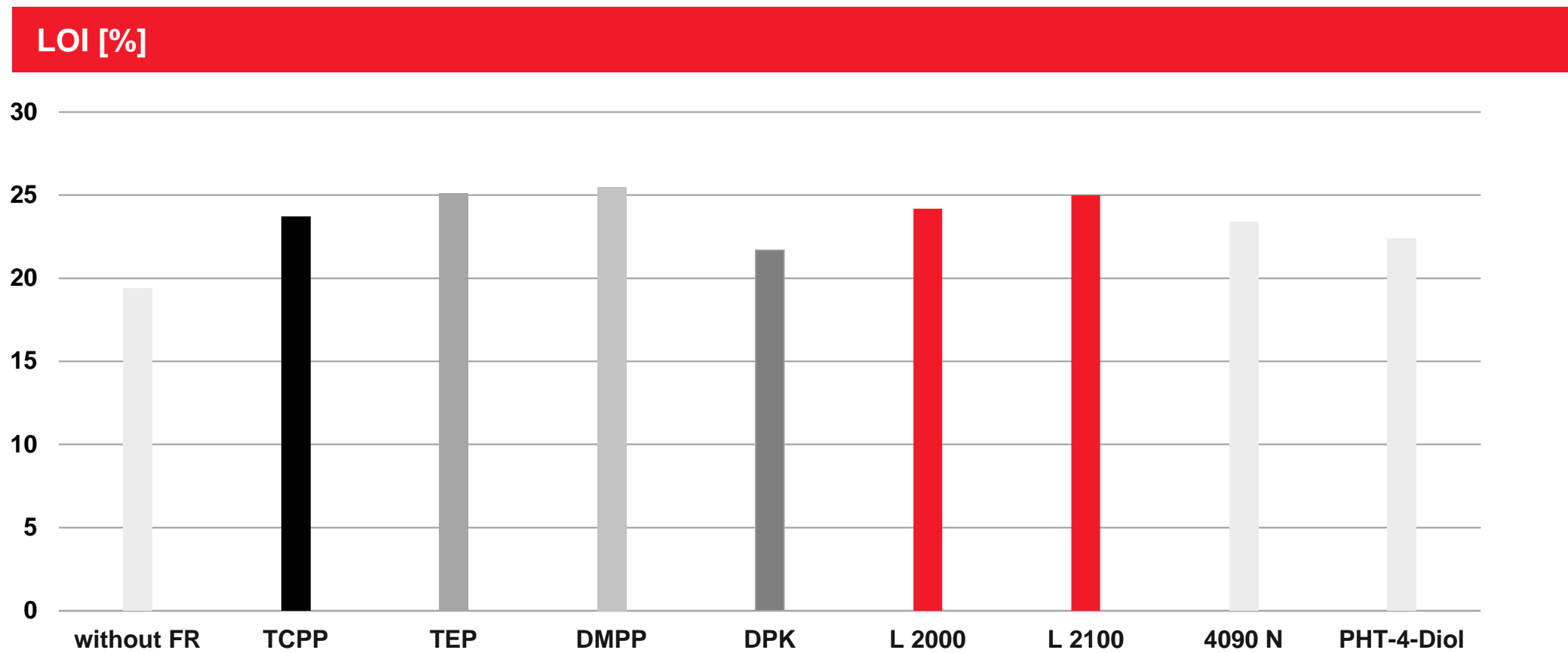
Compressive strength (EN 826)

LANXESS
Energizing Chemistry



PIR foam LOI values

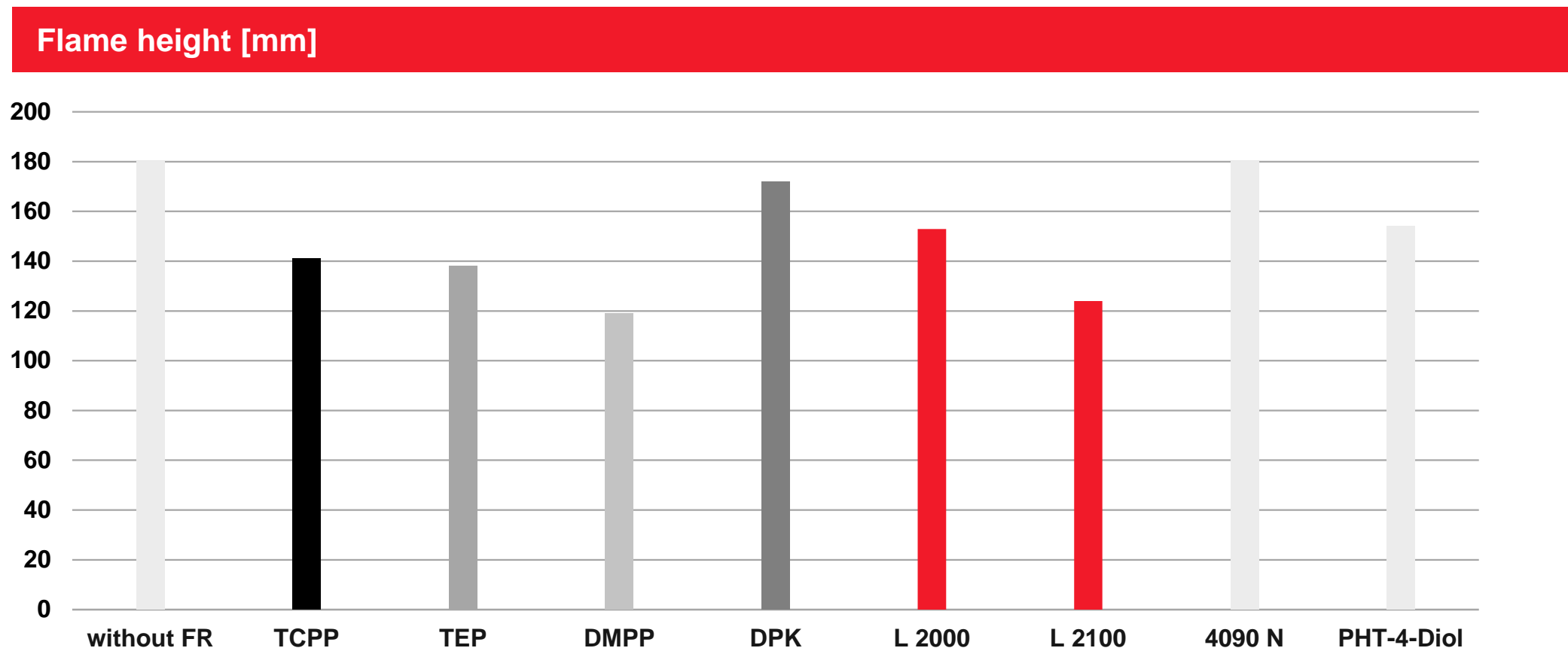
LANXESS
Energizing Chemistry



PIR foam

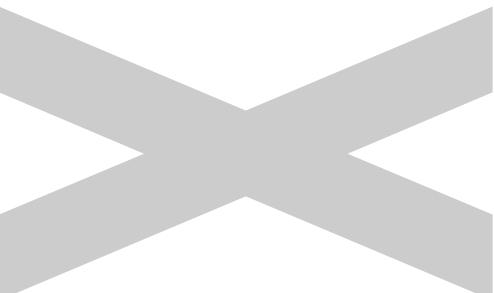
EN ISO 11925 – flame height

LANXESS
Energizing Chemistry



Disflamoll® / Reofos®

Flame retardants for TPU



PUBLIC

Flame retardants for thermoplastic polyurethane

LANXESS
Energizing Chemistry

Disflamoll® 51092

- Butylated triphenyl phosphate
- Phosphorus content: 8,5 %
- Viscosity: 100 mPa·s (20°C/68°F)



Disflamoll® DPK

- Cresyl diphenyl phosphate
- Phosphorus content: 9,1 %
- Viscosity: 46 mPas (20°C/68°F)



Reofos® 50, 65, 95

- Isopropylated triphenyl phosphates
- Phosphorus content: 8,4 / 8,1 / 7,6 %
- Viscosity: 49 / 57 / 93 mPas (25°C)



Flame retardants for TPU

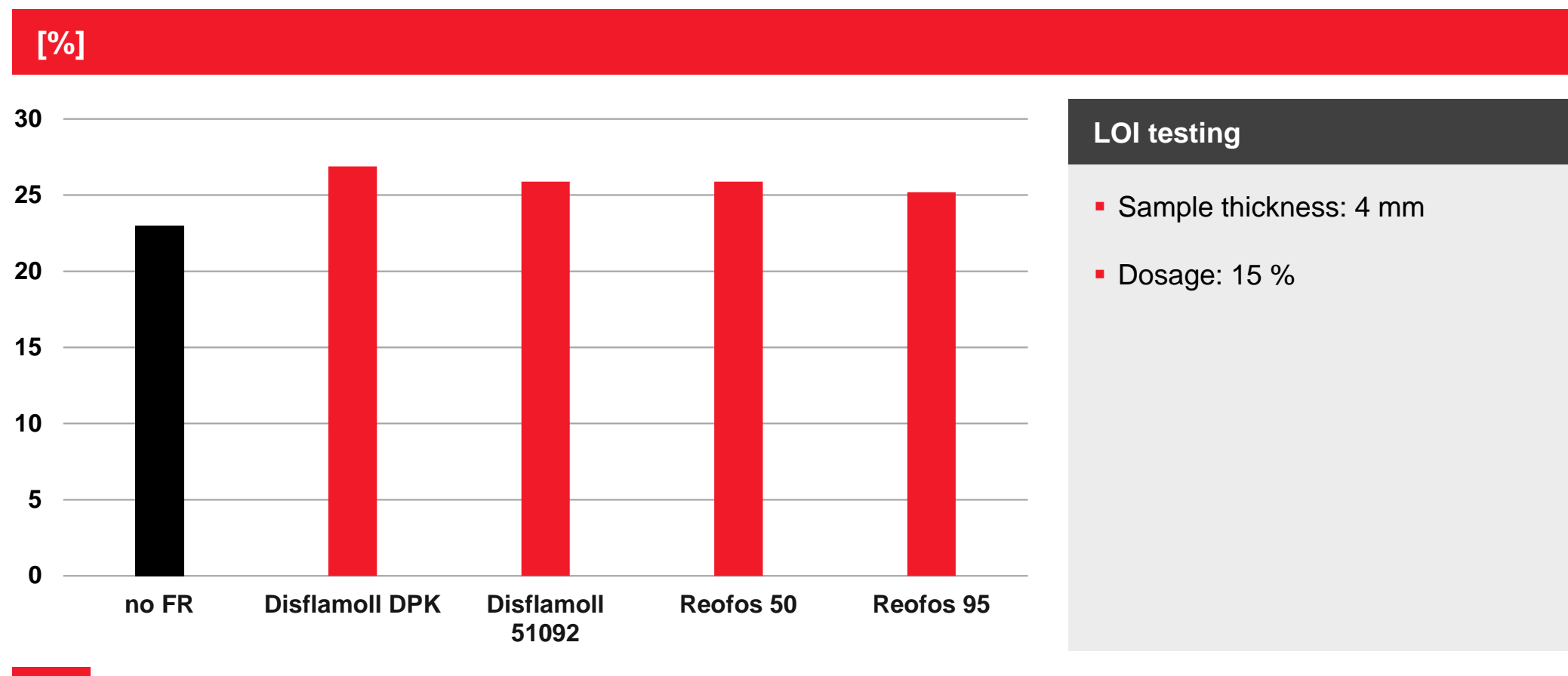
Comparison in TPU (15% in polyether TPU)



Properties	Units	Without FR	Disflamoll DPK	Disflamoll 51092	Reofos 50	Reofos 95
Shore A	-	83	80	77	79	77
Shore D	-	35	29	28	28	28
Tensile strength	MPa	47,4	37,8	44,1	41,1	46,6
Elongation	%	572	659	630	680	641
Tg (DSC)	°C	-39,6	-45,1	-42,4	-43,1	-42,4
LOI	%	23,0	26,9	25,9	25,9	25,2
Fire rating (2 mm)	UL 94 V	-	V 2	V 2	V 2	V 2

Flame retardants for TPU LOI – Polyether-TPU

LANXESS
Energizing Chemistry



Flame retardants for thermoplastic polyurethane Product overview – Conclusions



Disflamoll® 51092

- Suitable for polyester and polyether based TPU
- Good flame retardant efficiency

Disflamoll® DPK

- Suitable for polyester and polyether based TPU
- Good flame retardant efficiency
- Good plasticizing efficiency

- Suitable for polyester and polyether based TPU
- Good flame retardant efficiency

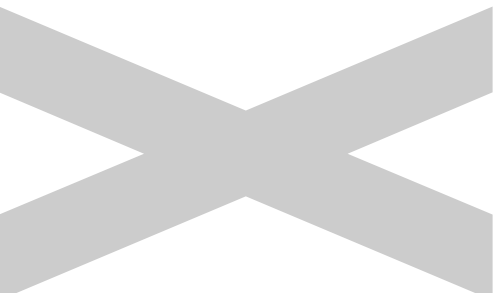
- Suitable for polyester and polyether based TPU
- Good flame retardant efficiency
- Low volatility

Reofos® 50

Reofos® 95

Stabaxol®

Highly effective anti-hydrolysis stabilization for polyester PU and TPU

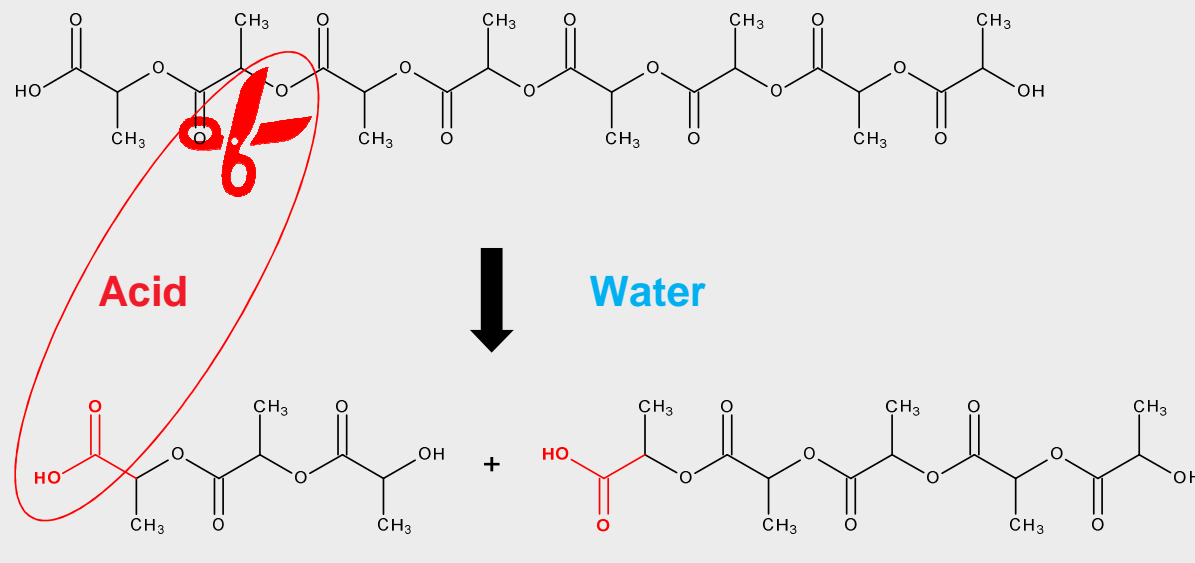


PUBLIC

Stabaxol®

What is hydrolysis?

LANXESS
Energizing Chemistry



No stable processing
(Low melt stability)

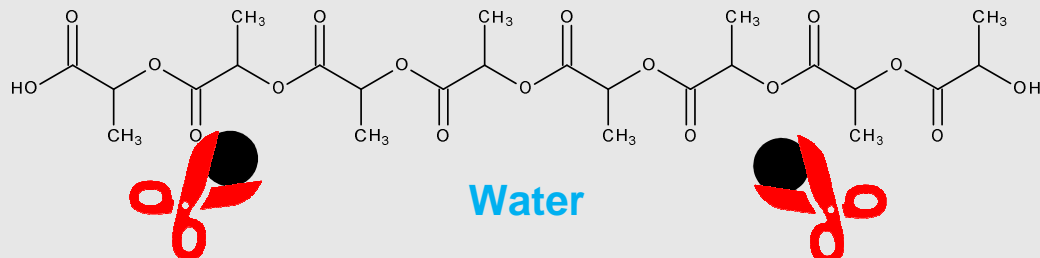
Polymer degradation

No stability in application
(Limited hydrolysis resistance)



Stabaxol®

Mode of function

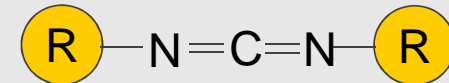


Carbodiimides react with carboxylic acids
(e. g. COOH end groups in polyesters)

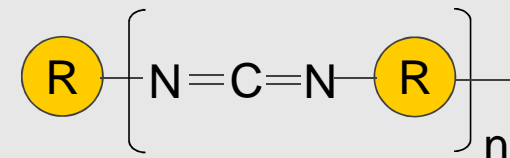
- Hydrolysis is an autocatalytic process accelerated by acids
- LANXESS carbodiimides react **selectively** as carboxylic acid scavengers
- **Carbodiimides significantly slow down the degradation process**
- Selectivity: - COOH > - NH₂ > - OH >> H₂O

Carbodiimides:

- Monomeric Type



- Polymeric Type



Sterical hindrance results in

- Thermal stability
- Long term hydrolysis protection
- Storage stability

Stabaxol®

Product range and recommended use



Product	Applications								
Active ingredients	PET	PBT	PLA	PU	PA	PU rubber	TPU	TPE-E	EVA
Stabaxol® I	<input type="checkbox"/>	<input type="checkbox"/>	<input type="checkbox"/>	<input checked="" type="checkbox"/>		<input type="checkbox"/>	<input type="checkbox"/>		<input type="checkbox"/>
Stabaxol® I LF	<input type="checkbox"/>	<input type="checkbox"/>	<input type="checkbox"/>	<input type="checkbox"/>		<input type="checkbox"/>	<input type="checkbox"/>	<input type="checkbox"/>	<input checked="" type="checkbox"/>
Stabaxol® L	<input type="checkbox"/>	<input type="checkbox"/>	<input type="checkbox"/>	<input checked="" type="checkbox"/>		<input type="checkbox"/>	<input type="checkbox"/>		<input type="checkbox"/>
Stabaxol® P	<input checked="" type="checkbox"/>	<input checked="" type="checkbox"/>	<input checked="" type="checkbox"/>	<input checked="" type="checkbox"/>	<input type="checkbox"/>	<input checked="" type="checkbox"/>	<input checked="" type="checkbox"/>	<input checked="" type="checkbox"/>	<input checked="" type="checkbox"/>
Stabaxol® P 100	<input checked="" type="checkbox"/>	<input checked="" type="checkbox"/>	<input checked="" type="checkbox"/>		<input type="checkbox"/>	<input checked="" type="checkbox"/>	<input checked="" type="checkbox"/>	<input checked="" type="checkbox"/>	<input checked="" type="checkbox"/>
Stabaxol® P 110	<input checked="" type="checkbox"/>	<input checked="" type="checkbox"/>	<input checked="" type="checkbox"/>		<input type="checkbox"/>			<input checked="" type="checkbox"/>	<input checked="" type="checkbox"/>
Stabaxol® P 200				<input type="checkbox"/>			<input type="checkbox"/>		<input checked="" type="checkbox"/>
Masterbatches (standard grades)									
Stabaxol® KE 7646				<input checked="" type="checkbox"/>					
Stabaxol® MB PET 3040				<input checked="" type="checkbox"/>					
Stabaxol® MB TPE 6030							<input checked="" type="checkbox"/>		
Stabaxol® MB TPE 6040							<input checked="" type="checkbox"/>		

possible use

recommended use

Tailor-made solutions for custom-made masterbatches based on different polymer types are also available.

Stabaxol®

Product Portfolio Overview



Description and Performance of Stabaxol®

	Stabaxol I	Stabaxol P200	Stabaxol P	Stabaxol P100
Delivery form	Crystallized melt	Powder	Liquid	Powder, Pastilles
Chemical description	Monomeric	Monomeric	Oligomeric	Polymeric
Melting-temperature	ca. 40°C	ca. 53°C	5°C	60 – 90°C
Molecular-weight	360 g/mol	360 g/mol	2.000 g/mol	3.000 g/mol
Application polymers	(PET), (PBT), TPU, PU, EVA, Adhesives	TPU, PU, Adhesives	PET, PBT, TPU, EVA, (Adhesives)	PET, PBT, PA, TPU, TPEE, (EVA)
Benefits	<ul style="list-style-type: none">- Fast reaction- High efficiency- <u>Cost effective</u>	<ul style="list-style-type: none">- Easy handling- Good solubility in Polyester Polyol- <u>No off-gassing</u>	<ul style="list-style-type: none">- Long-term stability- Low off-gassing	<ul style="list-style-type: none">- Very good long-term stability- Low off-gassing- Good thermal stability

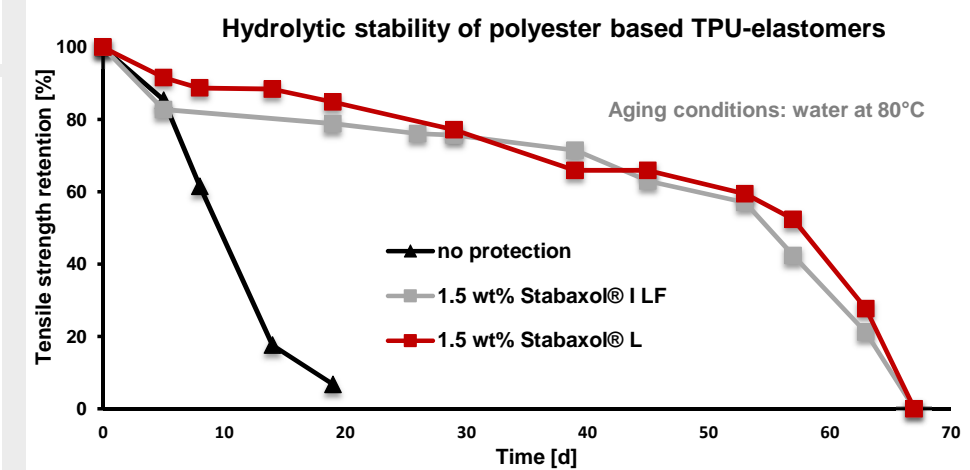
PUBLIC

New development products

Stabaxol® L

LANXESS
Energizing Chemistry

Description	<ul style="list-style-type: none">▪ Monomeric carbodiimide▪ Liquid or solidified melt▪ NCN-content: > 8 wt%
Application	<ul style="list-style-type: none">▪ TPU- and cellular PU-elastomers, PET▪ Injection molding, sealing, shoe systems▪ PU hot/cold casting systems▪ Rollers, automotive auxiliary springs
Properties	<ul style="list-style-type: none">▪ Excellent hydrolysis protection in TPU-elastomers, PET▪ Very reactive acid scavenger even at low temperatures▪ Reduced off-gassing and higher thermal stability in comparison to Stabaxol® I▪ No labeling (based on the required tox-data for 100 tons REACH registration)



Stabaxol® Application

LANXESS
Energizing Chemistry

PET

Fibers, films, screens, filters

PBT

Sheathing for optical fibers, injection-molded articles for electrical/electronic applications

PLA

Automotive, electronics, appliances, construction, bath and office equipment

PA

Monofilaments, industrial injection moldings, tubes, containers

TPE-E

Cable sheathing, industrial injection moldings

TPU

Cable sheathing (automotive), shoe systems, injection molding (electrical/electronic), sealings

PU

PU hot/cold casting systems (automotive auxiliary springs, **Vulkollan®** applications), ester flexible foam, rollers

PJ Rubber

Rollers, drive belts, membranes, seals

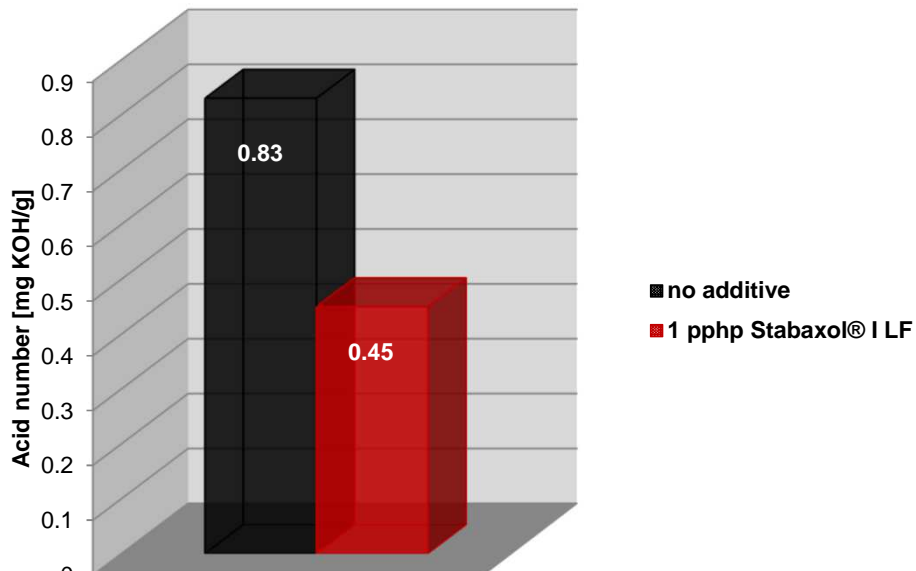


Application as acid scavenger

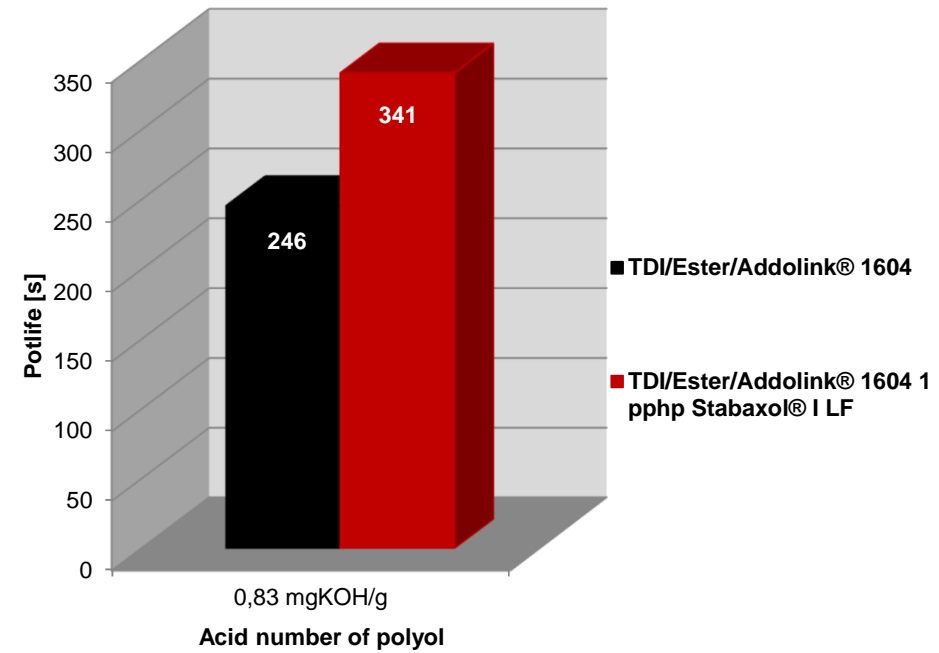
Stabaxol® I – Potlife extension

LANXESS
Energizing Chemistry

Acid value reduction in a polyester polyol
0.1 pphp NCN – reaction time: 0.5h @ 80°C



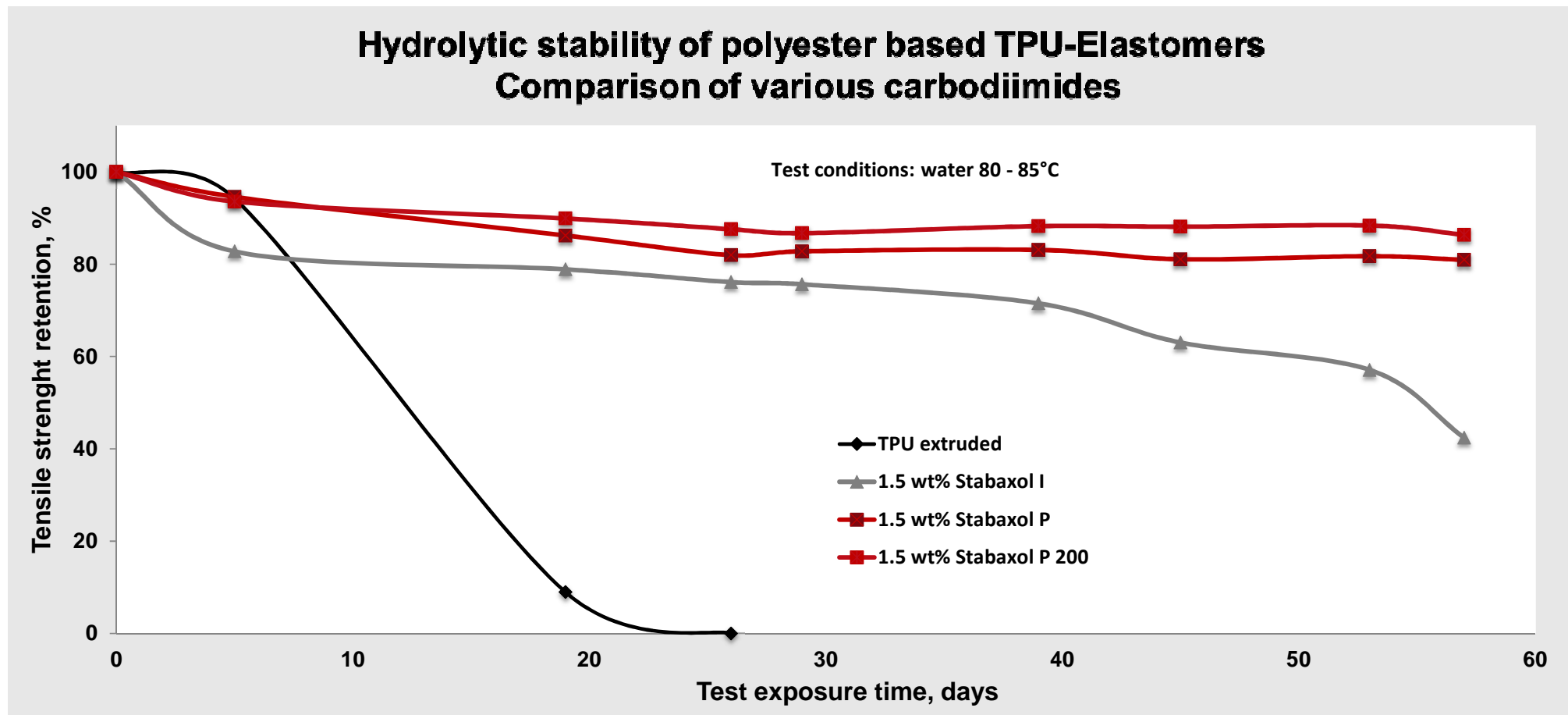
Potlife extension:
Hot Cast PU with amine crosslinker



Hydrolytic stability of TPU elastomers

Stabaxol® I / P / P200: Excellent performance (Compound)

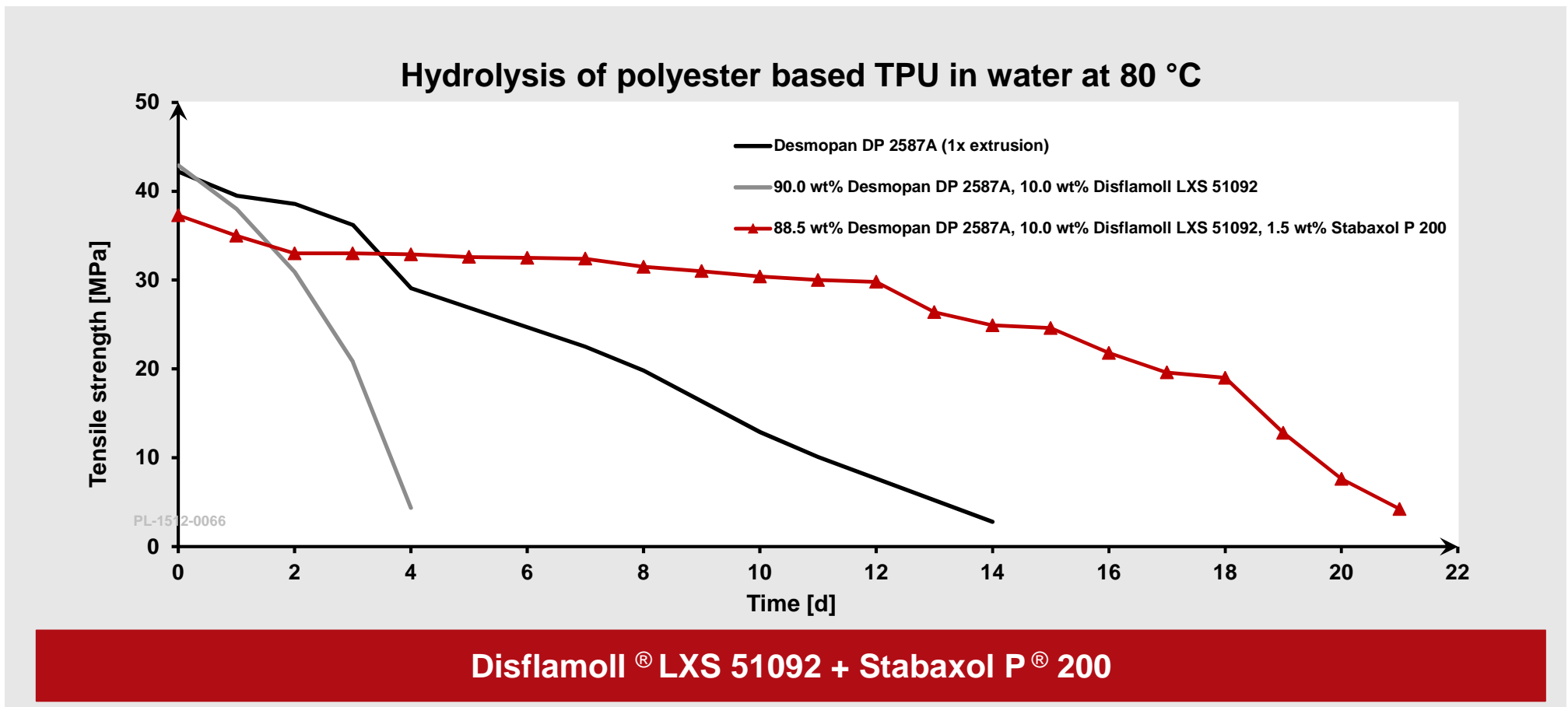
LANXESS
Energizing Chemistry

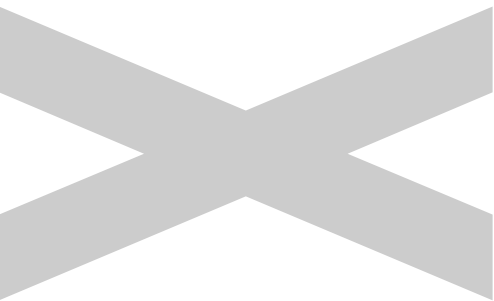


Hydrolytic stability of TPU

Stabaxol® P 200 in combination with Disflamoll®

LANXESS
Energizing Chemistry





Addolink®

Crosslinkers for Polyurethane Applications

PUBLIC

Addolink®: Typical Applications



Wheels & Rollers



Footwear



Mining Equipment



Dampening Elements



Printing Equipment



Pipeline Inspection

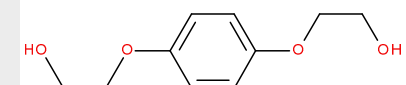
Addolink® crosslinkers are predominantly used in cast elastomers & TPU

HQEE*

LANXESS
Energizing Chemistry

Description

- Hydroquinone bis(2-hydroxyethyl)ether (HQEE)
- Melting point: min. 104 °C
- Water content: max. 0.1 %



Application

- Glycolic chain extender
- High performance hot cast elastomers with MDI-based prepolymers
- Especially useful for thermoplastic urethane elastomers (TPU)



Properties

- High purity product ($\geq 99.2\%$) with reduced amount of side products
- Very good mechanical & dynamical properties
- Good MbOCA** alternative with suitable MDI-based prepolymers



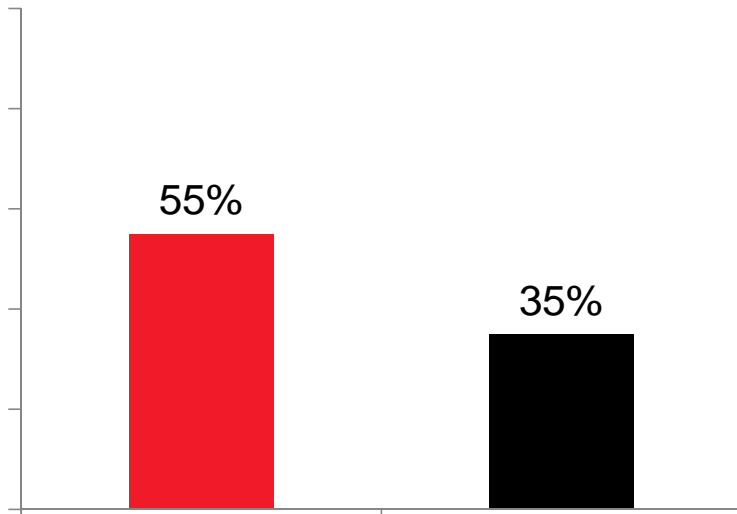
* Available under different trade names

** Sunset 22.11.2017. Extension of use in EU for a 4-year review period recommended by ECHA (as of 30.11.2017)

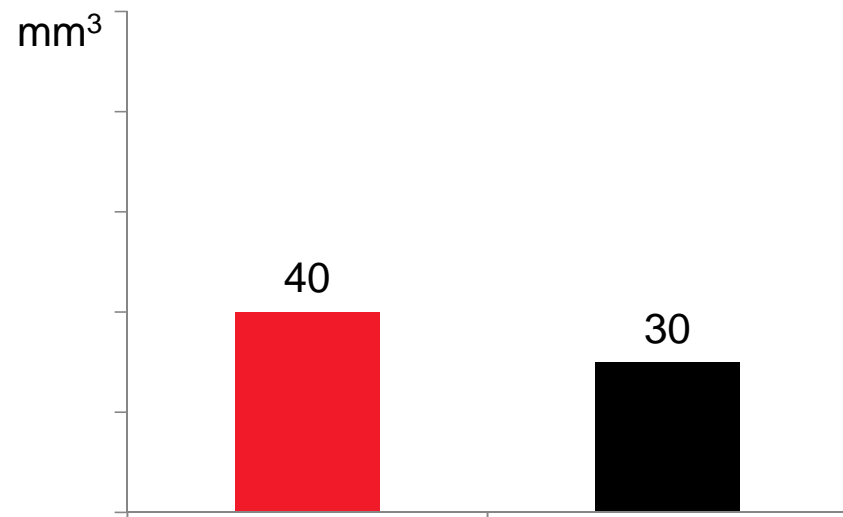
HQEE vs. 1,4-Butandiol (BDO)*

LANXESS
Energizing Chemistry

Compression Set



Abrasion



Chain extension with HQEE provides elastomers with better dynamic properties & lower abrasion

* Used as chain extender in MDI / Ester TPU, Shore D 60: lower values are better

HQEE: Typical End-Applications



Rollers & Wheels

For high dynamic load capacity or high speed applications,
e. g.: roller coaster, fork lift trucks etc.



Sealings

O-rings for high temperature and / or high pressure applications



Sporting Goods

Ski boots, wheels for roller-skates



Shoe Soles

Wear insert for high heels etc.



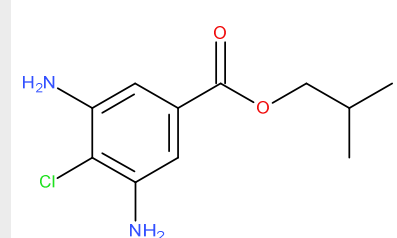
PUBLIC

Addolink® 1604

LANXESS
Energizing Chemistry

Description

- Isobutyl 3,5-diamino-4-chlorobenzoate (CDABE)
- Melting point: approx. 88 °C
- Water content: max. 0.15 %



Application

- Amine chain extender
- High performance hot cast elastomers with TDI-based prepolymers
- Especially useful **for large & intricately shaped parts**, e. g. pipeline pigs



Properties

- Very good mechanical & dynamical properties
- **Long pot life**, favorable classification
- Good MbOCA* substitute

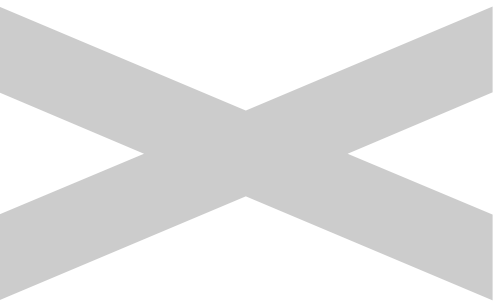


* Sunset 22.11.2017. Extension of use in EU for a 4-year review period recommended by ECHA (as of 30.11.2017)



Addocat®

Catalysts for Polyurethane Applications



PUBLIC

Addocat®: Complete Product & Application Overview



Addocat®	Rigid Foam				Flexible Foam			Elastomers			Coatings	Adhesives & Sealants	Special Characteristics
	Slab	Panels	Spray Foam	Appliance & Pipe Insulation	Ester	Ether	Molded-Integral	Cast	Cellular	TPU			
DB (BDMA)	■	■		■	■						■	■	Gelling co-catalyst, good emulsifier, improves flow and adhesion to facings, reduces friability in high-water formulations
PP (Blend of tert. amines)		■		■	■			■			■	■	Balanced catalyst, improves flow
SO (Tin(II) octoate)			■		■	■	■						Strong gelling catalyst for flexible foam
10/9 (Tertiary amine)											■	■	Mild gelling catalyst for wood coatings
105 (TEDA/DPG)	■	■	■	■	■	■	■	■			■	■	Strong multi-purpose gelling catalyst
108 (BDMAEE/DPG)	■	■	■	■	■	■	■						Strong blowing catalyst, improves flow
117 (DMP)	■	■		■	■								Gelling co-catalyst, good solubilizer
118 (DMDEE)			■	■	■	■	■	■			■		Catalyst for 1K & spray foam, improves shelf-life
1221VN (Blend of tert. amines)	■	■											Balanced rigid foam catalyst
1656N (Blend of DBTL & TEA)	■												Used mainly in rigid slabstock
1926 (Blend of DMCHA & polyol)	■	■		■									Improved metering compared to DMCHA

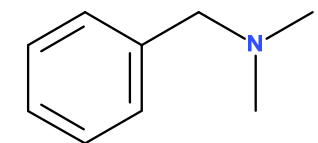
PUBLIC

Addocat® DB

LANXESS
Energizing Chemistry

Description

- Benzyldimethylamine (BDMA)
- Viscosity: 3 mPa·s
- Water content: max. 0.15 %



Application

- Rigid foam: panels, slab, *in-situ* foam, esp. high-water formulations
- Flexible foam: sole catalyst in ester-based formulations
- Also used in cold-cast elastomers, EP and UPE resins etc.



Properties

- Cost-effective, moderate back-end biased universal co-catalyst
- Reduces friability, provides tough & elastic surface
- Very good emulsifier, improves flow & adhesion to facings



PUBLIC

Addocat® PP

LANXESS
Energizing Chemistry

Description

- Blend of tertiary amines
- Viscosity: 3 mPa·s
- Water content: max. 0.5 %



Application

- CASE: coatings based on aliphatic isocyanates, cellular elastomers*
- Flexible foam: ester-based formulations
- Rigid foam: panels, appliance & pipe insulation



Properties

- Moderate activity balanced amine catalyst
- Improves flow
- Water soluble

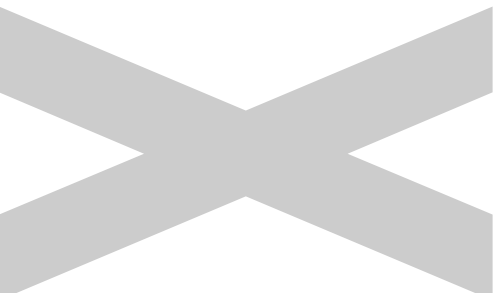


* Addocat® PP is used together with Addovate® SM, Addovate® DD 1092 and suitable Stabaxol® grades in the production of NDI-based high performance microcellular elastomers



Addovate®

Silicon-free Emulsifiers & Foam Stabilizers for Polyurethane Applications



PUBLIC

Addovate® : Typical Applications

LANXESS
Energizing Chemistry



Automotive upholstery



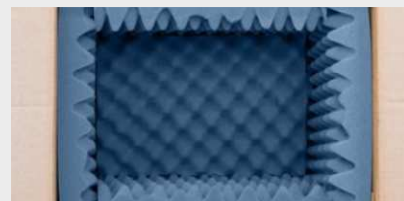
Textile lamination



Filters & sponges



Dampening elements



Packaging



Carpet underlay

Addovate® surfactants are predominantly used in ester flexible foam & cellular elastomers

PUBLIC

Addovate®: Product and Application Overview*



	Function			Main Application				
	Emulsifier	Stabilizer	Crosslinker	Technical		Textile	Low Odor / Fogging	Cellular Elastomers
Non-Ionic				Standard	Semi-rigid			
Addovate® EM	+++	+		■		■	■	
Addovate® WM	+++			■	■			
Addovate® 3240	+++			■			■	■
Ionic								
Addovate® DD 1092*	++							■
Addovate® SM*	++	++	+	■	■			■
Addovate® SV	++	++	+					■
Addovate® TX	+	+++	+	■		■		

* Used together with Addocat® PP and suitable Stabaxol® grades in the production of NDI-based high performance microcellular elastomers

Addovate® EM / TX

LANXESS
Energizing Chemistry

Description

- Addovate® EM: non-ionic emulsifier
- Addovate® TX: ionic emulsifier & foam stabilizer
- Often used together, but can be combined with other Addovate® grades



Application

- Textile grade ester foam, e. g. for textile lamination, paint rollers etc.
- Standard technical grade foam, e. g. sponges, packaging etc.
- Especially suitable for clickable foam



Properties

- Silicon-free, organic surfactants
- Very even cell size, no pin holes, excellent cell size control
- Less cutting loss due to a smaller edge zone



PUBLIC

Addovate® WM / SM

LANXESS
Energizing Chemistry

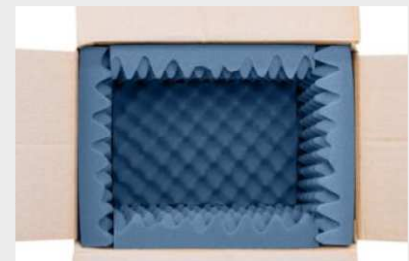
Description

- Addovate® WM: non-ionic emulsifier
- Addovate® SM: ionic emulsifier & foam stabilizer
- Typically used together, but can be combined with other Addovates®



Application

- Standard & semi-rigid technical foam, e. g. filters, sealants, packaging
- Water-blown & crosslinked cellular elastomers* (machine casting)
- Addovate® SM can be substituted with SV for hand casting



Properties

- Silicon-free, organic surfactants
- Small, even cell size



* Addovate® SM is used together with Addocat® PP, Addovate® DD 1092 and suitable Stabaxol® grades in the production of NDI-based high performance microcellular elastomers

Thank you for your attention

Disclaimer



This information and our technical advice – whether verbal, in writing or by way of trials – is subject to change without notice and given in good faith but without warranty or guarantee, express or implied, and this also applies where proprietary rights of third parties are involved. Our advice does not release you from the obligation to verify the information currently provided - especially that contained in our safety data and technical information sheets - and to test our products as to their suitability for the intended processes and uses. The application, use and processing of our products and the products manufactured by you on the basis of our technical advice are beyond our control and, therefore, entirely your own responsibility. Our products are sold in accordance with the current version of our General Conditions of Sale and Delivery.

Unless specified to the contrary, the values given have been established on standardized test specimens at room temperature. The figures should be regarded as guide values only and not as binding minimum values. Kindly note that the results refer exclusively to the specimens tested. Under certain conditions, the test results established can be affected to a considerable extent by the processing conditions and manufacturing process.

©2020 LANXESS. Addocat®, Addovate®, Addolink®, Adiprene®, Disflamoll®, Levagard®, PHT4-Diol™, Stabaxol®, Vibrathane®, LANXESS and the LANXESS Logo are trademarks of LANXESS Deutschland GmbH or its affiliates. All trademarks are registered in many countries in the world.

LANXESS Deutschland GmbH, D-50569 Köln

BU PLA (Polymer Additives)

PUBLIC



000569

NASA CONTRACTOR
REPORT



NASA CR-12

C.1

NASA CR-1262

LOAN COPY: RETURN TO
AFWL (WLIL-2)
KIRTLAND AFB, N MEX

HUMAN SURVIVAL IN
AIRCRAFT EMERGENCIES

by Charles A. Yost and Ronald W. Oates

Prepared by

STENCIL AERO ENGINEERING CORPORATION

Asheville, N. C.

for

NATIONAL AERONAUTICS AND SPACE ADMINISTRATION • WASHINGTON, D. C. • JANUARY 1969



0060569

NASA CR-1262

HUMAN SURVIVAL IN AIRCRAFT EMERGENCIES

By Charles A. Yost and Ronald W. Oates

Distribution of this report is provided in the interest of information exchange. Responsibility for the contents resides in the author or organization that prepared it.

Prepared under Contract No. NASw-1530 by
STENCIL AERO ENGINEERING CORPORATION
Asheville, N.C.

for

NATIONAL AERONAUTICS AND SPACE ADMINISTRATION

For sale by the Clearinghouse for Federal Scientific and Technical Information
Springfield, Virginia 22151 - CFSTI price \$3.00

ABSTRACT

A general study was performed to outline methods for the improvement of human survival in civilian aircraft emergencies. Survival condition criteria, accident statistics and human tolerance limits have been surveyed with respect to those aircraft used in two categories: certificated air carriers and general-private aviation (including official executive aircraft). The methods presented in this report for aircraft occupant survival improvement fall into the general areas of occupant protection through seat design and occupant restraint improvement to withstand impact accelerations which are applied to the aircraft.



FOREWORD

This volume briefly describes how survival in aircraft emergencies can be improved by optimum aircraft interior and seat system design to aid occupant restraint, support and protection. This effort is conducted under the Life Support and Protective Systems subprogram of the Human Factors Systems Program, a line item of the Congressional Authorization to the National Aeronautics and Space Administration.

As a follow-on effort the Ames Research Center, Moffett Field, California, is conducting for the Human Factors Program a developmental effort to design, develop, and evaluate a prototype seat/restraint system for improved crash and vibration protection. The latest developments in energy-absorption techniques, protective structures, and full-body emergency restraint methods will be applied to the problem.

ACKNOWLEDGMENTS

The research study described herein was conducted by Stencel Aero Engineering Corporation under NASA Contract NASw-1530. The work was done under the auspices of Dr. W. L. Jones, Director, Biotechnology and Human Research Division and technical direction of Mr. Allan Merkin, NASA Headquarters, Washington, D.C.

Aircraft and accident statistics have been provided by the FAA and interpreted by the writers for graphical presentation. Definition of the most adverse environments in which a human might survive have been abstracted from the FAA-Civil Aeromedical Research Institute work, from NASA reports and the Flight Safety Foundation, Inc. test data. In addition, a number of agencies and investigators have been consulted in an effort to gain in-depth information rapidly for this report. These contacts have included:

1. NASA- Biotechnology and Human Research Division, Washington, D.C.
2. FAA - Mr. J. J. Swearingen, and Mr. A. H. Hasbrook, Civil Aeromedical Research Institute, Oklahoma City, Oklahoma
3. FAA - Mr. J. J. Carroll, Supersonic Transport-Safety Washington, D. C.
4. CAB - Mr. B. R. Allen and Mr. Hollowell, Bureau of Safety, Washington, D.C.
5. Mr. J. Lederer and Mr. Hallas, Flight Safety Foundation, Inc., Phoenix, Arizona
6. Dr. L. S. Higgins, M.D., Technology, Incorporated, San Antonio, Texas
7. Mr. J. H. Enders, NASA, Aeronautics Division, Washington, D. C.

TABLE OF CONTENTS

SUMMARY	1
INTRODUCTION	2
SURVIVAL CRITERIA	3
Survivable Aircraft Accidents	3
Crashworthiness	4
Occupant Flailing	5
Human Body Structure	6
AIRCRAFT EMERGENCY SURVIVAL METHODS	12
INTERNAL FUSELAGE IMPROVEMENTS	13
Occupant Protection & Interior Design Methods	14
Seat Design	15
Restraint Design	16
COMMERCIAL MULTI-ENGINE TRANSPORT SAFETY IMPROVEMENT	17
General Statistical Information	17
Transport Aircraft Seating & Restraint System Improvement	26
Energy Absorbing Seat Development	28
Integrated Safety Seat	29
Honeycomb Design for Impact Survival	29
GENERAL AVIATION SAFETY IMPROVEMENT	34
General Aviation Statistics	34
INTERNAL IMPROVEMENTS	40
Seat Attachment	40
HUMAN TOLERANCES	42
REFERENCES	53

SUMMARY

Survival in aircraft emergencies can be improved, generally speaking, by improved aircraft interior and seat design to aid occupant restraint and protection. This would reduce injuries and fatalities in those accidents in which the aircraft incurs substantial damage but nevertheless remains adequately intact for occupant survival.

This report emphasizes occupant seating and restraint improvement as related to:

- (1) certificated air carrier transport aircraft having large passenger capacity.
- (2) general/private aviation aircraft having a few occupants.

Aircraft accident statistics show that substantial damage is sustained in nearly 70 percent of all aircraft accidents but that the fuselage remains sufficiently intact for human survival. Occupants can be protected against injury in this type of accident by means of energy absorption seat designs, protective seat structure with improved full body restraint, and safety consciousness in interior cabin decor. Internal improvements would therefore have beneficial utilization in the majority of aircraft accidents and provide immediate areas for improvement.

INTRODUCTION

The Civil Aeronautics Board classifies an aircraft accident as the occurrence incident to flight in which, as a result of the operation of an aircraft, any person (occupant or non-occupant) receives fatal or serious injury, or any aircraft receives substantial damage. An aircraft accident incident to flight is further defined as an accident which occurs between the time an engine or engines are started for the purpose of commencing flight until the aircraft comes to rest with all engines stopped for complete or partial deplaning or unloading. It excludes death or injuries to persons on board which result from illness, altercations, and other incidents not directly attributable to flight operations. This report refers to an aircraft emergency as a situation in which an aircraft accident results.

The problem of improving the chance of human survival in aircraft emergencies arises out of the increasing numbers of persons using aircraft as well as the widely diversified performance and application of these aircraft. The provision of survival aids to meet an aircraft emergency have not kept pace with the capability of an aircraft to transfer people into environmental conditions beyond human tolerance. The problem is most acute in all fields of civil aviation where manufacturing and operating economics are strong factors.

This report presents concepts, analyses, and evaluation of practical survival methods that may be applied to civilian aircraft. Two categories of aircraft have been considered in the study: (1) certificated air carrier aircraft, and (2) general private aviation aircraft (including executive official aircraft.) Consideration is given to human tolerance, aircraft impact velocity and angle, the type of aircraft operation, the accident statistics that indicate predominate problem areas, and survival improvement concepts that can be applied inside of the aircraft to accomplish human protection.

The study as reported, proceeds first to define the extent of the survival improvement problem in terms of aircraft accident statistics; and in terms of physical factors such as velocity, acceleration, and human tolerance.

Thereafter, methods for survival improvement are presented that would be applied internal to the aircraft to maintain conditions of occupant tolerance by means of seat design and occupant restraint.

SURVIVAL CRITERIA

Survivable Aircraft Accidents

There are many conditions that an occupant is exposed to and must withstand in order to survive an aircraft accident. Assuming the aircraft fuselage remains structurally intact, the passenger must be protected from severe impact forces, smoke, fire and fumes, and then he must be given a means for immediate evacuation. The first and foremost requirement to be met in order for the occupant to survive is that the aircraft fuselage must remain substantially intact. While fires must be suppressed and the passengers must be protected from smoke and fumes, and then evacuated, none of these can be very useful without maintaining structural integrity of the occupant area.

This report deals primarily with the problem of protecting the aircraft occupants from severe impact forces. A survivable aircraft accident is therefore defined for this study as one in which the occupied cockpit and/or fuselage remain relatively whole after impact. The methods studied and presented in this report are therefore concerned with occupant structural protection; and improving the occupant seat and restraint structure so as to be compatible with human impact and acceleration tolerances.

Two aspects of survival criteria exist. One has to do with the aircraft structure capability and the other has to do with the occupant-seat structural capability. Since the imposed forces are dependent upon the velocity changes that occur with distance and time, it is possible to present the limits of structural capability in these terms. Similarly, the occupant has acceleration tolerances beyond which he sustains injury. An estimate of these limitations are given in Figure 1, and expressed in terms of velocity change and deceleration distance.

As shown in Figure 1, one real limit placed upon the occupant is that available distance under which he may be decelerated. This limit is placed upon the occupant by surrounding seats, by the cockpit envelope, or by the distance from the bottom of the seat to the floor. The occupant must be decelerated within this space limitation.

Data on the acceleration tolerance of typical aircraft occupants (men, women and children) is not available. While it is known that some persons have experienced and tolerated very high

acceleration forces, with a wide variety of passengers a 10 g limitation would be reasonable for design. With a 10 g limitation for design and the space available to the seat for displacement it can be seen in Figure 1 that the relative occupant velocities with objects in the cabin should be limited to about 25 ft/sec. Velocities in excess of this amount are likely to cause injury to the passenger.

Crashworthiness

Figure 1 gives some idea of the limits for aircraft structure and for occupants under a crash environment. The aircraft longitudinal deceleration distance covers a wide range because of various horizontal sliding resistance conditions. Horizontal velocities in excess of about 180 ft/sec. might be tolerated by the aircraft provided it does not meet strong vertical obstacles, steep embankments, or have severe attitudes. Sliding action permits the deceleration distance in the longitudinal direction to be much larger than the actual length of the aircraft. Objects approached longitudinally may often result in the fuselage remaining relatively intact.

The ability of the aircraft fuselage to attenuate vertical velocity is fixed by the fuselage diameter. Vertical velocity tolerance is therefore much less than that for the longitudinal direction. The only means attenuating the vertical velocity is crushing of the aircraft diameter. In the case of most transports, perhaps four or five feet of fuselage can be deformed before the interior cabin floor structure reaches ground level. As illustrated in Figure 1, this deformation might allow a 30 or 40 foot per second vertical velocity to be tolerated and still maintain reasonable occupied fuselage structural integrity.

Approximate survivable impact conditions found in some transport crashes investigated by Av-Ser (reference 3 and 7) were as follows:

- (1) 150 knots forward speed
- (2) 15 degrees nose down pitch angle
- (3) 30 degrees yaw angle to either side of the longitudinal axis of the aircraft.
- (4) a resultant crash force angle within an arc extending from 15 degrees above to 45 degrees below the longitudinal aircraft axis in the vertical plane and parallel to the longitudinal axis.
- (5) impact against and a deceleration on reasonably level terrain having the general density of plowed ground.

These conditions are generally in keeping with those outlined in Figure 1. The velocity and impact angle at which the fuselage commences to undergo severe destruction is shown in Figure 2. This is roughly compatible with the Av-Ser findings for survivable-unsurvivable conditions found in some transports; as well as being roughly compatible with Figure 1. To this date, very little test data is available that would allow a more exact definition of the survivable accident boundaries for aircraft structures.

Looking at Figure 2 it can be seen that the region for survivability extends up to an aircraft velocity of about 140 miles per hour for horizontal impact angles. As the flight path angle increases the toleration of the aircraft decreases, until at about 70 degrees, the tolerable velocity probably drops to near zero.

Occupant Flailing

Design improvement for occupant protection requires that space be available for the occupant to decelerate, and requires full restraint of the occupant in his seat (reference 3.4, 3.5). In current seats, particularly in general aviation, cabin conditions are prevalent that cause the occupant to become injured from impact with rigid structures.

Case histories show that 70 to 80 percent of all general aviation injuries in crash decelerations are a result of face or head impacts caused by upper torso and head flailing. Improved occupant restraint design incorporating upper torso restraint would immediately decrease the injury index in these survivable crashes.

To provide some idea of flailing sweep, Figure 3 shows the motions of fifth and ninety-fifth percentile subjects accelerated forward over a tight safety belt. Reference 2.2, 215. The subjects were displaced by a 1 g force so the sweep presented must be considered as a minimum strike distance. The impact velocity of the head during these test exceeded 12 ft/sec.

In actual crash conditions larger magnitudes of body movement can be expected since impact forces are likely to be greater than 1 g and the passenger seat belts would probably be loosely fastened. While it is not practical to allow

amount of space needed so that the occupant could flail without impacting any structure, it is practical to restrain the occupant such that his head and torso are unable to flail. Shoulder and lap restraint alone would eliminate a large number of impact injuries.

Figure 3(b) illustrates the number of injuries that have been incurred on various parts of the body in a large number of light aircraft accidents. This injury pattern of 800 survivors in light aircraft accidents shows that, in light planes at least, the greatest number of injuries occur to the head and torso. This is almost entirely a result of body flailing at impact. The need to restrain the body above the waist is apparent and should be incorporated.

Human Body Structure

Bones provide the rigid framework for the body to carry loads and to protect the vital organs such as the heart, brain, and lungs from injury. The ligaments act to hold the bone joints together and cartilage furnishes elastic connective tissues which protect the bones at the joints from shock and give the skeleton more flexibility. Figure 4 illustrates the arrangement of the human skeleton, and identifies the major skeletal parts by their technical names.

The engineer is concerned with the body as a structural load carrying system for dynamic and static loads. The body, being a composite of flexibly connected rigid members, must be externally restrained to prevent excessive momentum or force to build up between the parts. For a seated aircraft passenger undergoing rapid decelerative forces, the body masses requiring restraint are the pelvis region, the upper chest area and the head. While restraint of the arms and legs would also be desirable, movement of these body parts and their possible injury are not directly fatal. While methods for such total restraint would be desirable, it would present much difficulty in practice.

The head mass must be restrained from fore and aft whiplash motions that can be developed on the 7 cervical vertebrae. Failure to restrain the head permits severe neck strains and head velocity conditions to develop.

The upper torso must be restrained to prevent pivoting motions about the pelvic regions. The majority of the body mass is in the upper torso, contained in the boundary of the rib cage and dorsal vertebrae, with the dorsal vertebrae acting as attach points for the ribs. This section therefore forms a relatively

rigid structure for restraint support. Movement of the upper torso is therefore in a rigid fashion about the lumbar vertebrae and pelvic region when a lap restraint is employed. Without upper torso restraint, the torso momentum would transfer to the pelvic region.

The pelvic region must be restrained to avoid bending of the lumbar vertebrae and to prevent motion of the pelvic and fore-leg masses. The lumbar vertebrae and the lower dorsal vertebrae receive very little support from the rib cage structure. Vertical compressive accelerations of the upper body are therefore almost wholly supported by this vertebrae column section and can be expected to experience more severe stresses than the upper portions of the back bone structure. Ruptured discs are fairly common and might therefore occur frequently in this section if it is not firmly supported.

The skeletal structure, as shown in Figure 4, and the distribution of masses and hinge regions of the body indicate a need for body restraint, during impact, extending from the pelvis region up to and including the head. The relative masses of the various body parts are approximated as listed in Figure 4. Reference 3.6 points out that shoulder straps fastened to the lap belt can apply forces that lift and reduce the lap belt effectiveness.

VELOCITY - DISTANCE - TIME (SURVIVAL CRITERIA)

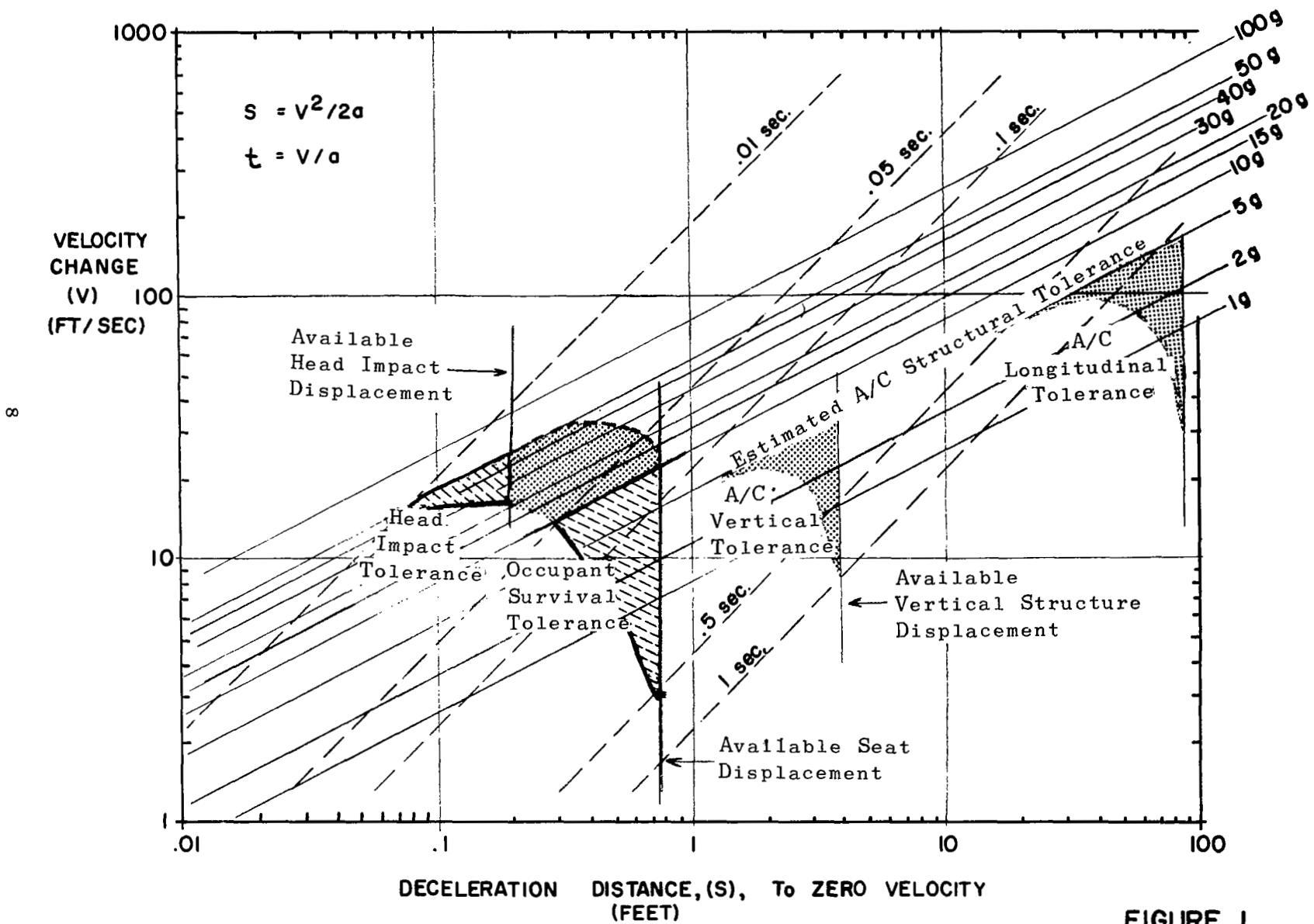


FIGURE 1

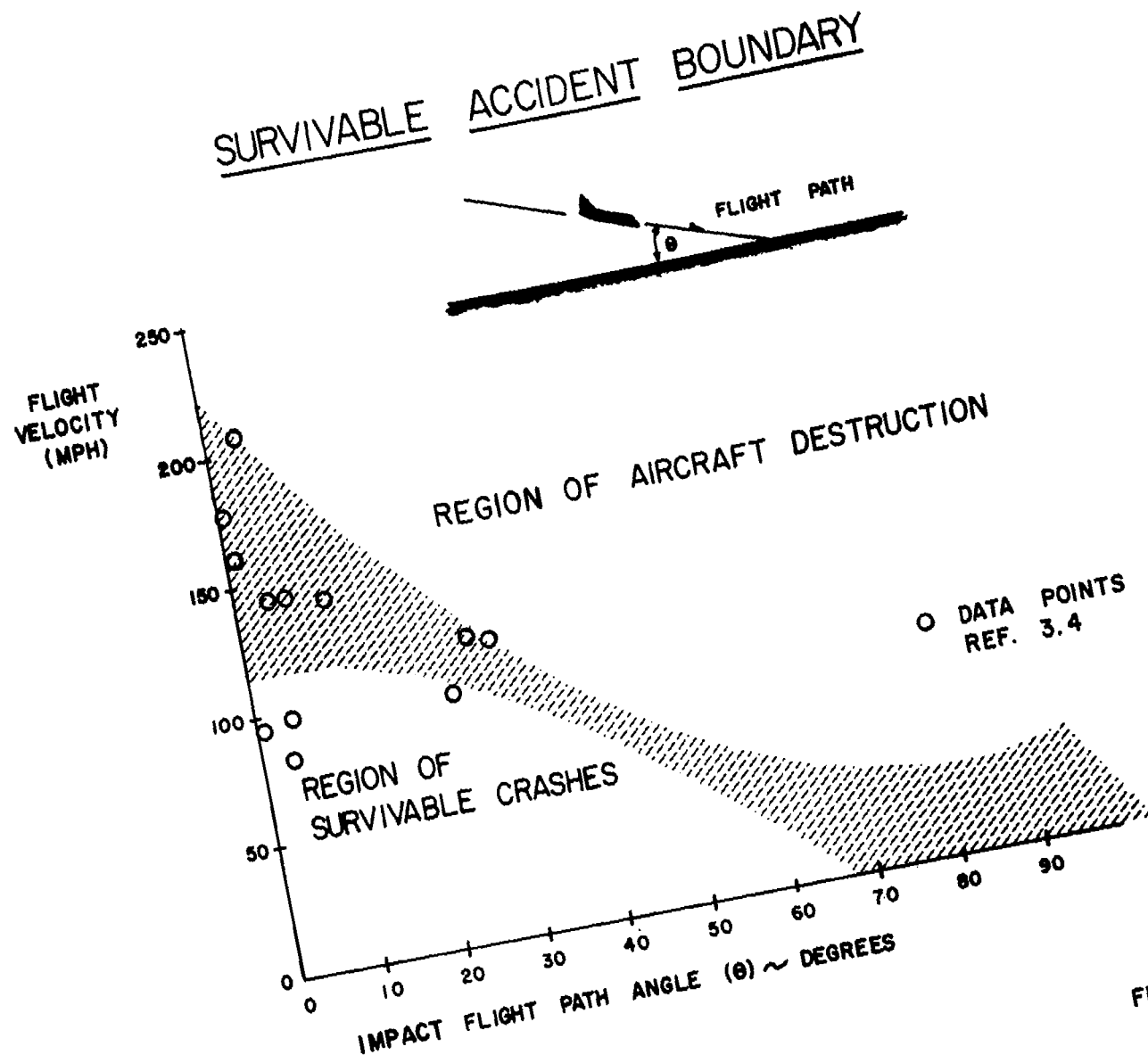
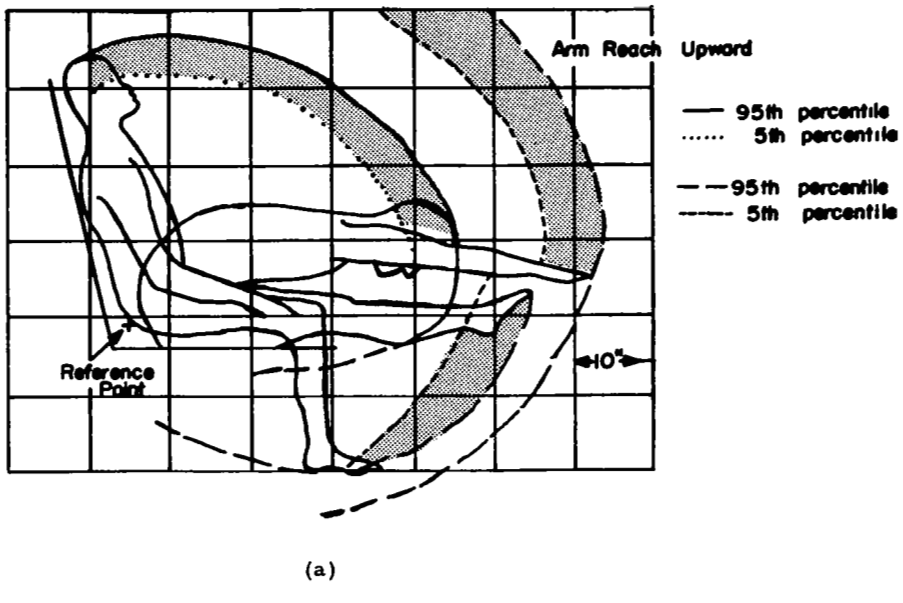


FIGURE 2

RESTRAINED HUMAN IMPACT ENVELOPE



REF: AM 62-13

**RESTRAINED HUMAN INJURY AREAS
LIGHT AIRCRAFT CRASHES**

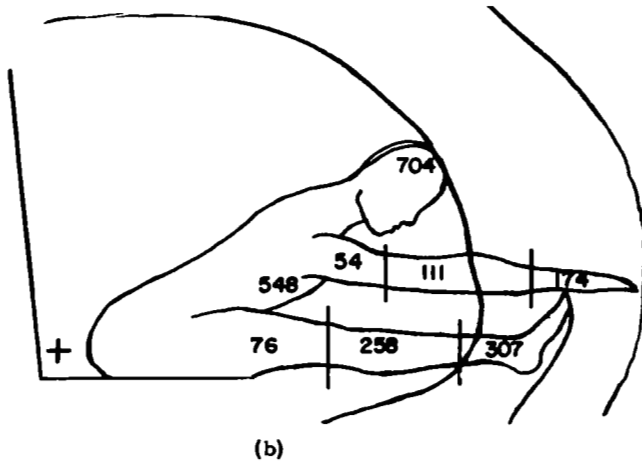


FIGURE 3

SKELETAL STRUCTURE
NOMENCLATURE

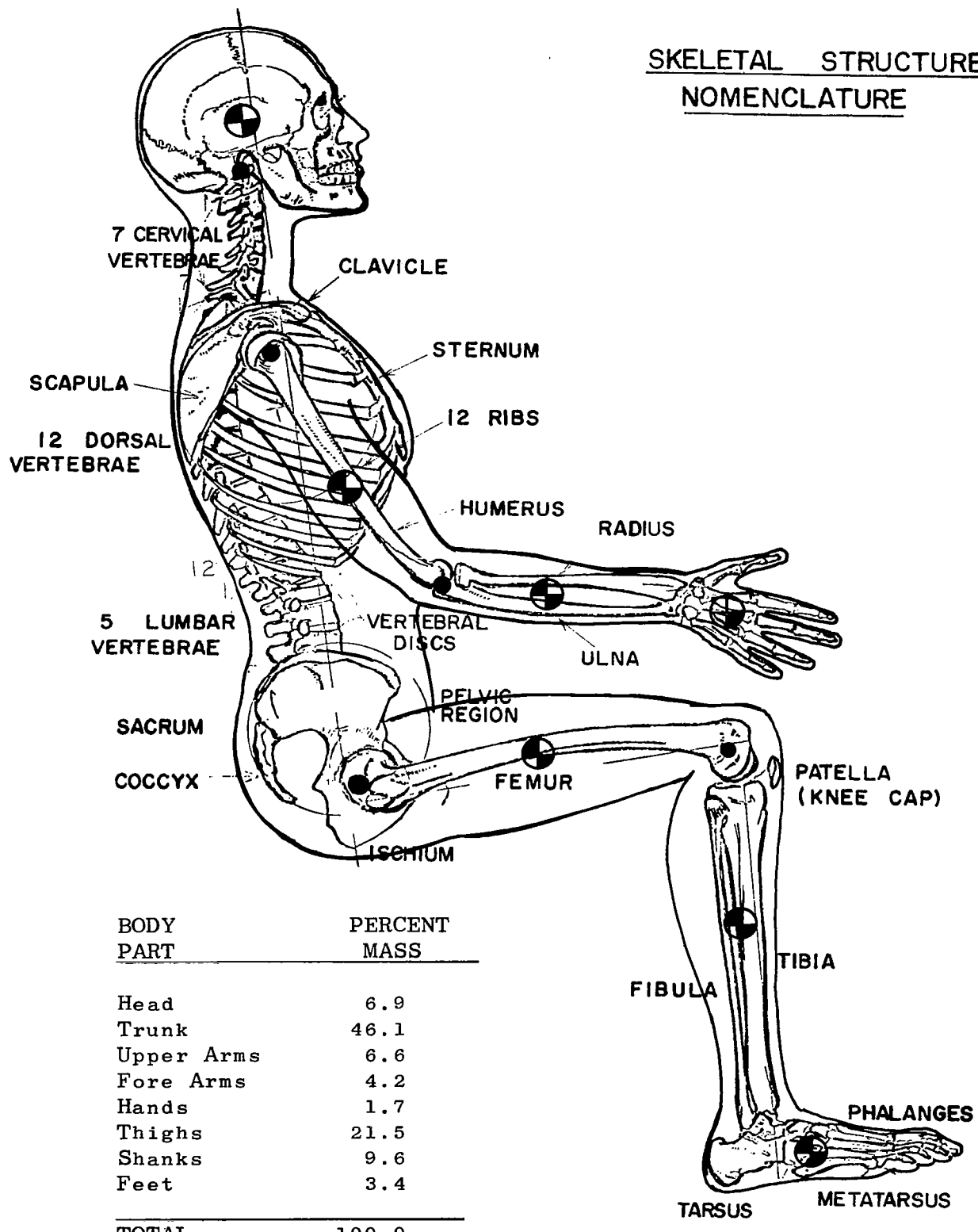


FIGURE 4

AIRCRAFT EMERGENCY SURVIVAL METHODS

Internal survival improvement methods in this report contain design objectives for occupant seating and restraint. Other areas for improvement, such as fire suppression, smoke and fume protection and evacuation aids are not elaborated in this study.

There are a number of methods that could be applied in an aircraft emergency to protect the occupants from severe injury. Only a few of these methods can be applied at an acceptable price to the user. Figure 5 shows some of the methods that might be applied to assist survival in aircraft emergencies. These methods are presented in chart form. The kind of methods that could be applied are divided into three basic modes of flight: take-off, in-flight, and landing. The methods are further divided into applications to general aviation and commercial aviation, and executive aircraft. Those methods that appear reasonable to apply in a given flight mode and a particular type of aircraft are indicated by a solid dot.

AIRCRAFT EMERGENCY METHODS

METHOD	TAKE-OFF			IN-FLIGHT			LANDING		
	G	C	E	G	C	E	G	C	E
INTERIOR CRASH PROOFING	●	●	●				●	●	●
CRASH CAPSULES			●						●
FULL BODY RESTRAINT	●	●	●	●	●	●	●	●	●
ENERGY ABSORBING SEAT	●	●	●				●	●	●

C = COMMERCIAL AIR CARRIER

E = EXECUTIVE OFFICIALS

G = GENERAL AVIATION

FIGURE 5

INTERNAL FUSELAGE IMPROVEMENTS

Efforts to improve aircraft interiors are a result of accidents wherein the aircraft cabin has remained adequately intact for human survival but the occupants have, nevertheless, died or were seriously injured because of fumes, fire, inadequate seat tie-down/seat belt restraint, or impact with local hard objects placed too close for crash safety. A summary of notes by J. J. Carroll⁴ and published reports by A. H. Hasbrook⁷, combined with that data obtained by the Flight Safety Foundation, Inc.³ point out that the interior design considerations for crash survival should include crashworthiness features such as:

- (1) Secure seat tie-down and seat energy absorption properties.
- (2) Secure occupant restraint.
- (3) Removal of lethal objects and surfaces from the occupant-impact envelope.
- (4) Secure attachment of interior furnishings.
- (5) Suppression of smoke and fire.
- (6) Quick routes for evacuation.

Much remains to be done toward defining quantitative values to meet these requirements. In this respect, aircraft manufacturers have pointed out the need for accident survival methods/criteria that is of definite argument based on clear evidence and of a quantitative nature for design and test.

Work at the Civil Aeromedical Research Institute (CARI) has been extensive in defining human body impact limits and injury levels.² The CARI work, combined with the aircraft crash test data of the Flight Safety Foundation, Inc.³ provides additional views on how aircraft interiors may be designed to improve chances for occupant survival.

2.2

S. R. Mohler and J. J. Swearingen estimate that possibly one half of all fatalities occurring annually in survivable aircraft accidents could be prevented if aircraft design were to include conditions for human tissue protection during impact. These authors further detail three principles for delethalization:

- (1) Eliminate and/or redesign cabin objects which can cause puncture wounds upon bodily impact.
- (2) Design and install a seat-restraint system (seat belt and shoulder harness) which will securely hold a human body under brief transient forces as high as 25 g. (Ref. 3.6, 1.1.4.3.1). Tolerance to impulsive loading under severe body restraint

may be taken as: (Ref. 3.6)
Longitudinal - 45 g for 0.10 sec.
25 g for 0.20 sec.

Lateral - 20 g for 0.10 sec.

Vertical - (Eyeballs down) 25 g for 0.10 sec.
(Eyeballs up) 15 g for 0.10 sec.

- (3) Design instrument panels and all other areas of likely body contact so that upon impact the greatest amount of deformation and material rearrangement would occur in the structures and not in the human body.

Occupant Protection & Interior Design Methods

Improvements for the occupant in the aircraft interior are effective under flight conditions where the aircraft is in a velocity and attitude condition that would allow impact to occur without severe destruction of the fuselage. Granting such impact conditions, the interior improvements are concerned primarily with occupant protection; thus, the removal of dangerous furnishings, sharp or hard surfaces and loose objects that might impact with the occupant is compatible design for aircraft emergencies.

Occupant seating and restraint represents a major area of interior design that could be improved with immediate benefits for occupant protection. For emergencies, full body restraint is essential to keep the occupant from flailing and impacting with surrounding hardware. In large passenger aircraft, seat and restraint design improvements are most essential to meet take-off and landing emergencies. Certain types of aircraft that undergo severe jostling conditions in-flight would also be made more comfortable with a full body restraint system on the pilot.

Where an aircraft undergoes crash type conditions, the occupant protection can be improved by designing seats to absorb high energy pulses. Force limiting energy absorbing devices (Ref. 3.5) would reduce high peak forces and allow the seat to remain attached to the basic aircraft structure and maintain the occupant position in the seat at lower force levels. Such seat design would be immediately useful to all aircraft types. At the present time seats are not designed to absorb high energy impacts and therefore frequently come loose from the airframe structure.

Another form of protection for the occupant would be crash

capsules. The nature of crash capsules would require them to be special structures within the airframe designed to resist and absorb impact at higher energy levels than the aircraft itself. Such devices do not appear economically practical for most aircraft; however, crash capsules may be useful for special executive application wherein a maximum protective security is more essential than the usual economic considerations for the aircraft.

Seat Design

The integral parts of a passenger seat system at the present time are the restraint belt, belt anchorage, seat portions which carry belt loads, cushion support and seat anchorages to the floor structure. Improvement is needed in the design of these components.

The use of ductile structures is desirable since this would allow deformations and attenuation precluding complete seat failure. Whenever practical, passenger seats should only be attached to a surface of structural continuity, such as the cabin floor. Attachments to differing structure surfaces, such as wall-floor combination structure, can deform differently to impose severe torsion on the seat ties, resulting in greater seat tiedown stresses and deformation damage.

Aircraft seat design provides one immediate improvement avenue for occupant safety. Seats may be improved by giving design attention to the following items:

- (1) Minimize seat mass, particularly in the upper parts of the seat back to reduce impact acceleration moment forces.
- (2) Avoid the exposure of hard structures where body impact may occur.
- (3) Use ductile, energy absorbing materials for primary seat structure.
- (4) Provide exo-skeletal seat structure for occupant protection.
- (5) Provide crushable impact attenuating surfaces.
- (6) Increase floor attachment joint flexibility to reduce bending stresses.
- (7) Build in seat safety aids against smoke, fumes, heat, vision and decompression.
- (8) Extend upper seat back above the head level for head protection.

Restraint Design

When an aircraft cockpit or cabin area remains relatively intact after a crash impact, definite improvements would be realized if the passenger or crew member were more adequately restrained.

Restraint design is an integral part of the seat system and needs design effort to:

- (1) Improve belt latch resistance against accidental release. For instance, some belt latches are susceptible to accidental release.
- (2) Provide restraint devices for upper torso and head in severe emergencies.

Head injuries take a heavy toll either directly by puncture wounds or indirectly by stunning blows. These injuries prevent rapid occupant exit before fire consumes the aircraft. Head and shoulder restraint is therefore essential to prevent excessive head travel and to provide a degree of safety to many who are at present killed or who suffer severe injuries to head or face.

Deceleration tests have demonstrated that when a man is well restrained by seat and shoulder harnesses, and in good condition he can tolerate crash force peaks from 15 to 45 g's (ref. 3.6). This substantiates the belief that people should survive impacts where the structures remain primarily intact since these structures fail at much lower g-forces.

COMMERCIAL MULTI-ENGINE TRANSPORT SAFETY IMPROVEMENT

General Statistical Information

A commercial air carrier is an operator who has been issued a Certificate of Public Convenience and Necessity by the CAB. The two main categories of air carriers are the Certificated Route Carriers and the Supplemental Carriers.

Figure 6 is a bar graph that shows each major type and number of aircraft in operation by the certificated route air carriers as of December, 1965. Boeing, Douglas, Lockheed and Convair Corporations provide the greatest majority of the currently used commercial aircraft. Of the 2104 fixed wing aircraft listed as held by the air carriers, only about 1875 are actually used for passenger operations. The number of commercial aircraft in active service (Figure 8) has only varied about 2½% since 1957. The service provided by these aircraft is shown in Figure 7 as accumulated by all the aircraft, and again in Figure 8 as an annual average allotted to each aircraft. Currently, the average transport aircraft travels 700,000 miles flies 2100 hours and makes 2200 departures per year.*

The annual number of commercial carrier accidents is small when compared to the large number of aircraft operations during that period. Figure 9 shows an average of about 80 accidents to occur annually, out of the four million flight departures.

Taking into account the total number of accidents that occur annually, Figure 10 shows about one accident to occur per 50,000 departures, and coincidentally, about one accident to occur per every 50,000 flight hours. This averages about 11,000 departures or flight hours per day, so that some kind of aircraft accident might be expected to occur every five days.

The reliability of aircraft transport systems is difficult to express in a simple manner because of numerous operating variables.

*The statistics found in this section were derived from the "FAA Statistical Handbook of Aviation" and from the Civil Aeronautics Board Annual "Statistical Review" and have been interpreted by the authors for presentation in this report.

Using the conglomerate of overall departure and flight time statistics and assuming all events to be equally probable, the reliability of the operating aircraft transport system could be expressed as:

- (1) Reliability = 0.99998 that any one departure will be accident free, or perhaps
- (2) Reliability = 0.99998 that any one hour of operation will be accident free.

This represents extremely good system reliability; however, it is a grossly simple interpretation and does not represent effects of individual case factors of time, distance, departures, maintenance, weather, etc. While the accident rate is extremely small, the massive quantities of air carrier operations still inevitably result in a significant total number of accidents and fatalities as shown in Figure 11.

There were 1642 fatalities in commercial aviation during the period from 1960 through 1964 as a result of 64 fatal accidents. These fatalities were distributed in categories as shown in Figure 12 and are summarized by Table 1.

TABLE 1

	Percent of all accidents	Percent of all fatal accidents	Percent of all fatalities
Take-off and Initial Climb	14	20	25
Enroute	26	45	60
Approach and Landing	50	30	15

AIRCRAFT IN OPERATION BY
CERTIFICATED ROUTE AIR CARRIERS
DEC. 1965

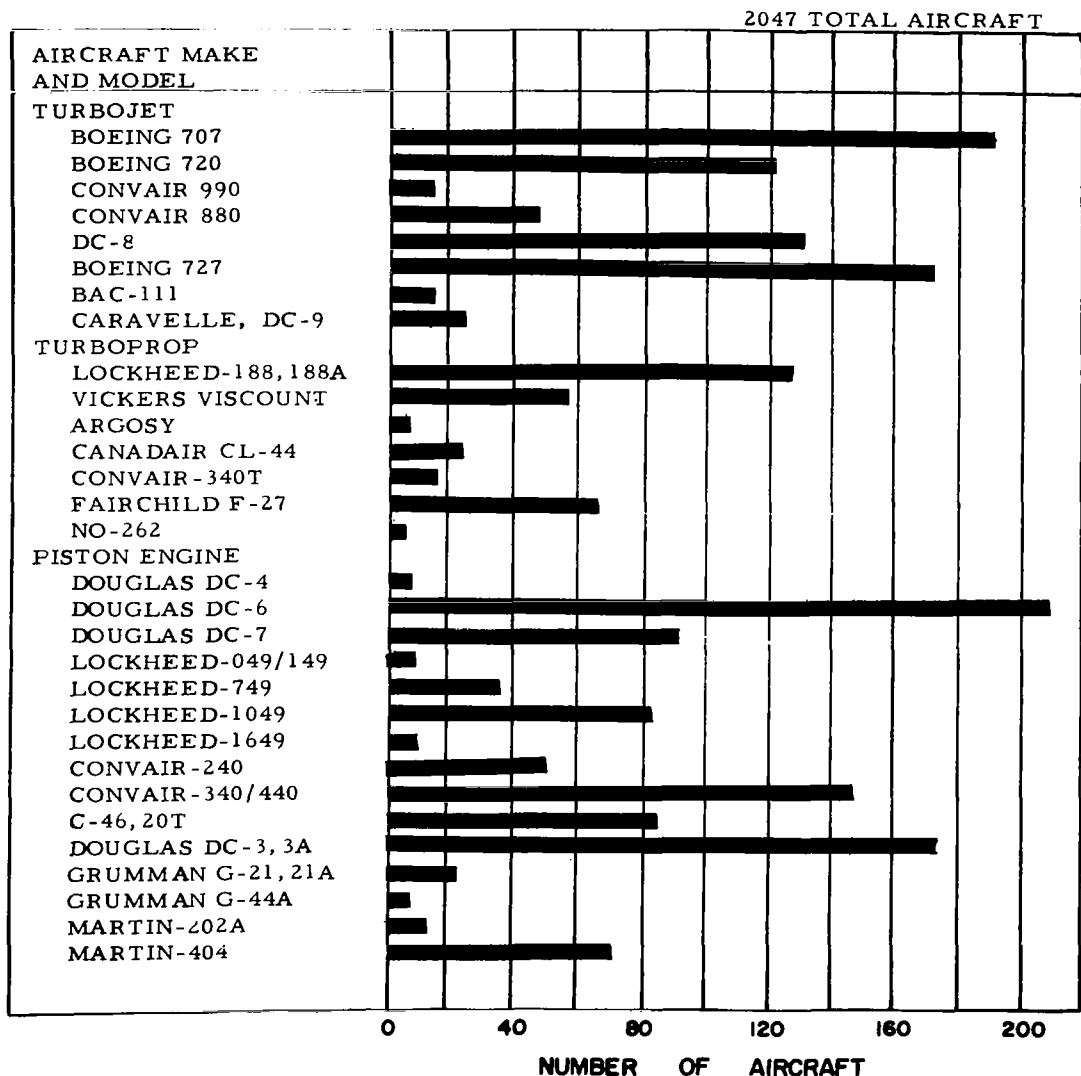


FIGURE 6

CERTIFICATED ROUTE
AIR CARRIERS
ALL SCHEDULED SERVICE

HOURS FLOWN
AND
DEPARTURES
($\times 10^6$)

MILES
FLOWN
($\times 10^6$)

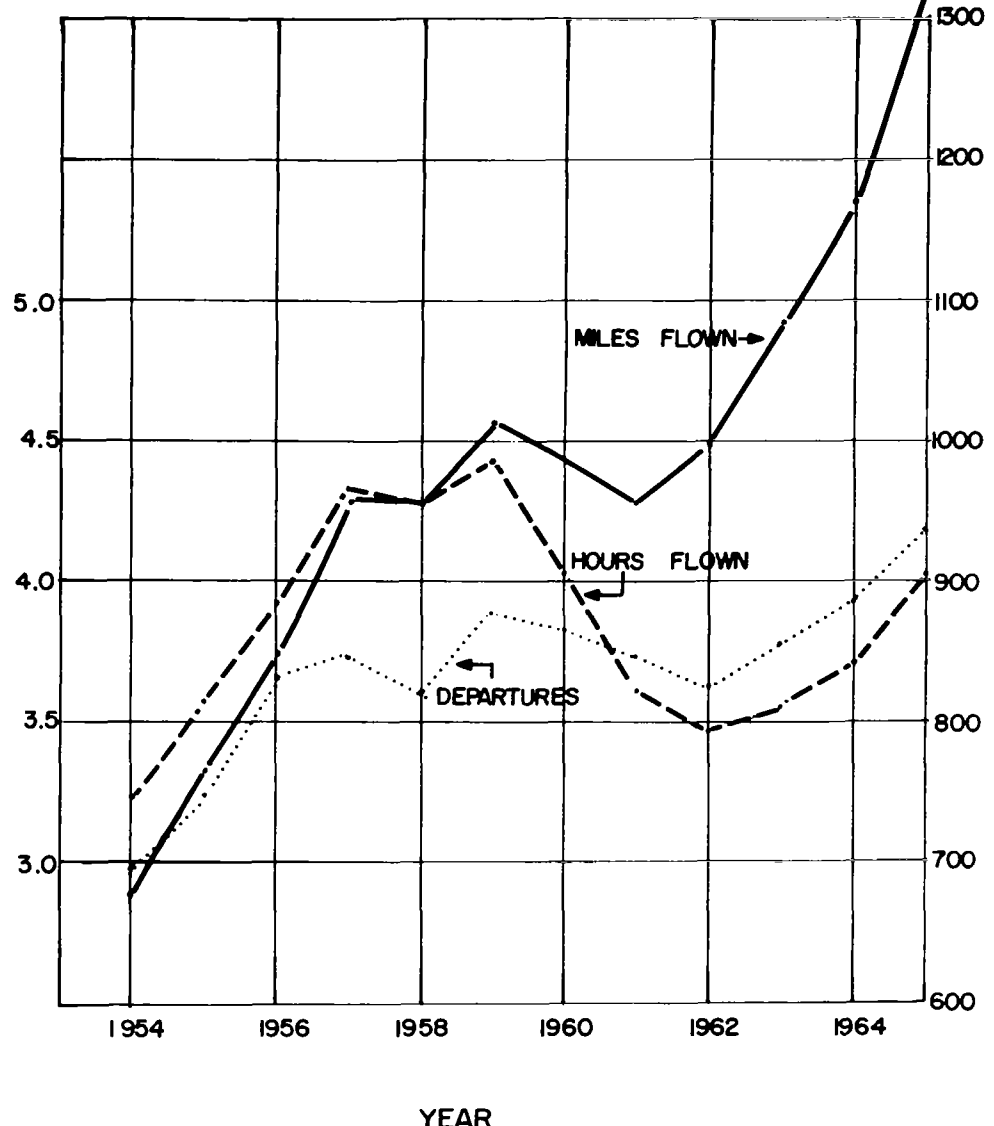


FIGURE 7

CERTIFICATED PASSENGER/CARGO
U.S. DOMESTIC & INTERNATIONAL AIR CARRIERS
OPERATIONS DATA
 (REF. 1966 FAA STATISTIC HANDBOOK)

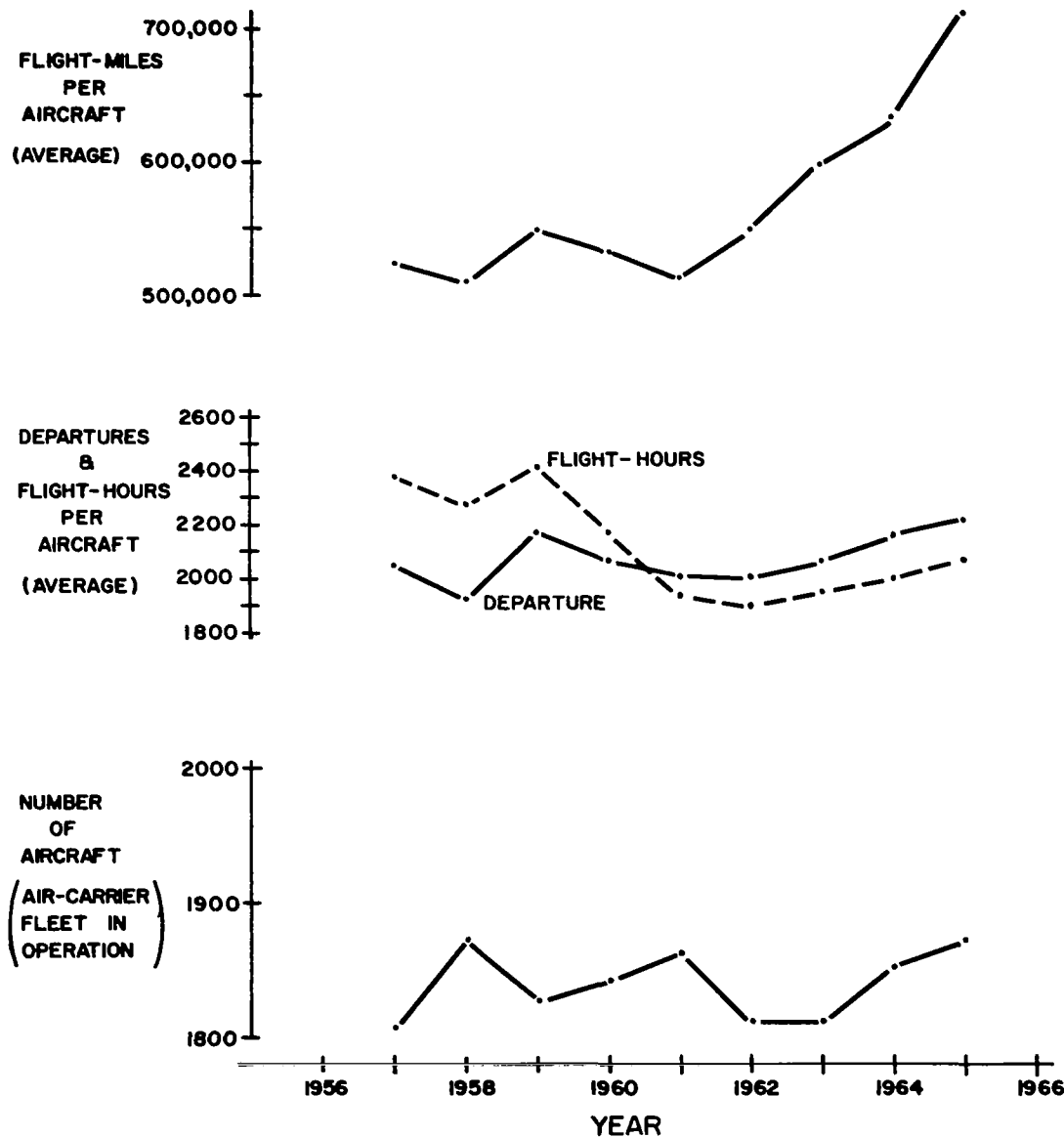


FIGURE 8

U.S. CERTIFIED ROUTE AIR CARRIERS
ALL OPERATIONS - NUMBER OF ACCIDENTS

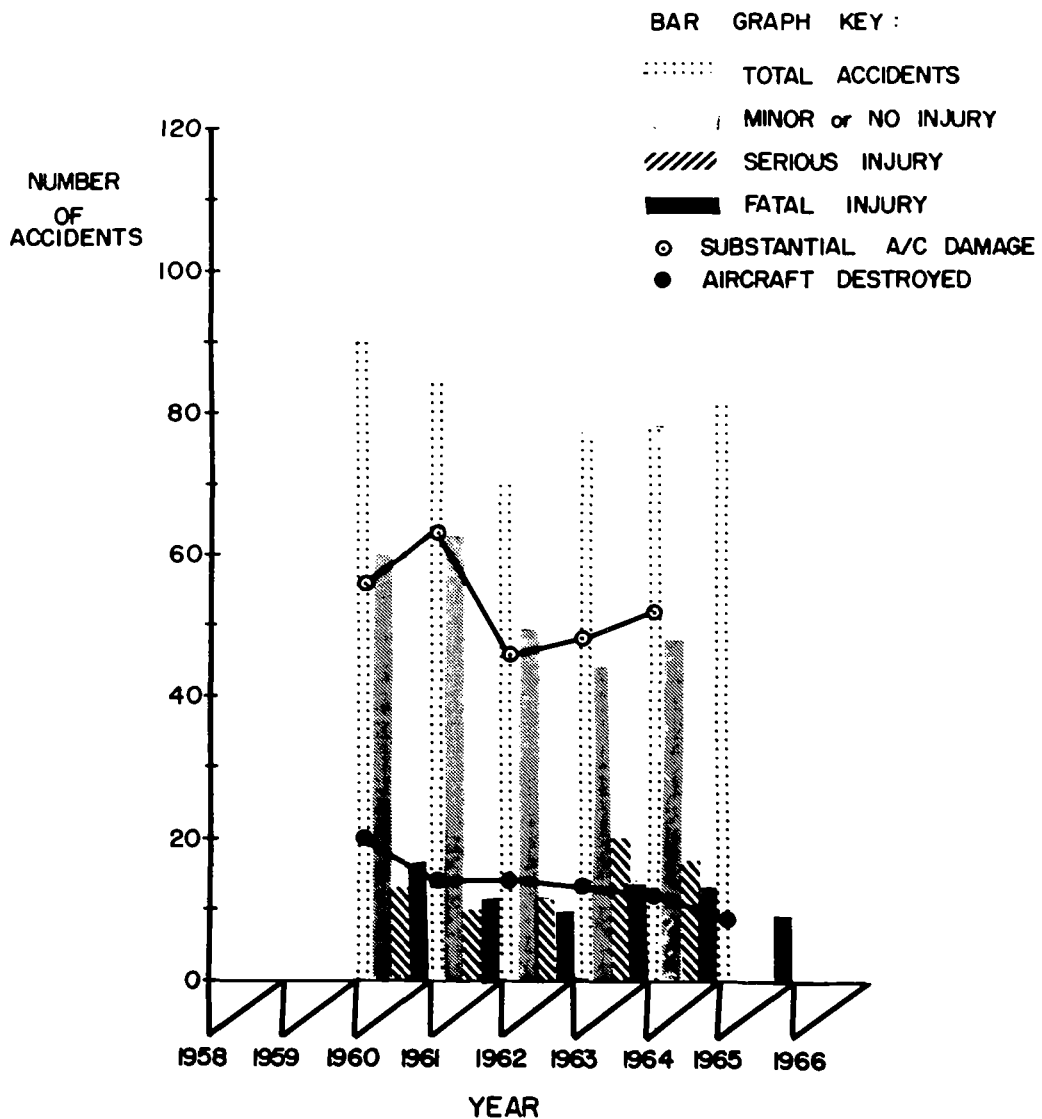


FIGURE 9

CERTIFIED PASSENGER/CARGO
U.S. DOMESTIC & INTERNATIONAL AIR CARRIERS
ACCIDENT RATE DATA

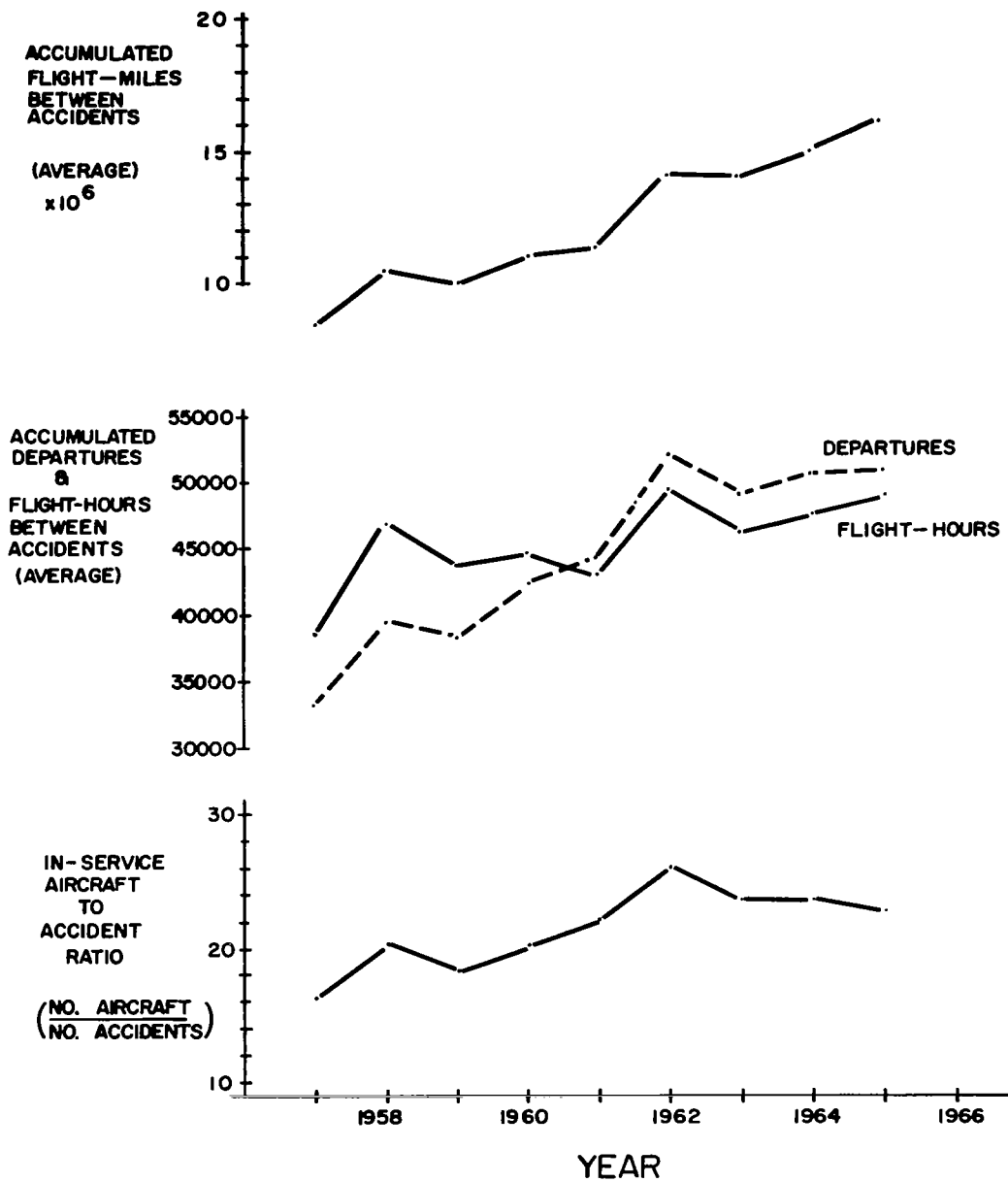


FIGURE 10

U. S. AIR CARRIERS
ALL OPERATIONS
FATALITIES PER FATAL ACCIDENT

1960-1965 INCLUSIVE

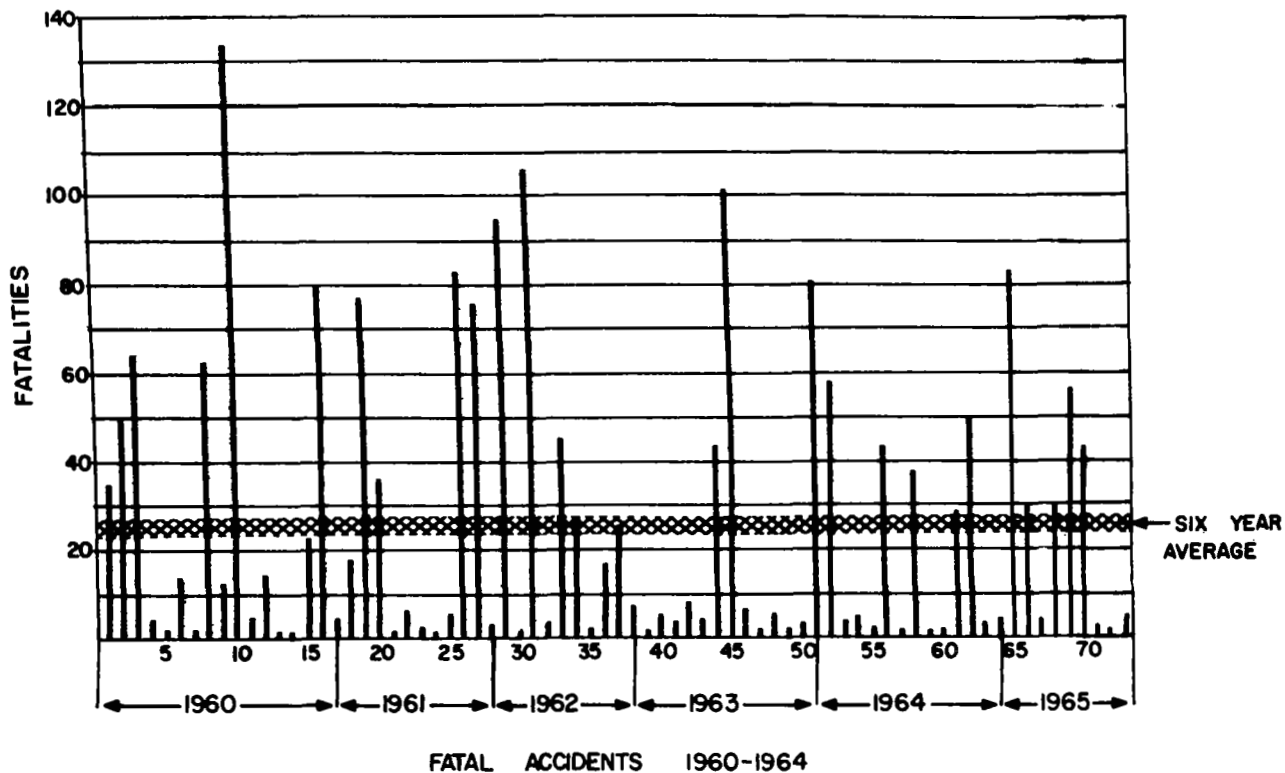


FIGURE 11

U.S. AIR CARRIER ACCIDENTS
1960-1964 INCLUSIVE

402 ACCIDENTS		64 FATAL ACCIDENTS		1642 FATALITIES			
PHASE OF OPERATION	ACCIDENTS PER PHASE	PERCENTAGE OF ALL ACCIDENTS		FATAL ACCIDENTS	FATAL %	ACC. % PER PHASE	FATALITIES
STANDING	2.9%	GROUND	14	3.5	1	7.14	2
TAKE-OFF	4.0	TAXIING	20	4.9	2	10.0	2
TAKE-OFF RUN	4.7						
INITIAL CLIMB	7.6	TAKE-OFF	56	13.9	12	21.4	404
CLIMB TO CR.	3.5						
ENROUTE CRUISE	14.5						
ENROUTE DESCENT FROM CRUISE	6.9	ENROUTE	106	26.4	29	27.36	972
APPROACH	11.8						
LEVEL OFF & TOUCHDOWN	13.8						
GO-AROUND	2.2	LANDING	204	50.8	20	9.8	262
ROLL-OUT	18.1						
TAXIING FROM LANDING	4.0						
OTHER	6.0	UNKNOWN	2	.5	0	0	0
TOTALS			402	100 %	64		1642

FIGURE 12

Transport Aircraft Seating & Restraint System Improvement

The number of transport aircraft emergencies is evident from the statistics of Table 1, Figure 11 and Figure 12. The multi-engine reciprocating and the jet engine aircraft are used primarily by commercial certificated air carriers and often carry over a hundred passengers each. The problem of improving survival in this class of aircraft is quite different from that associated with general aviation,

Passengers on any one transport flight may represent the whole spectrum of the population in age, health, size and occupation. A large number of persons seated in row fashion is also a characteristic of passenger transports that necessitates that the passenger remain seated and be protected in that position until such time that the aircraft has come to a stop and orderly evacuation can begin.

One of the most difficult problems confronting designers for improved protection of occupants is the fact that occupants vary over such a large range. The methods used to improve human survival during transport emergencies must therefore be compatible with all persons. The improvement of passenger seat design and restraint must take the wide variation of occupants into account. The techniques for energy absorption and restraint are thereby complicated.

The skeleton shown in Figure 4 represents the structure of an average adult as he might be seated in a passenger aircraft. The locations and relative masses are also shown for each major body segment. The body mass segment data is derived in part from a study on body segment parameters. Looking at the body as a non-rigid physical structure with mass centers and flexible joints, it is apparent that both upper and lower torso restraint is required to prevent spine bending and head-flailing motions that could cause serious injuries. The rapid motion of the head mass on the neck vertebrae structure and the strain developed by suddenly stopping this mass even without impact is the cause of many neck injuries. Similarly, acceleration forces acting to bend the spinal column impose severe compression and/or tension stresses on the vertebrae disc structure causing slipped disc and other forms of back injury.¹³ Some form of restraint is required to prevent these body displacements, since muscle response and strength alone is inadequate to react to sudden impact forces.

Tests indicate that in some survivable crashes the local dynamic loads may reach 40 to 50 g's for short durations, measured in milliseconds.^{3,6} If the seats are unable to absorb this sudden impulse they will break loose.

The maximum forces developed on seat structure are a result of relative velocity mass accelerations and floor structural deformations. These develop under conditions of aircraft runway overshoot, or impact under adverse attitudes in which the fuselage meets sudden resistance and undergoes structural failure.

The occupant held seated in the aircraft can experience high accelerations if he develops independent velocity changes over a very short distance. Elasticity of the fuselage structure and free unrestrained motions of the occupant allow relative velocity to build up between the seats and various parts of the aircraft. It is in the arresting of these relative internal velocities that such short duration, high g-level forced (40-50 g's) may develop in the seat structure.

There are two practical requirements that must be met for improved occupant protection. One is that the occupant's vital parts must be kept from building up differential velocities in excess of about 30 or 40 feet per second. In addition, these differential velocities must be stopped within a space of about 6-8 inches to prevent excessive acceleration loads on the occupant. Secondly, the body loads must be transferred into the seat by a restraint and cushion support system that does not have significant rebound.

The seat may be thought of as being composed of three basic parts. Those parts are: the legs, which should be energy absorbing in order to transfer large quantities of energy without developing high peak loads; a supporting frame with cushions which would act to protect the occupant; and thirdly, some form of body restraint which is able to maintain the occupant in position regardless of his size or shape.

Seats that are suitable for providing a large amount of energy absorption and occupant protection should be mounted as single units; that is, they should not be structurally tied into pairs and triplets as an integral unit as currently practiced in passenger aircraft. This is not to say that individual energy absorbing seat designs couldn't be grouped in close doublet and triplet type arrangements, but rather that these seats would

have to have the capability of moving independently of one another under impact situations to avoid assymmetrical loading and to accomplish efficient energy absorption.

Features that could be incorporated in advance seat design are shown in Figure 13 entitled "Aircraft Seat Design Improvement for Impact". Some of the features pointed out in that figure are the high back protective head rests, the impact absorbing back structure, high energy dissipation cushions, high-energy dissipation stroking load limiting legs, and a full body restraint system. This may be compared with present seat designs which use rigid leg structures, lap belt restraint only, low energy absorption cushions, soft back structures and no head protection.

The simple technique of using the available seat spacing for stroking energy devices increases seat leg energy dissipation by a factor of about 6 without increasing the basic seat design strength. Using present seat design techniques and increasing the seat design strength to about 25 g's would only increase the energy absorption capabilities of present seats by about $2\frac{1}{2}$ times. By comparison, advanced energy absorption seat design, when increased to 25 g design strength level, would increase the energy absorption capability by a factor of 16. Such improvements are a result of allowing the seat to stroke in a controlled load limiting manner while absorbing energy throughout that stroke.

The ability to take advantage of an increased seat energy absorption capability lies in a full body restraint system that can transfer body loads into the seat in a simple practical manner.

Energy Absorbing Seat Development

One example of a light-weight, high-strength seat which is designed to offer maximum energy absorption is shown in Figure 14. Energy absorption is provided by extensible attenuators in forward and vertical loadings. This seat is designed for impact attenuation for the dynamic load conditions of 20 g-vertical and 20 g forward within a 30 degree arc to either side, as well as for 10 g's laterally. This seat strength is based upon an occupant weight of 225 pounds.

Seat weight is kept to a minimum through the use of aluminum honeycomb construction in all structural panels. Less cushions and mounting tracks, the seat weights approximately 35 pounds.

Integrated Safety Seat

Referring to Figure 3a, it can be seen that a passenger who is restrained only by a seat belt is thrown forward from the waist up. The torso and head swings through an arc such that the head would impact into the front seat or panel objects. The legs also swing such that they would impact similar objects.

Figure 15 illustrates an integrated safety seat concept and one method whereby the body could be restrained from the waist to the head. The restraint method uses a body curtain which is stored on the top of the seat back beneath the upholstery. Ordinarily, the curtain is not used; however, in an emergency it would be a simple matter to reach above the head and pull the curtain down over the body and fasten it to the seat belt. This method of body restraint has the advantage of not interfering with the passenger comfort unless an emergency occurs. The curtain would be sufficiently porous and resilient to permit both breathing and force distribution. In addition to the face curtain, the seat shown in Figure 15 features energy-absorbing leg supports and a high seat back extending above the head level in order to protect the head from flying objects.

Energy absorbing supports are sufficiently rigid to resist normal passenger loads; however, under the much higher forces of a crash, the legs would deform and absorb energy in the process of seat stroking. Further study is required on this type of seating, both from the standpoint of detail structure and from the standpoint of accommodation.

Other features that might be considered in the design of a safety seat to meet passenger requirements include such things as air supply, food trays, ready-to-serve food packages, trash collection units, minor first-aid needs, smoke-heat-vision protective devices, and floatation gear.

Honeycomb Design for Impact Survival

Aluminum honeycomb is an effective mechanical energy absorber and is finding increased use in the control of forces to decelerate objects.¹¹ Materials such as sponge, solid rubber, cork, and paper wadding generally exhibit spring characteristics with an attendant rebound problem.

Aluminum honeycomb has the unique property of failing at a constant load with complete dissipation of energy that would otherwise be released in rebound. The initial peak at which compressive failure begins can be eliminated by pre-crimping the honeycomb core to produce slight initial compressive failure. When exposed to further loading the pre-crimped core proceeds to carry the crushing load at a near linear rate. Such control appears attractive in safeguarding human occupants in aircraft crash conditions.

As an example of aluminum honeycomb's ability to attenuate human impact loads, consider this representative case:

Assuming the impacting mass to be the human head with a weight of about twelve (12) pounds and assuming that the occupant is restrained by a seat belt, the head could be expected to impact a forward surface (instrument panel, seat back, etc.) at a velocity of over 40 ft/sec. Under these conditions, approximately 320 ft-lb of kinetic energy would be dissipated at head impact. Without a yielding material to absorb this energy, death is certain. However, rough calculations indicate that such an impact upon an aluminum honeycomb (3003 aluminum, 3/4 inch cell, and a .004 inch foil gage)¹² section with a thickness somewhat over 3 inches could be tolerated by the human head.

$$\text{Kinetic energy at impact} = E_k = \frac{WV^2}{2g} = \frac{(11.5)(42)^2}{64.4} = 320 \text{ ft.-lb.}$$

$$\text{The rate of deceleration is approximated by : } A = V^2 / 2S_c$$

It appears practical to pad areas of likely body contact in all types of aviation vehicles with honeycomb or similar material to improve survival.

AIRCRAFT SEAT DESIGN IMPROVEMENT FOR IMPACT

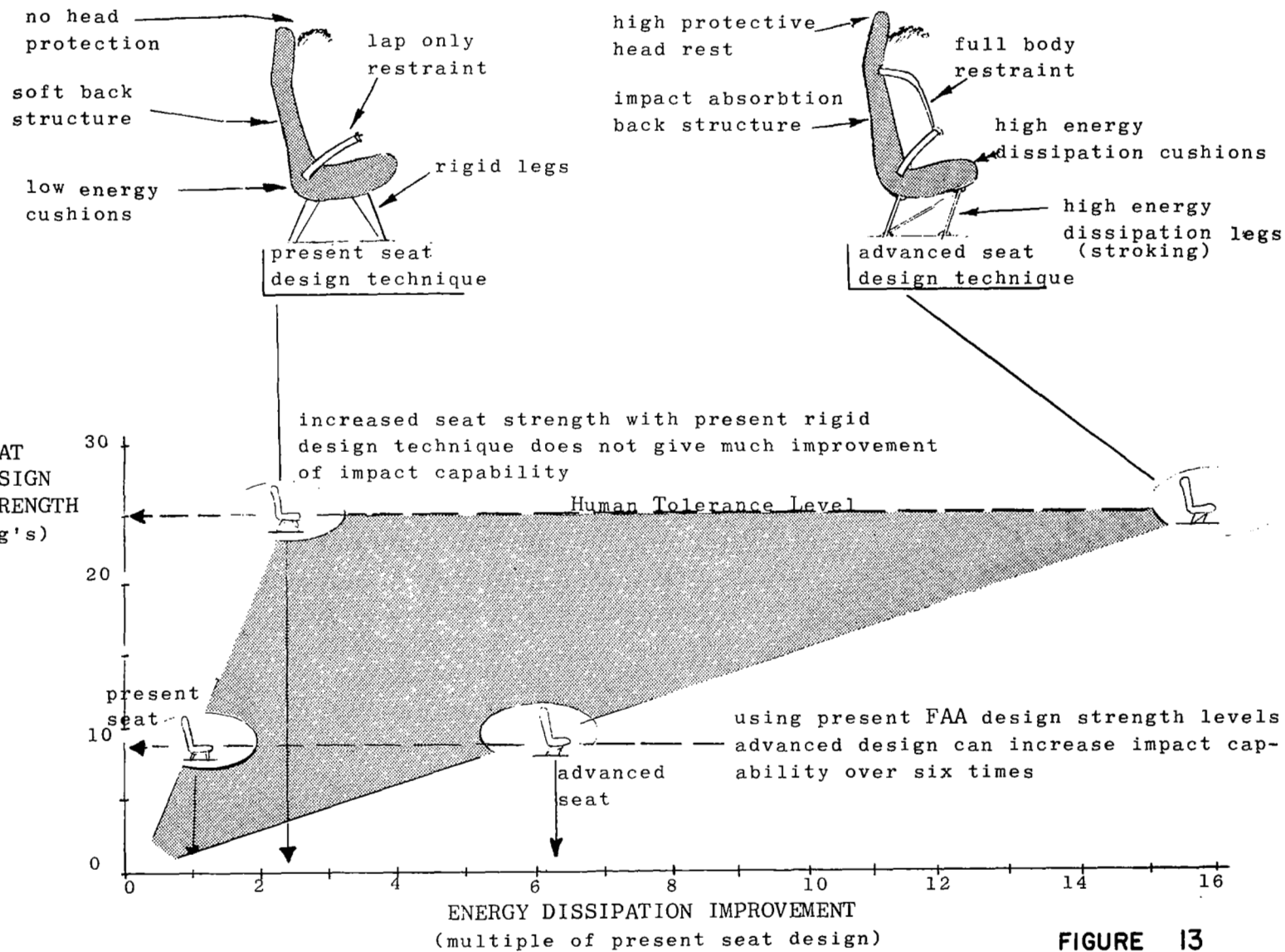


FIGURE 13

20-G ENERGY ABSORBING SEAT

(REF. U.S. NAVY CONTRACT N600 (9) 62456)
NET CUSHION HELICOPTER SEAT
STENCIL AERO ENGINEERING CO.

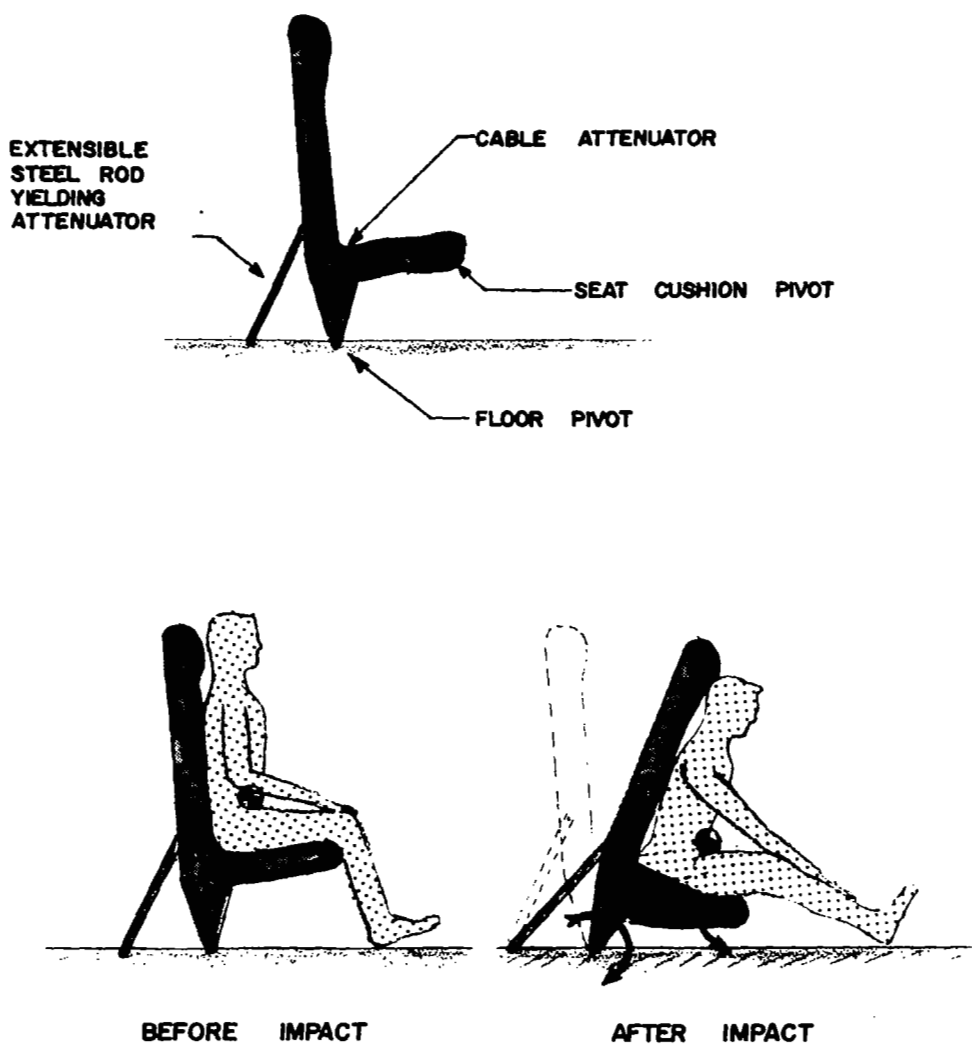


FIGURE 14

INTEGRATED SAFETY SEAT
(ENERGY ABSORBING)

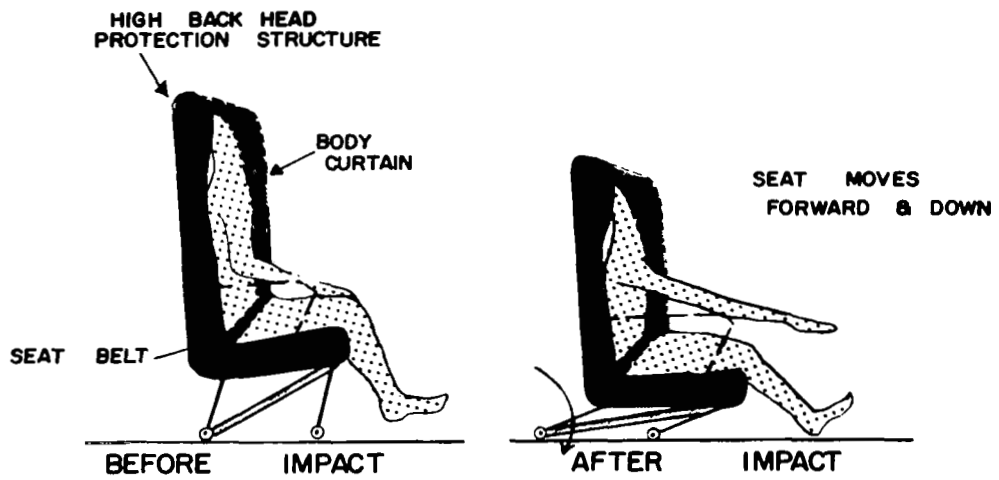
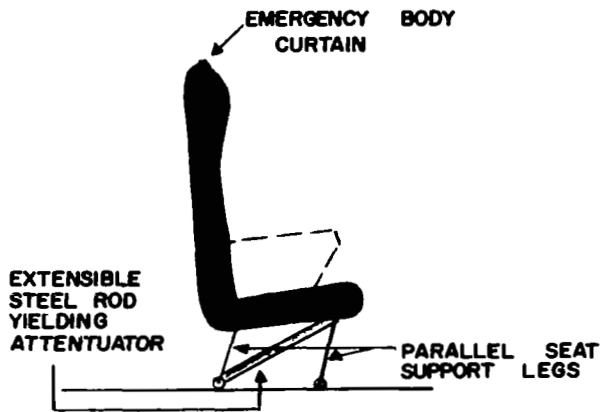


FIGURE 15

GENERAL AVIATION SAFETY IMPROVEMENT

General Aviation Statistics

U.S. General Aviation includes all domestic civil flying other than scheduled and related flying of public airlines. Over the past several years the annual flying time of general aviation has been about four times the flying time of domestic public air carriers.

General aviation flying is categorized by five types: pleasure, business, aerial application, instruction and commercial/miscellaneous.

General aviation pleasure flying accounted for about 25% of the total flying hours and for one-half of the pilot fatalities in the 1962-63 period.

The second highest accident mortality rate is experienced in commercial air taxi service, fire control activities, and miscellaneous flying. While the time spent in commercial flying is nearly the same (25%) as in pleasure flying, the actual number of deaths was only about one-third that of pleasure flying.

Business flying has experienced a somewhat better accident record than commercial flying. Business flying utilizes aircraft to transport executives, sales personnel, etc., and accounts for roughly two-fifths of the total flying time in general aviation. In 1962-63 the fatality rate for business flying was 3.5 per 100,000 plane hours, or about 40 percent lower than for general aviation as a whole.

The instructional flying category consists of flight training of civilians under accredited instructor supervision. One-sixth of the total flying time was accounted for by instructional flying in 1962-63. However, this type of flying was responsible for only one-twentieth of all fatalities.

General aviation data presented in this section are for all flying categories and for all types of aircraft and includes over 90,000 aircraft of all types. This is twice the number of only ten years ago and the rapid growth continues. Figure 16 graphically portrays this rapid growth.

Annually, out of the general aviation aircraft, about one in 18 can be expected to have an accident of some type; one aircraft in 25 can be expected to receive substantial damage; one aircraft in 90 can be expected to be destroyed; and about one aircraft in 180 can be expected to include fatalities. The record of general aviation (Figure 16) shows that an accident occurs for every 4000 hours of accumulated flying time while the commercial air carrier record averages 50,000 flying hours between accidents.

Figure 17 shows the number of accidents currently at 5000 per year, of which 500 are fatal, and 1000 aircraft are destroyed. The actual number of fatalities has increased to over 1000 per year in apparent proportion with the increased number of aircraft. The rapid upward trend is shown in Figure 18.

A breakdown of general aviation accidents by phase of operation for year 1963 is shown in Figure 19. It is readily apparent that the largest single percentage of accidents occur during landing; however, only a small number of these end with fatalities. Most of the fatalities occur during normal cruise, or other in-flight conditions associated with bad weather, malfunction of systems, pilot error or unexpected collision.

GENERAL AVIATION - ALL TYPES AIRCRAFT

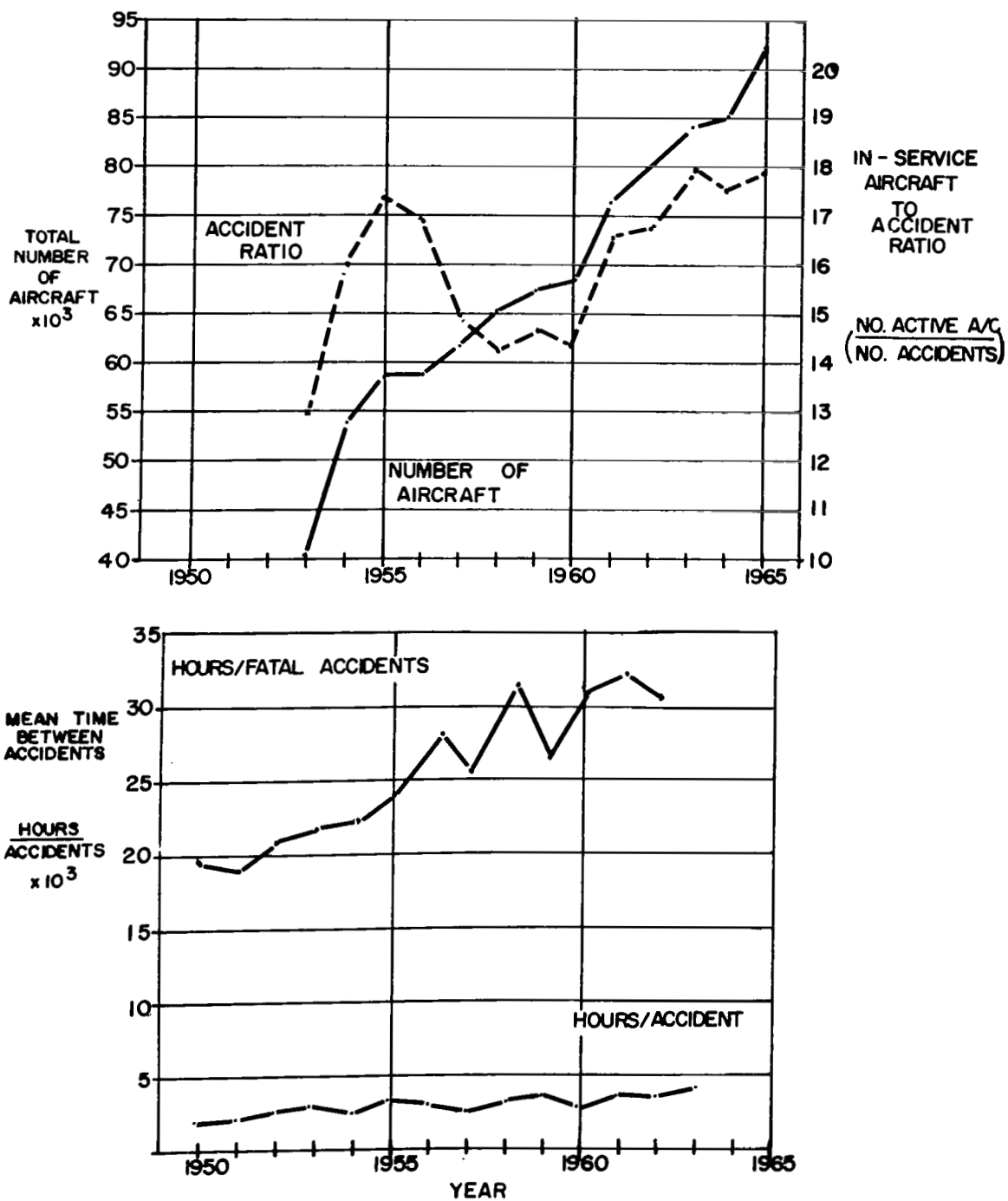


FIGURE 16

GENERAL AVIATION

ALL OPERATIONS - NUMBER OF ACCIDENTS

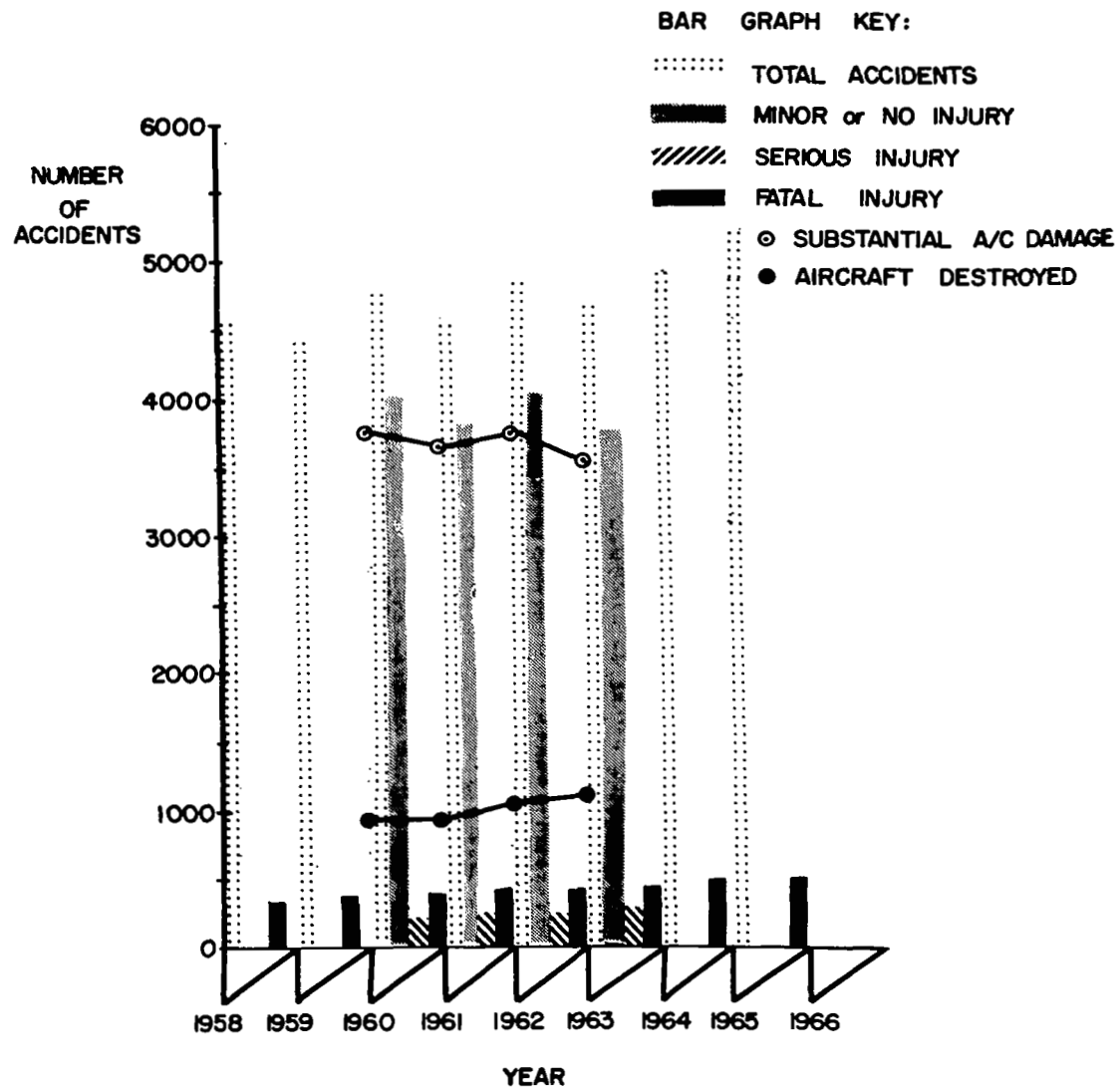


FIGURE 17

GENERAL AVIATION
ACCIDENT STATISTICS

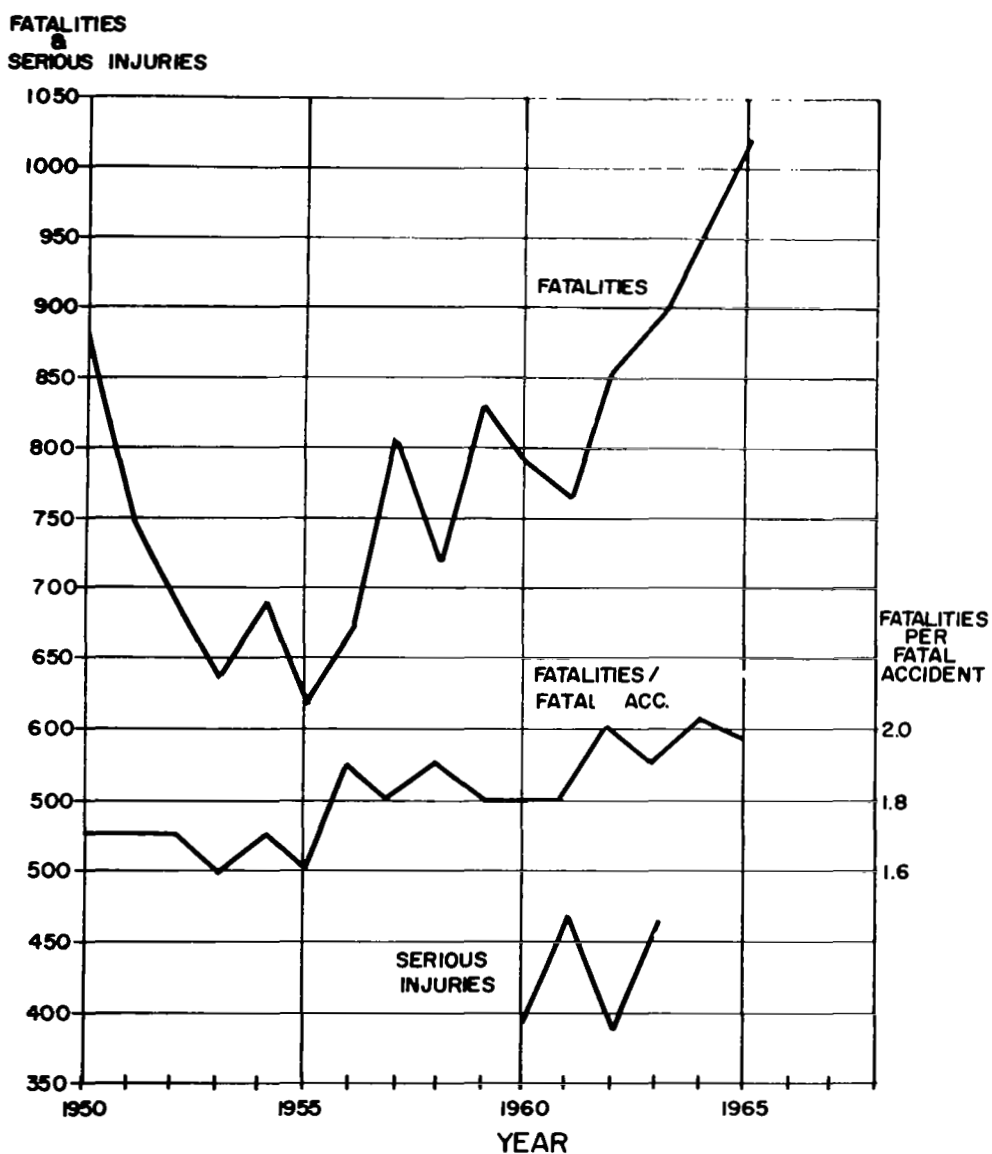


FIGURE 18

GENERAL AVIATION-ALL OPERATIONS
(63300 ACTIVE AIRCRAFT)

TYPICAL DISTRIBUTION OF ACCIDENTS BY PHASE-YEAR 1963

4690 ACCIDENTS - 462 FATAL - 295 WITH SERIOUS INJURY - 3913 WITH MINOR INJURY

1097 AIRCRAFT DESTROYED - 3550 AIRCRAFT SUBSTANTIALLY DAMAGED - 43 MINOR DAMAGE

893 FATALITIES - 462 SERIOUS INJURIES - 7336 MINOR INJURIES

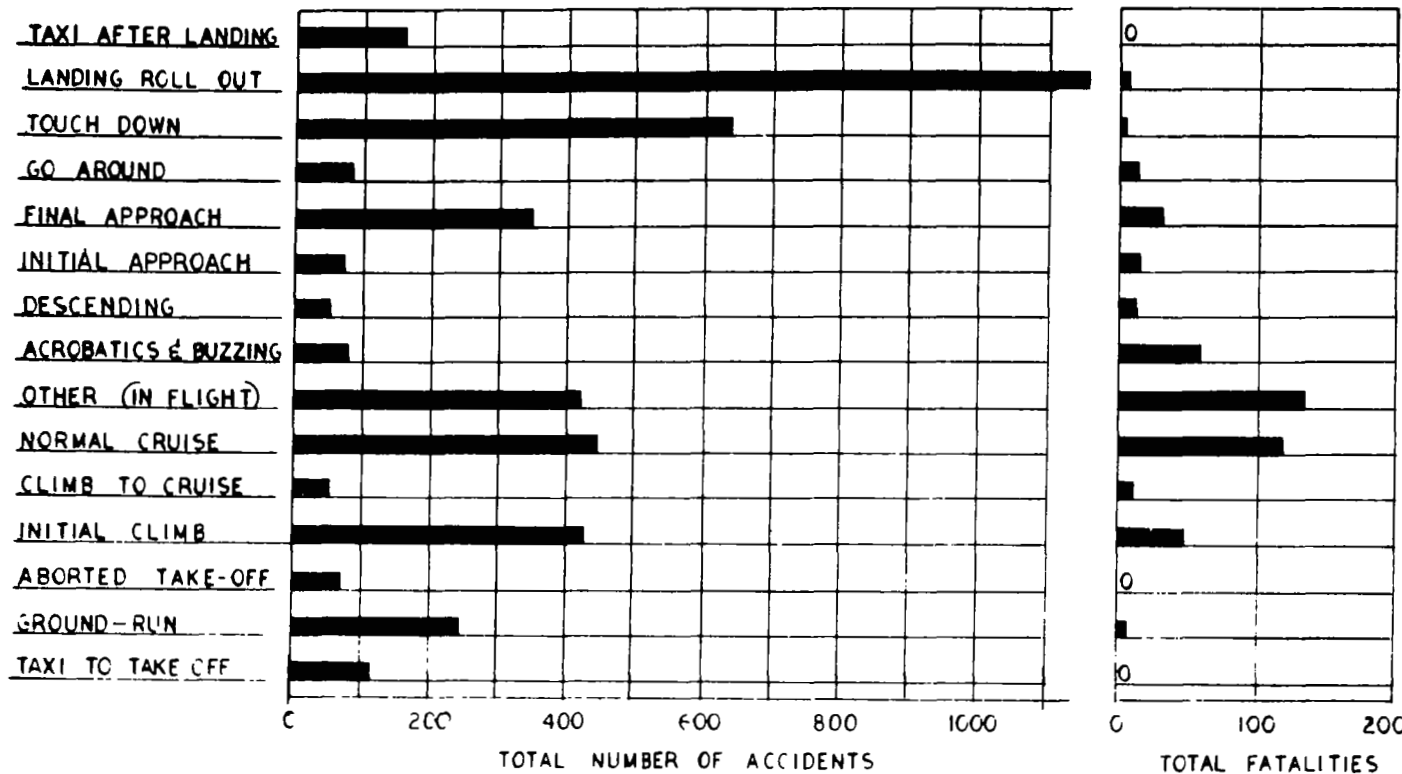


FIGURE 19

INTERNAL IMPROVEMENTS

Seat Attachment

Manufacturers of general aviation aircraft are obliged to observe the requirements of Federal Air Regulations Part 23, Airworthiness Standards: Normal, Utility, and Acrobatic Category Airplanes. Under the design requirements specified herein the seat structure with an occupant restrained by belt or harness should be capable of ultimate forces as follows:

Upward	3.0 g	(4.5 g Acrobatic Category)
Forward	9.0 g	
Sideward	1.5 g	

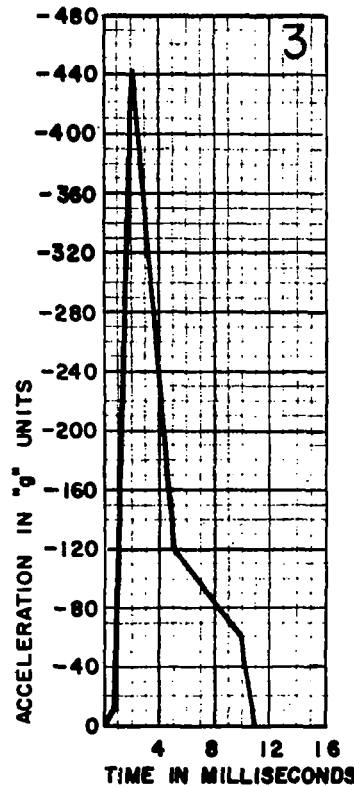
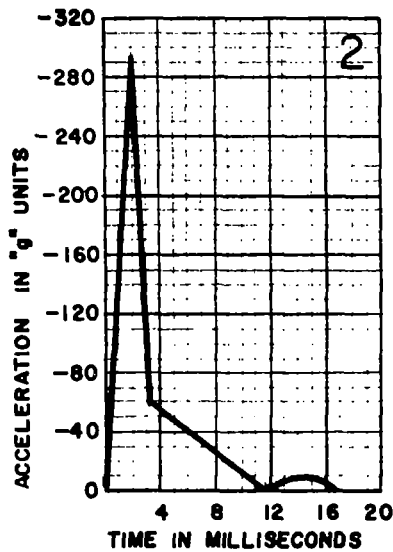
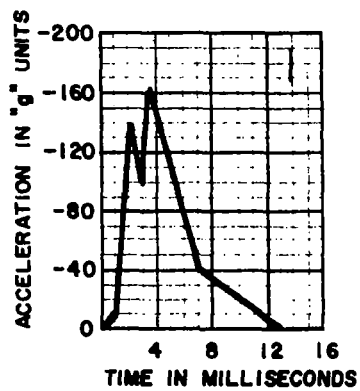
These force limits apply to minor crash conditions and provide a reasonable chance of escaping serious injury, but under certain conditions much higher peak g's may be experienced. Seats may break loose under this loading and point out the need for an energy absorbing seat attachment.

The need for full body restraint is apparent from Figure 3 and from Figure 20, which shows g-force curves obtained from catapulting an instrumented dummy head against a typical unprotected light aircraft instrument panel. As noted, the lowest impact velocity produced a peak g value of over 160 g. The rigid panel did not deform so the head impacted the panel over a very small area. The forehead is the strongest part of the face, but it cannot withstand a force of 80 g's on one square inch of area without fracture. Therefore, all injuries depicted in Figure 20 would cause fatal head injuries.

HEAD IMPACT ACCELERATIONS

G-FORCE CURVES OBTAINED WITH HEAD IMPACTS ON A TYPICAL LIGHT-AIRCRAFT INSTRUMENT PANEL AT VELOCITIES OF (1) 17.6 FT/SEC., (2) 26.7 FT/ SEC., AND (3) 42.2 FT / SEC.

T4



REF. AM 66-12

FIGURE 20

HUMAN TOLERANCES

This section presents a number of graphical data related to human tolerances for acceleration, impact, temperature, and decompression. These data were gathered from the NASA SP-3006 "Bioastronautics Data Book" and FAA reports AM 66-12, and AM 66-18 written by J. J. Swearingen, of the Civil Aeromedical Research Institute. These particular graphs have been selected because of their direct relationship to aircraft accident survival.

The graphs in this section are provided mainly as supplementary survival criteria data.

Figure A-8 shows the relationship of maximum acceleration and onset rate for stopping distances from 4 to 8 inches from a 30 ft/sec. impact velocity.¹¹ The most efficient use of stopping distance is produced by an infinite onset rate. This is represented by the minimum g, infinite onset point of each curve. A triangular time history is represented by the maximum g end point of each curve. The points between these two extremes represent trapezoidal time histories with specific onset rates and a finite crushing time at constant g. For protection of humans, the areas of high g and low onset rate are of interest. Superimposed on this figure are the approximate acceleration tolerances¹⁰ for humans with acceleration duration time labeled for each data point.

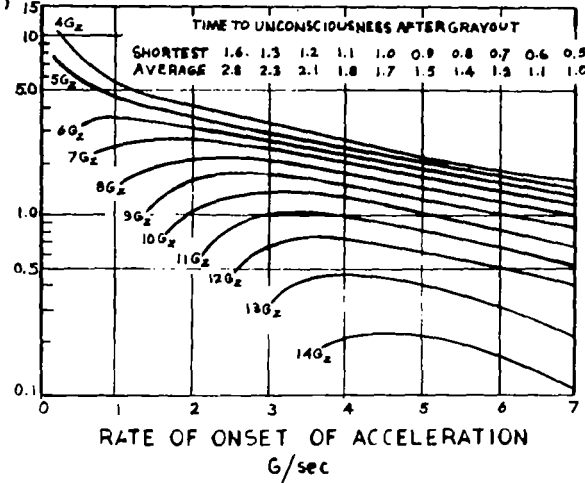
For impact durations of less than 0.07 seconds, it is assumed that the body acts as a rigid mass with no fluid shifts occurring.¹¹ Thompson assumed that structural limits for body tissue are in excess of 200 g, and constructed the tolerance curve of Figure A-9. The magnitude of peak g may range up to 45 g for impacts of greater than 0.07 second duration, hence there is infinite slope for the tolerance curve in this area. For impacts of less duration time, up to about 200 g, the tolerance limit is represented by the criteria that $2V = 100$ ($V = 50$ fps) and for this area the tolerance curve is horizontal. The validity of this concept is indicated by the data points on Figure A-9.

Based on these test results, and shown in Figure A-10, A.B. Thompson states that the ultimate human limits to entire body impact is somewhere in the range of 45 and 55 psi impact force. The physiological shock yield point lies somewhere between 28 and 32 psi for transverse accelerations.

ACCELERATION TOLERANCE

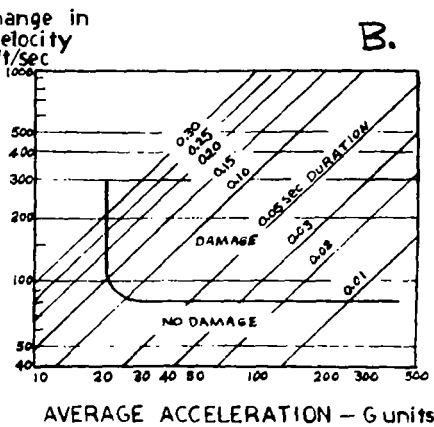
REF. NASA SP-3006

Time
to
grayout
(sec)



A.

change in
velocity
ft/sec

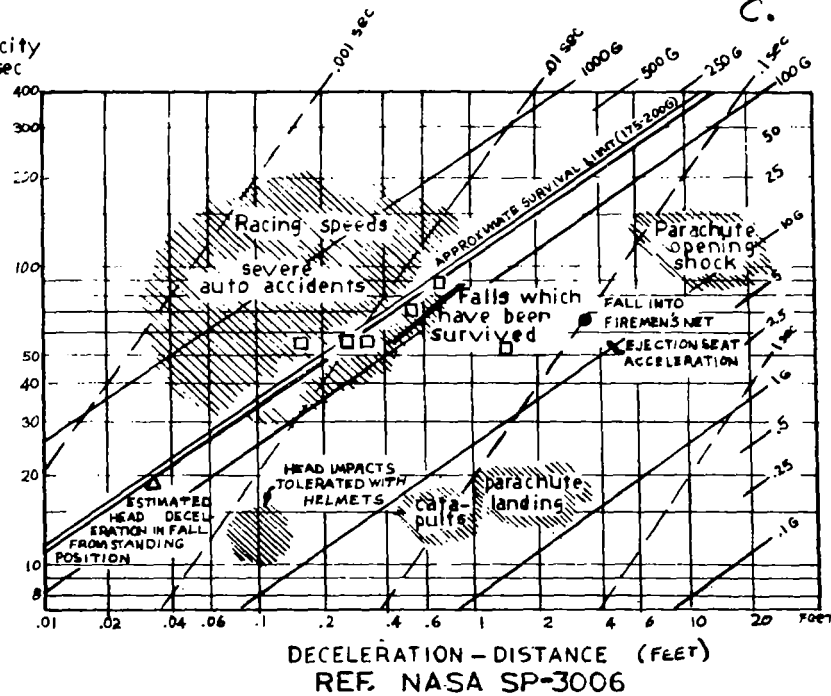


B.

RATE OF ONSET OF ACCELERATION
G/sec

AVERAGE ACCELERATION - G units

velocity
ft/sec

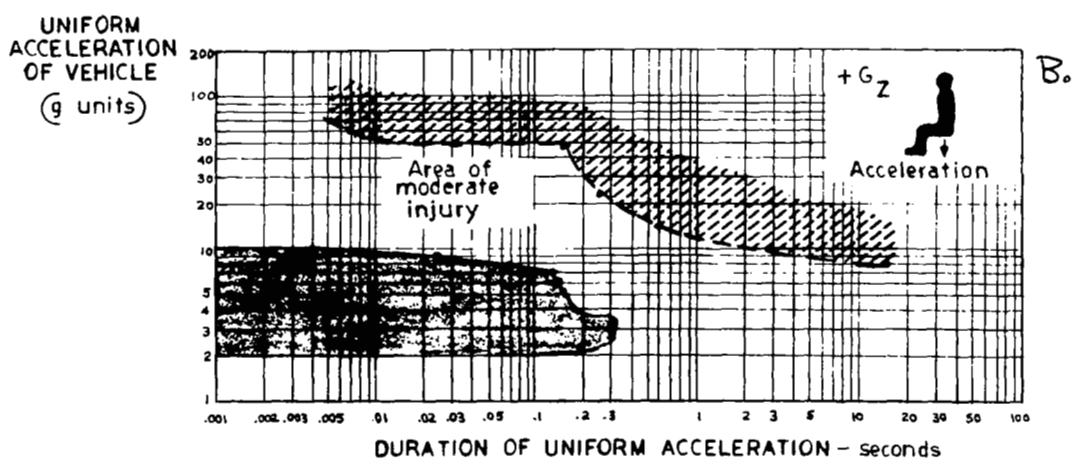
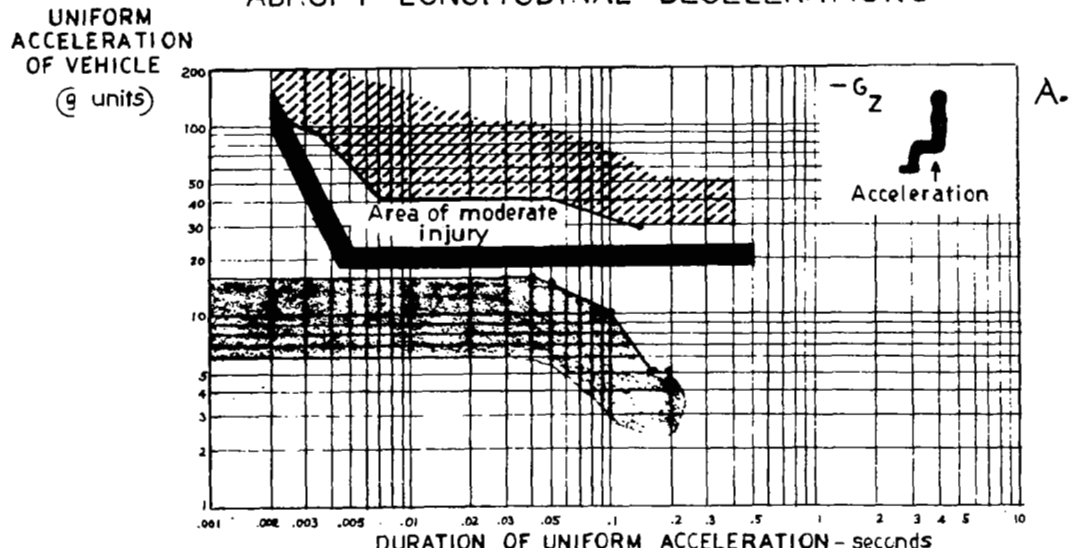


C.

DECELERATION - DISTANCE (FEET)
REF. NASA SP-3006

FIGURE A-1

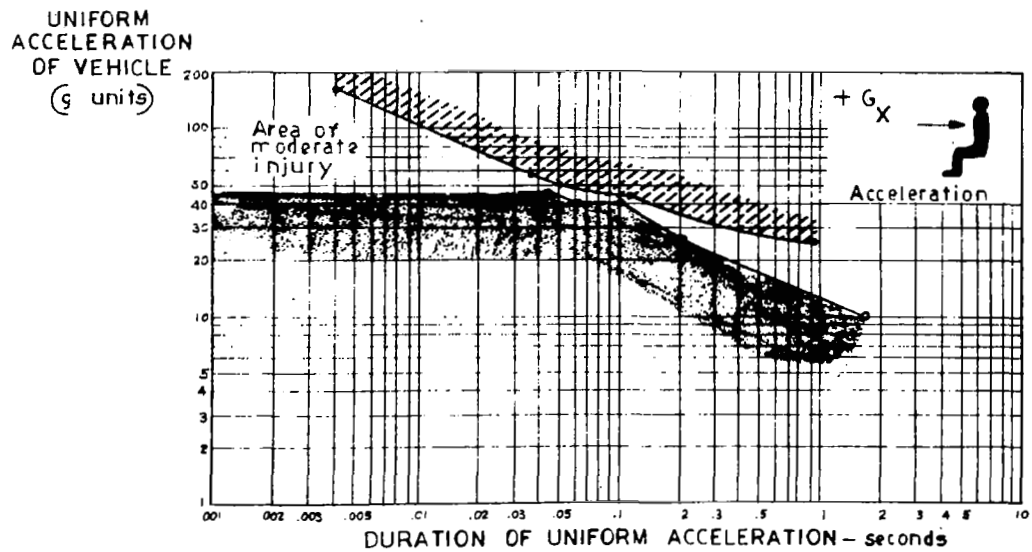
ABRUPT LONGITUDINAL DECELERATIONS



REF. NASA SP-3006

FIGURE A-2

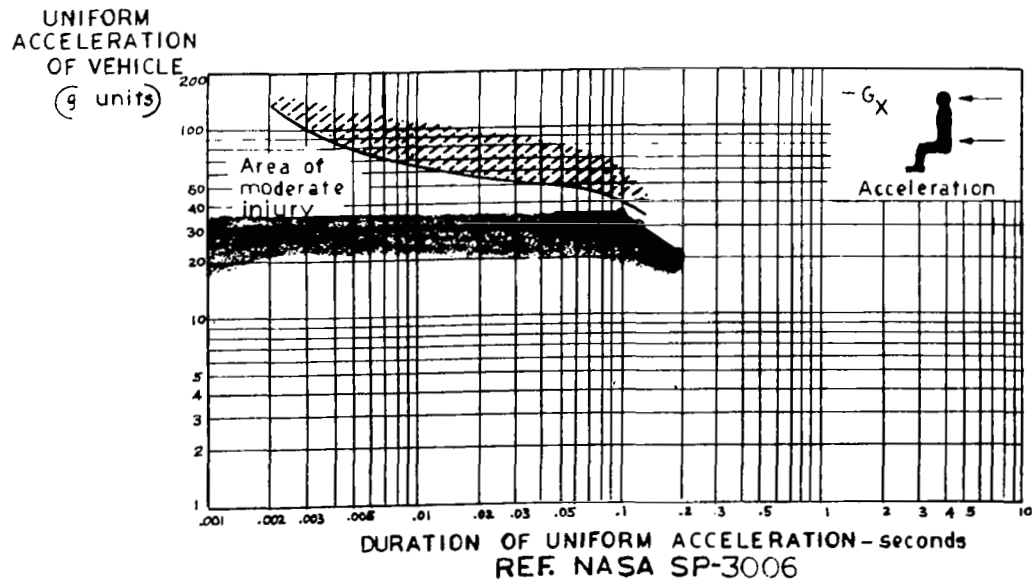
ABRUPT TRANSVERSE DECELERATIONS



A.

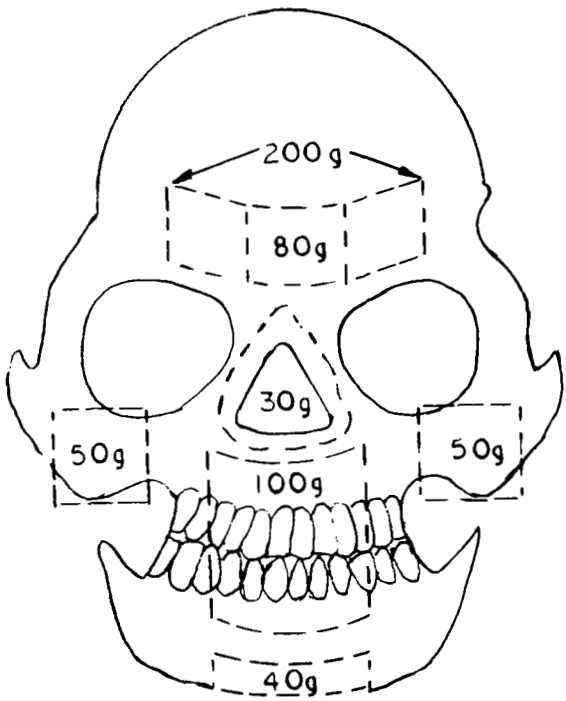
||||| SEVERE INJURY

— AREA OF UNINJURED



B.

FIGURE A-3



SUMMARY OF MAXIMUM TOLERABLE IMPACT FORCES ON A PADDED DEFORMABLE SURFACE

Ref. J. J. Swearingen AM-66-16
CIVIL AEROMEDICAL RESEARCH INSTITUTE
Office of Aviation Medicine
Federal Aviation Agency

FIGURE A-4

HUMAN TOLERANCE TO TEMPERATURE

REF. NASA SP-3006

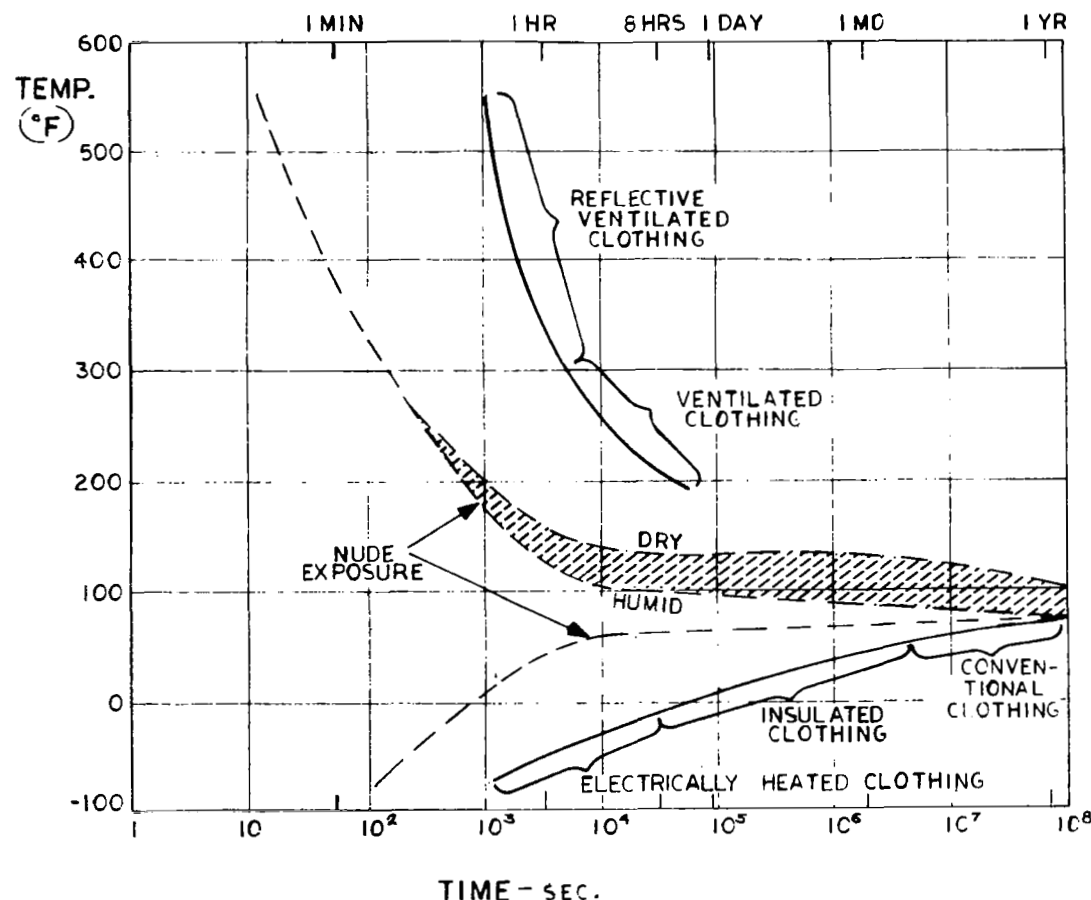
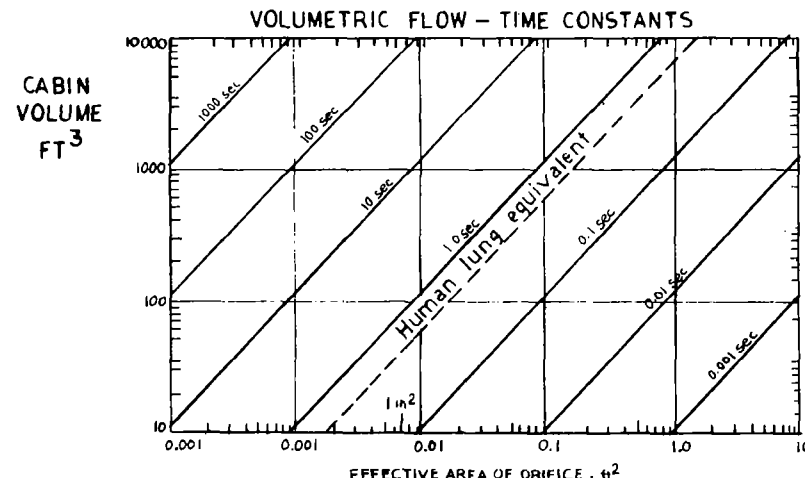
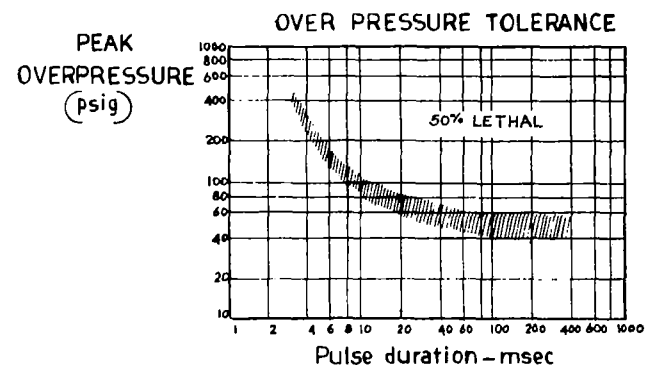
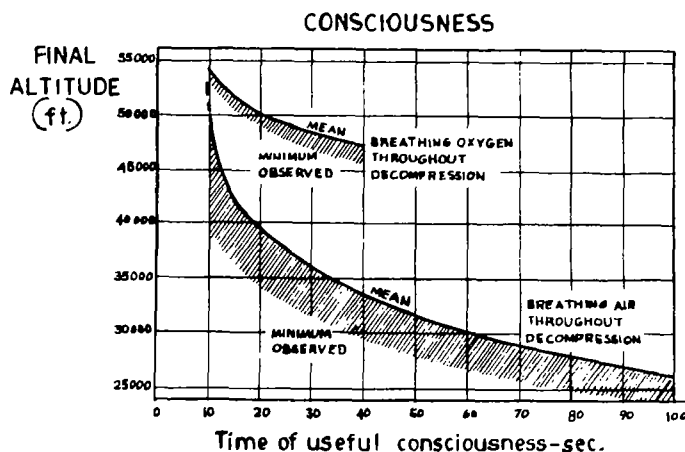


FIGURE A-5

DECOMPRESSION DATA



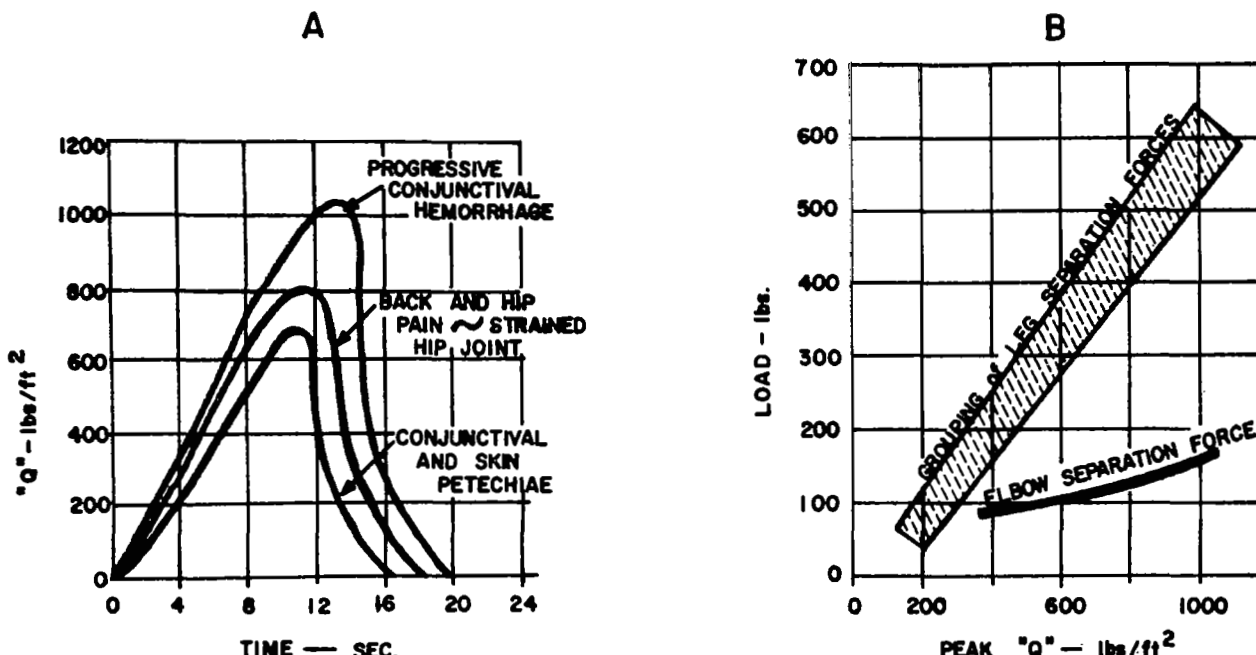
84



REF. NASA SP-3006

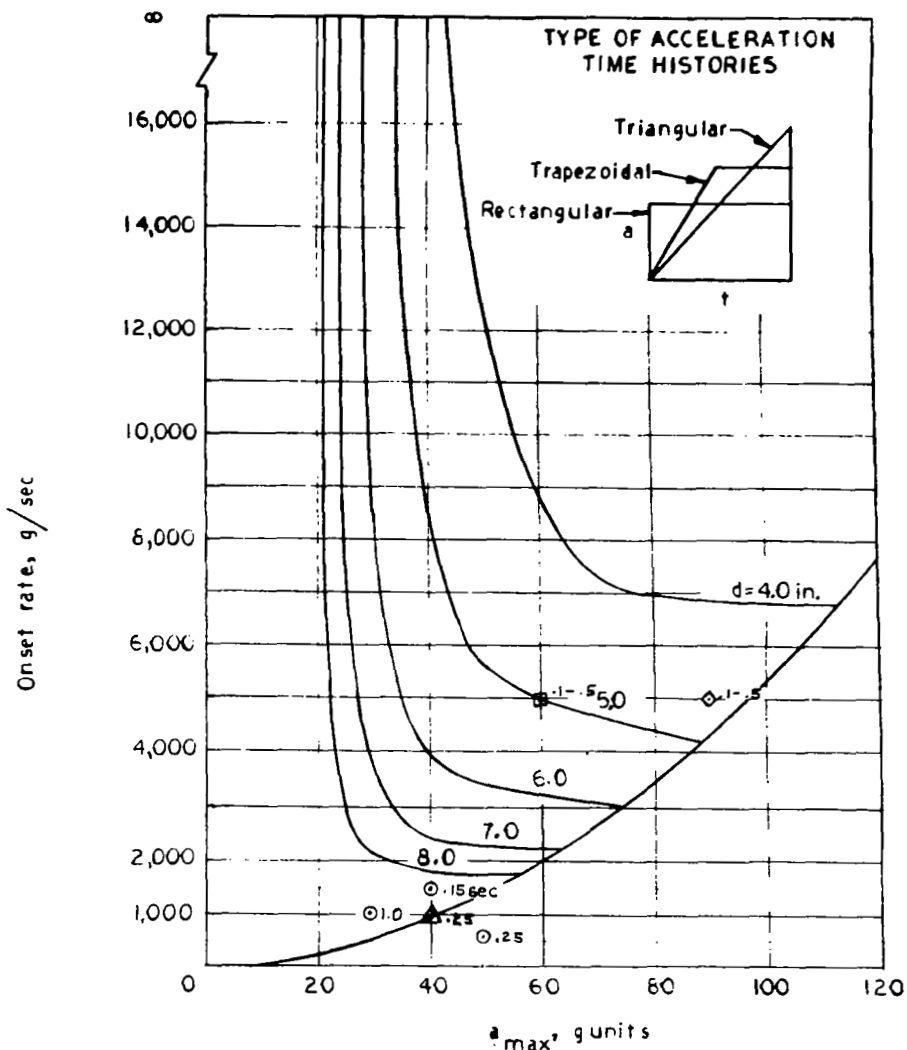
FIGURE A-6

MECHANICAL EFFECTS OF HIGH DYNAMIC PRESSURES



REF. NASA SP-3006

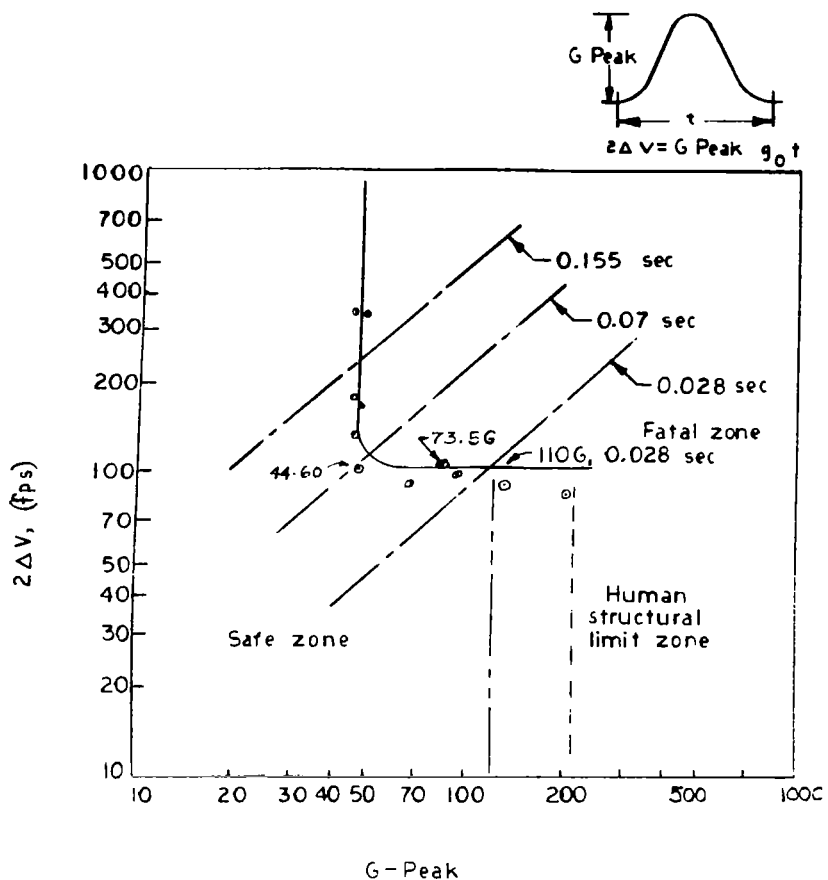
FIGURE A-7



Variation of maximum acceleration and onset rate for constant values of stopping distance for an impact velocity of 30 ft/sec.

REF. NASA TECH. NOTE D-158

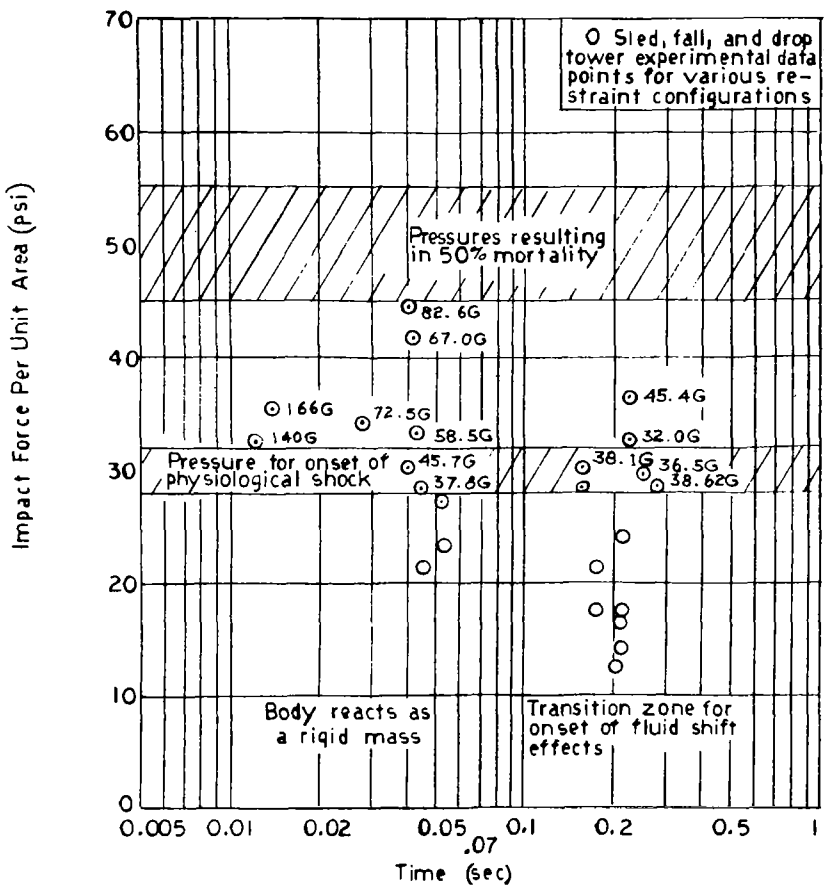
FIGURE A-8



-Human Transverse Impact Tolerance,
 $2\Delta V$ Versus Peak G

REF. ASD-TDR-63-173

FIGURE A-9



Human Transverse Impact Tolerance as
Defined by Unit Impact Pressure and Time

REF. ASD-TDR-63-173

FIGURE A-10

REFERENCES

1. "Safety Considerations for Passengers and Crew" By: James E. Dougherty and Richard B. Stophlet, Federal Aviation Agency, Washington, D.C.; AIAA Third Annual Meeting; Boston, Massachusetts, November 1966; AIAA Paper Number 66-844
2. Civil Aeromedical Research Institute, Oklahoma City, Oklahoma Federal Aviation Agency, Office of Aviation Medicine
 - 2.1 Swearingen, John J.
"Tolerances of the Human Face to Crash Impact"
AM 65-20, July 1965
 - 2.2 Mohler, S.R. And Swearingen, J.J.
"Cockpit Design for Impact Survival"
AM 66-3, February 1966
 - 2.3 Swearingen, J.J., Hasbrook, A.H., Snyder, R.G.
"Kinematic Behavior of the Human Body During Deceleration"
AM 62-13, June 1962
 - 2.4 Swearingen, J.J.
"Injury Potentials of Light Aircraft Instrument Panels"
AM 66-12, April 1966
 - 2.5 DeHaven, H.
"The Site, Frequency and Dangerousness of Injury Sustained by 800 Survivors of Light Plane Accidents"
Department of Public Health and Preventative Medicine,
Cornell University, Medical College, July 1952
3. Flight Safety Foundation, Inc., Phoenix, Arizona
 - 3.1 "Full Scale Dynamic Crash Test of a Lockheed Constellation Model 1649 Aircraft" - Technical Report
RPT. FAA-ADS-38 October 1965
By: Flight Safety Foundation
Contract No. FA-WA-4569
FAA Aircraft Development Service
 - 3.2 "Full Scale Dynamic Crash Test of a Douglas DC-7 Aircraft"
Technical Report
RPT. FAA-ADS-37 April 1965

References - Continued:

3. 3.3 Tecom Technical Report 66-77, January 1964
Experimental Research
"CH-21A Helicopter Airframe Deformation Under a
Dynamic Crash Condition"
U.S. Army
Transportation Research Command
Ft. Eustis, Virginia
- By: Flight Safety Foundation; W.H. Reed, D. F.
Carroll; Contract DA 44-177-AMC-888(T)
J.L. Reed, Project Engineer
Lt. Col. T. C. Woodbury Johnson, Group Leader
Larry M. Hewin, Technical Director
- 3.4 "Floor Accelerations and Passenger Injuries in Transport Aircraft Accidents" AV-Ser 66-19; Haley, Turnbow and Walhout. USAAVLABS TR67-16.
- 3.5 "Aircraft Passenger-Seat-System Response to Impulsive Loads" AV-Ser 66-20; Turnbow, Collins, Cromock & Myklestal, USAAVLABS TR 67-17.
- 3.6 "Crash Survival Design Guide" AV-Ser USAAVLABS TR-67-22, Turnbow, et.al.
- 3.7 "Body Segment Parameters"
New York University
School of Engineering & Science
TR #1166.03, by Drillis & Contini
4. Consolidated Notes on Aircraft Safety, J.J. Carroll;
(unpublished) FAA Headquarters, Washington, D. C.
5. "Bioastronautics Data Book", NASA SP-3006
6. Seribner, Kimball J., Captain, Pan American Airways
"Emergency Barriers for Transport Aircraft"
Space and Flight Equipment Association Third National
Flight Safety Survival and Personnel Equipment Symposium,
October 1965
7. Design of Passenger "Tie-Down", Sept. 1965, CSDM #1,
AV-SER-44-0-66, A. Howard Hasbrook, Aviation Crash
Injury Research of Cornell University
8. "Janes, All the Worlds Aircraft, 1966-67", McGraw-Hill.

9. CAB Accident Investigation Report taken from Aviation Week and Space Technology, September 6, 1966, p. 113.
10. "Investigation of Crew Escape System Surface Impact Techniques for Advanced Aerospace Vehicles" ASD-TDR-63-173.
11. "Limited Investigation of Crushable Structures for Acceleration Protection of Occupants of Vehicles at Low Impact Speeds" NASA Technical Note D-158, October 1959
12. "Energy Absorption Properties of Aluminum Honeycomb", Hexcel Products, Inc., TSB-110, January 1, 1960.
13. "Phase IV - Investigation of Strength of Isolated Vertebrae" October 1966, Technology Inc. TI 1313-66-4 NASw-1313 L.S. Higgins, J.F. Crocker

See discussions, stats, and author profiles for this publication at: <https://www.researchgate.net/publication/336318314>

Mathematical modeling of polyurethane foam elasticity measuring process

Conference Paper · October 2019

CITATIONS

0

READS

188

4 authors:



Amna Bajtarevic-Jelec

University of Zenica

13 PUBLICATIONS 2 CITATIONS

[SEE PROFILE](#)



Sabahudin Ekinovic

University of Zenica

64 PUBLICATIONS 296 CITATIONS

[SEE PROFILE](#)



Fuad Hadžikadunić

University of Zenica

56 PUBLICATIONS 28 CITATIONS

[SEE PROFILE](#)



Amra Talić - Čikmiš

University of Zenica

10 PUBLICATIONS 6 CITATIONS

[SEE PROFILE](#)

Some of the authors of this publication are also working on these related projects:



Co-processing of municipal waste as alternative fuel in the cement industry [View project](#)



Bending Stresses in Layers of Wood with Numerical Verification [View project](#)

Mathematical modeling of polyurethane foam elasticity measuring process

Amna BAJTAREVIĆ¹⁾

Sabahudin EKINOVIĆ¹⁾

Fuad HADŽIKADUNIĆ¹⁾

Amra TALIĆ-ČIKMIS¹⁾

1) Faculty of Mechanical Engineering
University of Zenica, Fakultetska 1,

Bosnia and Herzegovina

amna.bajtarevic@mf.unze.ba

sekinovic@mf.unze.ba

hfud@mf.unze.ba

acikmis@mf.unze.ba

Original scientific paper

Abstract: Nowadays, production of upholstered furniture and similar products could not be possible without material which is called polyurethane foam. According to main application of this material, elasticity is one of the most important characteristic. The focus of this paper is based on polyurethane foam elasticity measuring by testing of steel ball elastic rebound. In order to determining steel ball elastic rebound dependency from change of foam hardness and ball diameter, regression analysis is performed.

Keywords

polyurethane foam

elasticity

elastic rebound

regression analysis

1. Introduction

Polymer materials are the most used materials for production of furniture, besides wood, glass and metal. Specific polymer material which is called polyurethane foam (hereafter: PU foam), is made by chemical reaction of two main substances polyol and isocyanate with additives [1]. Production of upholstered furniture and sleep products is not possible without this material. According to the main use, important characteristics of PU foam are: density, hardness, elongation, plasticity and elasticity. The last above mentioned characteristic is considered as the most important because it determines quality and competitiveness of final product. Very common method of PU foam elasticity analysis is measurement of steel ball elastic rebound that is defined by standard ISO 8307. Method is based on free fall of ball from defined high and rebound high measure.

In the domain of stochastic modeling, method of mathematical modeling of polynomial is used for determining of functional dependence between dependent magnitude (y) and independent magnitudes (x_i). Accordingly, dependence is defined by regression model in the form of $y=f(x_i)$ [2]. In this paper, method of mathematical modeling of polynomial is conducted to defining dependence of elastic ball rebound (y) from ball diameter (x_1) and foam hardness (x_2). Mathematical principle of this dependency is not known in advance.

2. The main characteristics of measurement subject and process

2.1. Term of polyurethane foam

Two main raw materials for production of PU foam are petroleum products: polyol and toluene diisocyanate, e.g. "TDI". Additional substances are activators: Sn-octoate, Sn-isooctoate, stabilizers and others [3]. In short, process of PU foam production is started with dosage main raw materials via dispensing pumps with additives to the "head for mixing" of machine that working on principle of mixer. After process of mixing, homogenous mixed raw materials flow to the special container where chemical reactions are happened. From that container material is started to foam and flow through canal, so in place of special bath, block of PU foam is formed. Produced blocks are stored in storage shed for ripening process that lasts 48 hours. Matured blocks can be stored or processed on machines for PU foam cutting.

The main characteristics of PU foam are defined by proportion of main raw materials and additives. Types of PU foam are distinguished by characteristics of density and hardness. Four main parameters of PU foam such as type of foam, level of hardness, value of density and value of hardness are shown in standard mark of this material, as it is shown in figure 1.

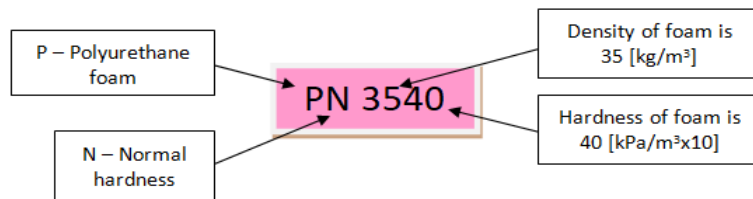


Figure 1. Marking of PU foams

2.2. Analysis of PU foam elasticity

Polyurethane foams are high-elastic materials therefore their main application is material for production of upholstered furniture and systems for sleep (mattresses, toppers and etc.). Elasticity testing methods for foams are very similar such as methods for steel. Specimen of foam is exposed tension force until fracture. Length of elongation before fracture is measured magnitude. However, foam is very nonplastic material, so after fracture, parts of specimen are returned to the original form and dimension [3]. On the other hand, for above mentioned application of foams, it is very important to analyze characteristic of elastic rebound for PU foams.

Clearly, this property is crucial for quality of final product in which main material is PU foam.

Elasticity analysis of polymer materials by measuring of elastic rebound is defined by standard ISO 8307 [4]. Equipment for this measuring consists of vertical, transparent tube with defined scale and diameter from 30 till 65 mm, steel ball and other devices for automatic reading of rebound. Diameter of steel ball should be 16 ± 5 mm while mass should be in tolerance of 16.8 ± 1.5 g. Measuring is performed by releasing of steel ball from 500 ± 5 mm height. Fault of measuring could be happened if steel ball make contact with internal surface of tube. In that case, measuring would be invalid.

In figure 2, sketch of equipment for elastic rebound measuring is shown.

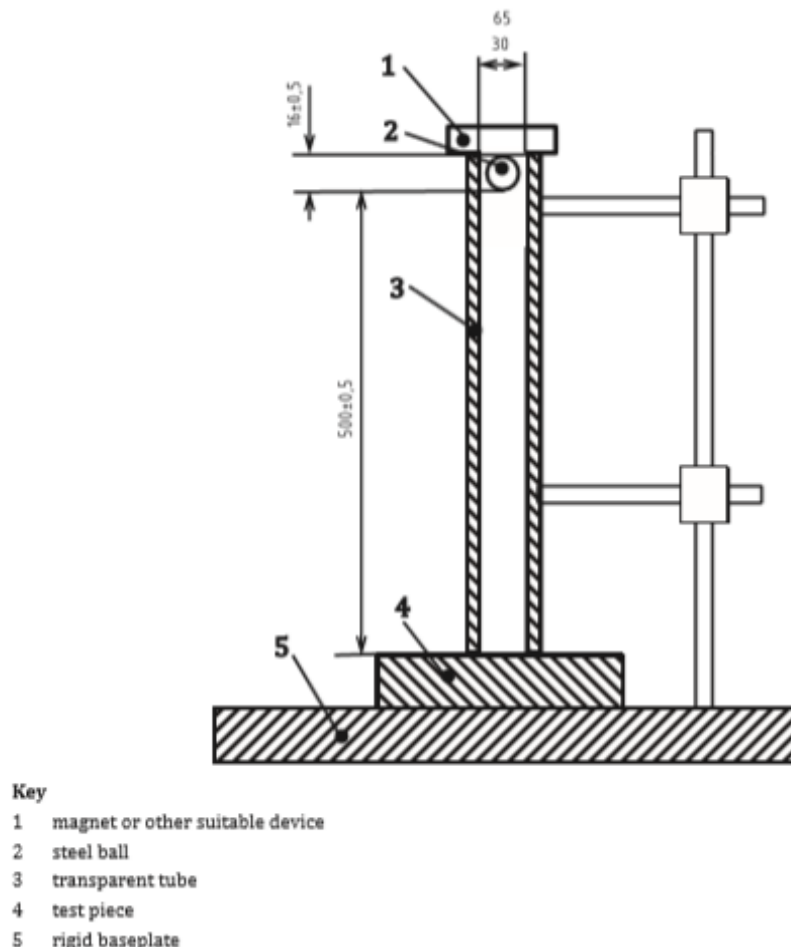


Figure 2. Equipment for elasticity analysis of polymer materials defined by ISO 8307

Dimensions of PU foam specimen should be 100x100x100 [mm]. Tested specimen is mounted at position 4, as it is presented in figure 2.

3. Conducting an experiment

3.1. Defining of problem

Essence of this paper is based on procedure of conduction an experiment with processing of experimental results. Thus, mathematical model is established that shows results dependency of measuring from main factors. In fact, it should be defined dependency of elastic rebound for PU foam from steel ball diameter and hardness of foam.

3.2. Preparing of model

During experiment, simple device for testing PU foam elasticity with manual reading is used. Research is conducted in laboratory for stress and strain analysis at ambient temperature. Steel ball is released from height of 500 mm. Experiment requirement is to prepare three steel balls and three specimens of PU foam. It is important to emphasize that specimens are not subjected to any loads before experiment. Three types of PU foam are used, as follows:

- PE2520 – elastic PU foam, hardness: 2.0 kPa/m²
- PN3540 – PU foam with normal hardness, hardness: 4.0 kPa/m²,
- PT4060 – PU foam with increased hardness, hardness: 6.0 kPa/m².

Experiment is conducted by achieving of ball free fall. Measure of elastic rebound carried out according to scale of device. Simulation of experiment conducting is shown in the figure 3.

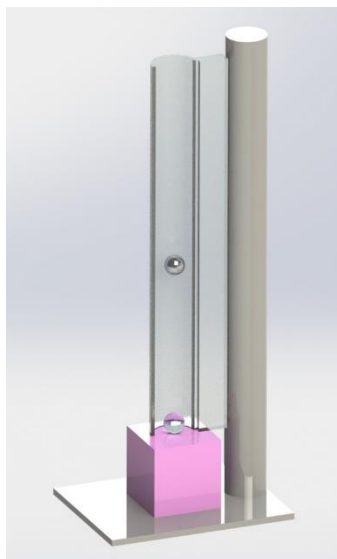


Figure 3. Simulation of experiment

Parameters of used factors are presented in table 1. As it is shown, three values of each factor are marked over three levels: upper, basic and lower. Distribution of levels is performed towards method of planning an experiment [5].

Table 1. Levels of used factors

Factor	Diameter of ball – factor X ₁ [mm]	Hardness of PU foam – factor X ₂ [kPa/m ²]
Upper level (+1)	22	6.0
Basic lever (0)	16.5	4.0
Lower level (-1)	11	2.0

4. Plan of experiment

Former research is conducted in order to defining if requested dependency can be express by mathematical model of first order with two levels of factors. Analysis is conducted by calculating of linear model in which is defined $N=2^k=2^2=4$. However, model is marked as inadequate by implementing of F-criteria.

Thus, this calculation is left out and analysis of model of second order is conducted.

In the theory of regression models, one of the most used is composition plan, especially, symmetrical composition plan that is applied in this paper too. Consequently, variables: $x_0, x_1, x_2, x_1x, x_1^2, x_2^2$ and results for three repetition in each point of plan are defined by experimental plan. Number of experiments is defined as:

$$N = 2^k + 2 \cdot k + n_0 = 2^2 + 2 \cdot 2 + 1 = 9 \quad (1)$$

Values from equitation (1) are defined as:

- N – total number of experiments,
- k=2 – number of factors,
- n_0 – number of experiments in central point.

Figure 4 represents scheme of composition orthogonal plan of second order.

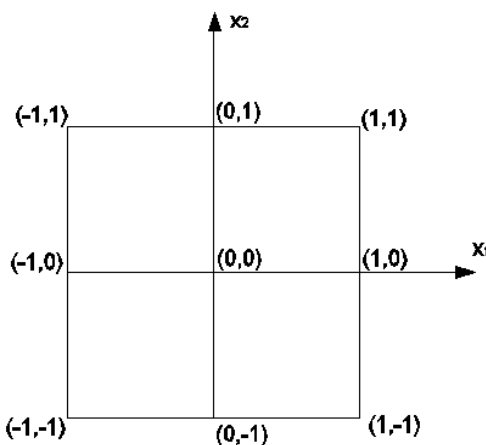


Figure 4. Scheme of orthogonal plan
In order to code main factors, equations of transformation are used, as it is shown:

$$x_i = \frac{X_i - X_{0i}}{w_i}$$

(2)

Values from equation (2) are defined as:

- x_i – coded value of factor,
- X_i – natural value of factor,
- X_{0i} – basic level of factor.

Accordingly, basic levels of factor are defined as:

$$X_{01} = \frac{X_{g1} + X_{d1}}{2} = \frac{22 + 11}{2} = 16.5$$

(3)

$$X_{02} = \frac{X_{g2} + X_{d2}}{2} = \frac{6 + 2}{2} = 4$$

(4)

Intervals of variation are calculated in next equations:

$$w_2 = \frac{X_{g2} - X_{d2}}{2} = \frac{6 - 2}{2} = 2$$

(5)

$$w_1 = \frac{X_{g1} - X_{d1}}{2} = \frac{22 - 11}{2} = 5.5$$

(6)

Coded values of factors are presented by next formulas:

$$x_{g1} = \frac{X_{g1} - X_{01}}{w_1} = \frac{22 - 16.5}{5.5} = 1 \quad (7)$$

$$x_{d1} = \frac{X_{d1} - X_{01}}{w_1} = \frac{11 - 16.5}{5.5} = -1 \quad (8)$$

$$x_{g2} = \frac{X_{g2} - X_{02}}{w_1} = \frac{6 - 4}{2} = 1 \quad (9)$$

$$x_{d2} = \frac{X_{d2} - X_{02}}{w_1} = \frac{2 - 4}{2} = -1 \quad (10)$$

Condition of orthogonal is shown as:

$$\alpha^2 = \frac{1}{2} \cdot \left[\sqrt{(2^k + 2 \cdot k + n_0)} - 2^k \right] \quad (11)$$

$$\alpha^2 = \frac{1}{2} \cdot \left[\sqrt{(2^2 + 2 \cdot 2 + 1)} - 2^2 \right] = 1 \quad (12)$$

$$\alpha = \pm 1 \quad (13)$$

New variable that makes orthogonal of plan matrix is:

$$\lambda_2 = N^{-1} \cdot \sum_{u=1}^n X_{iu}^2 = \frac{1}{9} (1^2 + 1^2 + 1^2 + 1^2 + 1^2 + 1^2) = \frac{2}{3} \quad (14)$$

Accordingly, new variables would be defined:

$$X_i' = X_i^2 - \lambda_2 \quad (15)$$

$$X_1' = X_1^2 - \frac{2}{3} \quad (16)$$

$$X_2' = X_2^2 - \frac{2}{3} \quad (17)$$

According to all calculations, plan experiment matrix could be defined, such as it is shown in table 2.

Table 2. Plan matrix of experiment

Experiment No	Factors								Results of measuring				
	x_0	x_1	x_2	x_1^2	x_2^2	x_1x_2	x_1'	x_2'	y_1	y_2	y_3	\bar{y}	\hat{y}
1	+1	-1	-1	+1	+1	+1	1/3	1/3	67.5	68	67	67.50	67.22
2	+1	+1	-1	+1	+1	-1	1/3	1/3	61	61.5	60	60.83	60.75
3	+1	-1	+1	+1	+1	-1	1/3	1/3	58	59	58	58.33	58.13

4	+1	+1	+1	+1	+1	+1	1/3	1/3	51	50	51.5	50.83	50.83
5	+1	-1	0	+1	0	0	1/3	-2/3	65	64	66	65.00	65.48
6	+1	+1	0	+1	0	0	1/3	-2/3	58.5	59	58	58.50	58.59
7	+1	0	-1	0	+1	0	-2/3	1/3	64.5	64.5	64	64.33	64.70
8	+1	0	+1	0	+1	0	-2/3	1/3	55.5	55	54.5	55.00	55.20
9	+1	0	0	0	0	0	-2/3	-2/3	63.5	63	63.5	63.33	62.76

5. Regression analysis

Regression model analyzed process of measuring could be shown by formula (18):

$$\hat{y} = \left(b_0 + \lambda_2 \cdot \sum_{i=1}^k b_{ii} \right) + \\ + \sum_{i=1}^k b_i \cdot x_i + \sum_{i < j}^k b_{ij} \cdot x_i \cdot x_j + \sum_{i=1}^k b_{ii} \cdot (x_i^2 - \lambda_2) \quad (18)$$

If new basic factor can be defined as:

$$\bar{b}_0 = b_0 + \lambda_2 \cdot \sum_{i=1}^k b_{ii} \quad (19)$$

Then, regression model is shown as:

$$\hat{y} = \bar{b}_0 + \sum_{i=1}^k b_i \cdot x_i + \sum_{j=1}^k b_{ij} \cdot x_i \cdot x_j + \sum_{i=1}^k b_{ii} \cdot x_i \quad (20)$$

Values of regression coefficient are calculated by following calculations:

$$\bar{b}_0 = \frac{\sum_{i=1}^N n_i \cdot \bar{y}_i}{\sum_{i=1}^N n_i} = \frac{\sum_{i=1}^9 3 \cdot \bar{y}_i}{3 \cdot (1+1+1+1+1+1+1+1+1)} \quad (21)$$

$$\bar{b}_0 = \frac{1}{9} (67.5 + 60.83 + 58.33 + 50.83 + 65 + 58.5 + 65.33 + 55 + 63.33) = 60.41 \quad (22)$$

Regression coefficients b_1 and b_2 are determined by formula (23):

$$b_j = \frac{\sum_{i=1}^N n_i \cdot x_{ji} \cdot \bar{y}_i}{\sum_{i=1}^N n_i \cdot x_{ji}^2} \quad (23)$$

Thus, values of coefficient are:

$$b_1 = \frac{\sum_{i=1}^9 3 \cdot x_{li} \cdot \bar{y}_i}{\sum_{i=1}^9 3 \cdot x_{li}^2} \quad (24)$$

$$b_1 = \frac{3 \cdot (-67.5 + 60.83 - 58.33 + 50.83 - 65 + 58.5)}{3 \cdot (1+1+1+1+1+1)} \quad (25)$$

$$b_1 = -3.44 \quad (26)$$

$$b_2 = \frac{\sum_{i=1}^9 3 \cdot x_{2i} \cdot \bar{y}_i}{\sum_{i=1}^9 3 \cdot x_{2i}^2} \quad (27)$$

$$b_2 = \frac{3 \cdot (-67.5 - 60.83 + 58.33 + 50.83 - 64.33 + 55)}{3 \cdot (1+1+1+1+1+1)} \quad (28)$$

$$b_2 = -4.75 \quad (29)$$

Coefficients with combined index are determined by:

$$b_{ij} = \frac{\sum_{u=1}^N n_u \cdot x_{iu} \cdot x_{ju} \cdot \bar{y}_u}{\sum_{i=1}^N n_u \cdot x_{iu}^2 \cdot x_{ju}^2} \quad (30)$$

$$b_{12} = \frac{\sum_{u=1}^9 n_u \cdot x_{1u} \cdot x_{2u} \cdot \bar{y}_u}{\sum_{i=1}^9 n_u \cdot x_{1u}^2 \cdot x_{2u}^2} \quad (31)$$

$$b_{12} = \frac{3 \cdot (67.5 - 60.83 - 58.33 + 50.83)}{3 \cdot (1+1+1+1)} = -0.21 \quad (32)$$

Coefficients of regression with similar index are determined by following calculation:

$$b_{ii} = \frac{\sum_{u=1}^N n_u \cdot x_{iu} \cdot \bar{y}_u}{\sum_{i=1}^N n_u \cdot x_{iu}^2} \quad (33)$$

$$b_{11} = \frac{3 \left[\frac{1}{3} (67.5 + 68.83 + 58.33 + 50.83 + 65 + 58.5) \right]}{3 \cdot \left(6 \cdot \frac{1}{9} + 3 \cdot \frac{4}{9} \right)} -$$

$$\frac{3 \left[\frac{2}{3} (64.33 + 55 + 63.33) \right]}{3 \cdot \left(6 \cdot \frac{1}{9} + 3 \cdot \frac{4}{9} \right)} = -0.72 \quad (34)$$

$$b_{22} = \frac{3 \left[\frac{1}{3} (67.5 + 68.83 + 58.33 + 50.83 + 64.33 + 55) \right]}{3 \cdot \left(6 \cdot \frac{1}{9} + 3 \cdot \frac{4}{9} \right)} -$$

$$b_{22} = \frac{3 \left[\frac{2}{3} (65 + 58.5 + 63.33) \right]}{3 \cdot \left(6 \cdot \frac{1}{9} + 3 \cdot \frac{4}{9} \right)} = -2.81 \quad (35)$$

If equitation (19) is used, value of factor b_0 is determined:

$$b_0 = b_0' - \lambda_2 \cdot \sum_{i=1}^k b_{ii} = b_0' - \lambda_2 \cdot (b_{11} + b_{22}) \quad (36)$$

$$b_0 = 60.41 - \frac{2}{3} \cdot (-0.72 - 2.81) = 62.76 \quad (37)$$

Therefore, expression for digression equitation in coded form is defined as:

$$\hat{y} = b_0' + b_1 x_1 + b_2 x_2 + b_{12} x_1 x_2 + b_{11} x_1' + b_{22} x_2' \quad (38)$$

Regression equitation in coded (39) and natural (40) form is determined by following expressions:

$$\hat{y} = 62.76 - 3.44x_1 - 4.75x_2 - 0.21x_1x_2 - 0.72x_1^2 - 2.81x_2^2 \quad (39)$$

$$\hat{y} = 23.1 + 3.78x_1 + 9.22x_2 - 0.019x_1x_2 - 0.131x_1^2 - 1.41x_2^2 \quad (40)$$

6. Dispersion analysis

Dispersion analysis is conducted in order to defining of factors significance. Conducting of dispersion analysis is very important for mathematical modeling. Thus, if one significant factor is missing, value of experiment fault decreases.

On the other hand, if all factors are included (also insignificant factors), research becomes very prolonged and expensive. In the theory of experimental researches, set of included factors affect at results of research by degree of its importance. To conclude, insignificant factors have to be found and excluded.

6.1. Dispersion of experiment

Dispersion of experimental results is defined by following expressions:

$$s^2(y) = \frac{1}{n} \cdot \sum_{v=1}^N f_v \cdot s_v^2 \quad (41)$$

$$s^2(y) = s_E^2 = \frac{S_E}{f_E} = \frac{1}{N \cdot (n-1)} \cdot \sum_{u=1}^N \sum_{i=1}^n (y_{ui} - \bar{y}_u)^2 \quad (42)$$

$$S_E = \sum_{u=1}^N \sum_{i=1}^n (y_{ui} - \bar{y}_u)^2 = (y_{11} - \bar{y}_1)^2 + \dots + (y_{93} - \bar{y}_9)^2 \quad (43)$$

$$S_E = (67.5 - 67.5)^2 + (68 - 67.5)^2 + (67 - 67.5)^2 + \dots + (63.5 - 63.33)^2 = 6.83 \quad (44)$$

Thus, dispersion of experiment is determined as:

$$s^2(y) = \frac{6.83}{9 \cdot (3-1)} = 0.379 \quad (45)$$

Values from equitation (45) are defined as:

- $N=9$ – number of different points.
- $n=3$ – number of experiment repetition in each point.

6.2. Dispersion of regression coefficients

Calculation of regression coefficients dispersion is shown by following expressions:

$$s^2(b_0') = \frac{s^2(y)}{\sum_{u=1}^N n_u} = \frac{0.379}{3 \cdot 9} = 0.01403 \quad (46)$$

$$s(b_0') = 0.1185 \quad (47)$$

$$s^2(b_i) = \frac{s^2(y)}{\sum_{u=1}^N n_u \cdot x_{iu}^2} \quad (48)$$

$$s^2(b_1) = \frac{s^2(y)}{\sum_{u=1}^9 n_u \cdot x_{1u}^2} = \frac{0.379}{3 \cdot (1+1+1+1+1)} = 0.02105 \quad (49)$$

$$s^2(b_2) = \frac{s^2(y)}{\sum_{u=1}^9 n_u \cdot x_{2u}^2} = \frac{0.379}{3 \cdot (1+1+1+1+1)} = 0.02105 \quad (50)$$

$$s(b_1) = s(b_2) = 0.1452 \quad (51)$$

$$s^2(b_{ii}) = \frac{s^2(y)}{\sum_{u=1}^N n_u \cdot x_{iu}^2} \quad (52)$$

$$s^2(b_{11}) = \frac{s^2(y)}{\sum_{u=1}^9 n_u \cdot x_{1u}^2} = \frac{0.379}{3 \cdot \left(6 \cdot \frac{1}{9} + 3 \cdot \frac{4}{9} \right)} = 0.06317 \quad (53)$$

$$s^2(b_{22}) = \frac{s^2(y)}{\sum_{u=1}^9 n_u \cdot x_{2u}^2} = \frac{0.379}{3 \cdot \left(6 \cdot \frac{1}{9} + 3 \cdot \frac{4}{9} \right)} = 0.06317 \quad (54)$$

$$s(b_{11}) = s(b_{22}) = 0.2513 \quad (55)$$

$$s^2(b_{ij}) = \frac{s^2(y)}{\sum_{u=1}^N n_u \cdot x_{iu}^2 \cdot x_{ju}^2} \quad (56)$$

$$s^2(b_{12}) = \frac{s^2(y)}{\sum_{u=1}^9 n_u \cdot x_{1u}^2 \cdot x_{2u}^2} = \frac{0.379}{3 \cdot (1+1+1+1)} = 0.0316 \quad (57)$$

$$s(b_{12}) = 0.1777 \quad (58)$$

$$s^2(b_0) = s^2(b_0') + \lambda_2^2 \cdot \sum_{i=1}^k s^2(b_{ii}) \quad (59)$$

$$s^2(b_0) = 0.01403 + \frac{4}{9}(0.06317 + 0.06317) = 0.0703 \quad (60)$$

$$s(b_0) = 0.265 \quad (61)$$

6.3. Defining of significance of regression coefficients

For estimation regression coefficient significance, Student criterion could be used. Criterion is conducted by determining of relation between absolute value of regression coefficient and dispersion of coefficient value. Calculated relation is compared with literature value [2]. If calculated relation is higher than literature value, factor is considered as significant. Thus, following condition is defined by criterion:

$$t_{ri} = \frac{|b_i|}{s(b_i)} \geq t_{t(f_0, \alpha)} \quad (62)$$

Literature value is defined by degree of freedom (f_0) and limit of significance ($\alpha=1-P$). In this case, for degree of freedom $f_0=27-9=18$ and defined limit of significance $\alpha=5$, according to table II [2], literature value $t_t=1.73$.

Calculation of relation between absolute value of regression coefficient and dispersion of coefficient value for each factor is determined as:

$$t_{r0} = \frac{|b_0|}{s(b_0)} = \frac{62.76}{0.265} = 236.83 > 1.73 \quad (63)$$

$$t_{r1} = \frac{|b_1|}{s(b_1)} = \frac{3.44}{0.1425} = 24.14 > 1.73 \quad (64)$$

$$t_{r2} = \frac{|b_2|}{s(b_2)} = \frac{4.75}{0.1425} = 32.71 > 1.73 \quad (65)$$

$$t_{r12} = \frac{|b_{12}|}{s(b_{12})} = \frac{0.21}{0.1777} = 1.18 < 1.73 \quad (66)$$

$$t_{r11} = \frac{|b_{11}|}{s(b_{11})} = \frac{0.72}{0.2513} = 2.86 > 1.73 \quad (67)$$

$$t_{r22} = \frac{|b_{22}|}{s(b_{22})} = \frac{2.81}{0.2513} = 11.18 > 1.73 \quad (68)$$

To conclude, factor b_{12} is insignificant, so it could be excluded from regression equitation. Therefore, final form of regression equitation is determined as:

$$\hat{y} = 23.1 + 3.78x_1 + 9.22x_2 - 0.131x_1^2 - 1.41x_2^2 \quad (69)$$

7. Determining of model adequacy

Condition of model adequacy is defined by Fisher-method, as follows:

$$F_r = \frac{\frac{S_{LF}}{f_{LF}}}{\frac{S_E}{f_E}} \leq F_t(f_1, f_2) \quad (70)$$

Literature value of F-distribution is determined by following parameters:

$$f_{LF} = N - m = N - (d + 1) = 9 - (5 + 1) = 3 \quad (71)$$

$$f_E = N_0 - N = 27 - 9 = 18 \quad (72)$$

Used magnitudes are defined as:

- $N=9$ – number of different points,
- $m=5+1$ – number of regression coefficients,
- $N_0=27$ – total number of conducted measurements,
- f_{LF} – number of degree of freedom, factor of distribution f_1 ,
- f_E – degree of freedom, factor of distribution f_2 .

According to above mentioned calculation, literature value [2] of F-criterion for defined f_1 and f_2 and limit of significance $\alpha=5\%$ is defined as $F_t=3.16$.

Dispersion for plan adequacy is determined by expression:

$$S_{LF} = n \cdot \sum_{u=1}^N \left(\bar{y}_u - \hat{y}_u \right)^2 = 2 \cdot [(67.5 - 67.21)^2 + \dots + \dots] = 2.627 \quad (72)$$

Therefore, by means of formula (70), adequacy of model is defined, as follows:

$$F_r = \frac{\frac{2.627}{3}}{\frac{6.83}{18}} = 2.31 < 3.16 \quad (73)$$

Concerning that calculated value is lower than value from literature, it can be concluded that hypothesis of model adequacy can be accepted. Researched process is adequately described by defined regression model.

8. Optimization of regression analysis factors

As it is calculated, defined regression model adequately (69) describes dependency of steel ball elastic rebound from ball diameter and hardness of PU foam. In order to get values of factors for the best case, e.g. the highest elastic rebound, mathematical calculation is conducted. Thus, factors x_1 and x_2 are optimized in order to determine its values for the highest value of \hat{y} .

$$\begin{aligned} 23.1 + 3.78x_1 + 9.22x_2 - 0.131x_1^2 - 1.41x_2^2 &= \\ &= -(0.131x_1^2 - 3.78x_1) - (1.41x_2^2 - 9.22x_2) + 23.1 = \end{aligned}$$

$$\begin{aligned}
 &= -\left(\sqrt{0.131}x_1 - \frac{1.89}{\sqrt{0.131}}\right)^2 - \left(\sqrt{1.41}x_2 - 4.61\right)^2 + \\
 &+ 23.1 + \left(\frac{1.89}{\sqrt{0.131}}\right)^2 + \left(\frac{4.61}{\sqrt{1.41}}\right)^2 = \\
 &\approx 23.1 + 27.28 + 15.07 - \left(\sqrt{0.131}x_1 - \frac{1.89}{\sqrt{0.131}}\right)^2 - \\
 &- \left(\sqrt{1.41}x_2 - \frac{4.61}{\sqrt{1.41}}\right)^2 \approx \\
 &\approx 65.45 - \left(\sqrt{0.131}x_1 - \frac{1.89}{\sqrt{0.131}}\right)^2 - \left(\sqrt{1.41}x_2 - \frac{4.61}{\sqrt{1.41}}\right)^2 \quad (74)
 \end{aligned}$$

Thus, the highest value of (74) will be achieved if

$$\sqrt{0.131}x_1 - \frac{1.89}{\sqrt{0.131}} = 0 \quad (75)$$

and:

$$\sqrt{1.41}x_2 - \frac{4.61}{\sqrt{1.41}} = 0. \quad (76)$$

If above mentioned equations are solved, requested values of x_1 and x_2 are:

$$x_1 = 14.42 \quad (77)$$

$$x_2 = 3.27$$

(78)

Accordingly, the highest elastic rebound, apropos the highest value of PU foam elasticity could be achieved in case of steel ball with diameter 14.42 mm (factor x_1) and PU foam with 3.27 kPa/m² of hardness (factor x_2).

9. Conclusion

Quality of polyurethane foam as main structural material in furniture industry is defined by main mechanical properties such as: density, hardness, elongation, permeability and elasticity. One of the basic methods for analysis of PU foam elasticity is method of measuring steel ball elastic rebound that is defined by standard ISO 8307. Above mentioned standard clearly describes instruments, equipment, conditions, preparation of specimens and procedure of conducting an experiment.

According to basic configuration of ISO defined procedure [4], procedure for conducting of experimental analysis in order to performing of regression analysis is defined. Thus, model that shows dependency of PU foam elasticity from steel ball diameter and PU foam hardness, as independently variables is set.

First conducted experiment presents analysis that is based on model of first order. It is proven that this

model is not adequate for describing of process. Finally, regression model of second order is carried out by setting of symmetrical composition plan with two independent factors.

Checking of significance of individual regression coefficients is achieved by Student method. It is proven that one of six coefficients is insignificant so it is excluded from model. Considering that factor b_{12} is shown as insignificant, it is concluded that mutually action of both factors does not have significant level of effect to process.

Fisher's method is used to define if set model adequately describes process PU foam elasticity measuring. It is shown that model of second order, made by two-factor plan with three iteration in each point of plan is adequate.

On the end, optimization is conducted in order to determine values of factor for the best case – case of the highest elasticity of PU foam. It can be concluded that if steel ball with diameter 14.42 mm and PU foam with hardness 3.27 kPa/m² are used, the height of rebound will be the highest, so elasticity of foam will be the most desirable.

10. References

REFERENCES

- [1] N.V. Gama, A. Ferreira, A. Barros-Timmons (2018), *Polyurethane foams: Past, Present and Future*, Materials 2018, MDPI, Basel, Switzerland
- [2] Jurković Milan (1999), *Matematičko modeliranje inženjerskih procesa i sistema*, Mašinski fakultet u Bihaću, Bihać
- [3] Rok Brinc (2007), *Poročilo nostranjega izobreževanja, Vlivanje pene*, Podgrad, Slovenija
- [4] Stanić Joko (1981), *Metod inženjerskih mjerena*, Mašinski fakultet, Beograd
- [5] Richard A. Jonson (2011), *Probability and Statistics for Engineers*, Pearson, Eighth Edition
- [6] Douglas C. Montgomery, *Design and Analysis, International Student Version*, John Wiley and sons, Eighth Edition

See discussions, stats, and author profiles for this publication at: <https://www.researchgate.net/publication/257603177>

Effects of BaSO₄, CaCO₃, Kaolin and Quartz on the Mechanical, Chemical and Morphological Properties of Cast Polyurethane

Article in Plastics Rubber and Composites · July 2012

DOI: 10.1179/1743289811Y.0000000035

CITATIONS

9

READS

2,304

4 authors, including:



Mahnaz Shahzamani

Academic Center of Education Culture and Research IUT branch

18 PUBLICATIONS 88 CITATIONS

[SEE PROFILE](#)



Payam Zahedi

University of Tehran

114 PUBLICATIONS 2,134 CITATIONS

[SEE PROFILE](#)

Some of the authors of this publication are also working on these related projects:



5-fluorouracil-loaded hydrogel scaffolds based on sodium alginate/xanthan/halloysite: Characterization, release behavior, and cancer cell death performance [View project](#)



EFFECT OF CROSSLINKING ON GLASS TRANSITION TEMPERATURE IN SYNTHESIS OF THIOL ACRYLATE-BASED LIQUID CRYSTALLINE ELASTOMERS [View project](#)

Effects of BaSO₄, CaCO₃, kaolin and quartz fillers on mechanical, chemical and morphological properties of cast polyurethane

M. Shahzamani¹, I. Rezaeian^{*2}, M. S. Loghmani¹, P. Zahedi² and A. Rezaeian²

For industrial applications of engineering polymers such as polyurethane, polyamides and polyesters, the addition of suitable reinforcing inorganic fillers is a practical and convenient method to achieve the desirable mechanical and chemical properties. In this study, the mechanical, chemical and morphological properties of cast polyurethane samples containing barium sulphate, calcium carbonate, kaolin and quartz fillers were investigated. In the formulation of these samples, the ranges of inorganic filler were 0–40 phr. The results of mechanical property tests, such as tear resistance, tensile strength, elongation at break, Young's modulus, hardness and abrasion resistance, were evaluated. The chemical resistance of the samples was determined against xylene and methyl ethyl ketone. The chemical resistance of the filled cast polyurethane was determined by the solubility parameters of polymer/solvent. Finally, the experimental results and SEM images showed that samples containing 30 phr calcium carbonate produced the best results.

Keywords: Polyurethanes, Fillers, Mechanical properties, Morphology, Chemical resistance

Introduction

Polyurethane cast elastomers have the most diverse range of polymers because of different raw materials that can be used for their production.¹ They are used in a variety of critical applications, including electrical encapsulates, abrasion resistance linings for pumps, chutes and conveyor belts, rollers, wiper blades, seals and gaskets and wheels for casters. Polyurethanes are being used in graphic rolls, offset printing rolls and in paper mill rolls.^{2,3} They also have wide applications in other industries such as paints, varnishes,^{4,5} foams, nanocomposite foams^{6,7} and medical implants.⁸ Polyurethanes are also used for nanoparticle filled composites.⁹ These varieties in the applications of polyurethanes have led to a widespread choice of raw materials for their production. The majority of polyurethane elastomers are based on diisocyanates, polyesters or polyethers long chains and bifunctional alcohols with short chains as chain extenders. In recent years, studies on polyurethanes and their derivatives have become an important research field. Polyurethanes derived from different polyols, diisocyanates and their characterisation have interested many researchers.^{10–14} On the other hand, castable polyurethanes are considered as an important part of polyurethane industries. These polymers are generally

produced by mixing two to five ingredients in a suitable mould at ~100°C, and the curing process is completed inside the mould after 6–18 h. For castable polyurethane products, it is essential to control the following parameters:¹⁵

- (i) the fillers used in polyurethane samples must be completely dry in order to prevent the formation of carbon dioxide and gas bubbles during the two-roll mill mixing process
- (ii) complete mixing of the filler particles and their breakdown in polyurethane matrix prevents the blooming process (a visible exudation or efflorescence on the surface of materials) and avoids sharkskin phenomenon as a surface defect in polymer melts
- (iii) a suitable filling of the mould is necessary in order to prevent viscous resin leakages and polyurethane shrinkage in the cast moulding process.

The purpose of adding mineral fillers to polymers has been primarily for cost reduction. In recent years, however, the fillers are more often used to fulfil a functional role, such as increasing the stiffness or improving the dimension stability of the polymers.¹⁶ For instance, the addition of zinc ferrite¹⁷ improves magnetic and dielectric properties, whereas the addition of calcium carbonate (CaCO₃),¹⁸ aluminium hydroxide,¹⁹ kaolin,²⁰ titanium dioxide, zinc oxide²¹ and silica²² reinforces mechanical properties. Furthermore, the use of metallic fillers increases acoustic properties in polyurethanes.²³

For polyurethane filled samples, an improvement in surface hardness, tensile strength (TS) and

¹Research & Development Department, Mobarakeh Industrial Rubber Company (MIRCO), PO Box 84861-35196, Isfahan, Iran

²School of Chemical Engineering, College of Engineering, University of Tehran, PO Box 11155-4563, Tehran, Iran

*Corresponding author, email rezaeian@ut.ac.ir

tensile modulus values was noticed by Roopa and Siddaramaiah.²⁴ They used different amounts of metakaolin in castable polyurethane, and investigated the physicomechanical properties and chemical resistance of filled chain extended polyurethane. Their results showed that with increasing the filler content in polyurethane matrix, the TS and chemical resistance of the samples against different solvents such as toluene and methyl ethyl ketone (MEK) were increased.

Gao *et al.*^{25,26} have investigated the preparation and characterisation of well dispersed waterborne polyurethane/CaCO₃ nanocomposites. It was found that well dispersion was obtained up to 6 wt-% of the surface treated CaCO₃ loading for polyurethane/CaCO₃ nanocomposite. Compared with the pure polyurethane, a significant improvement in thermal stability was observed with the addition of 6 wt-% of the surface treated CaCO₃. The experimental results suggested that the properties of nanocomposites were correlated with the dispersion of nano-CaCO₃ in polyurethane and the interfacial interactions between nano-CaCO₃ and polymer matrix.

In this work, a systematic study on cast polyurethanes containing different inorganic fillers was carried out. Four types of fillers [barium sulphate (BaSO₄), CaCO₃, kaolin and quartz (0–40 phr)] were added to polyurethane samples, and their mechanical, chemical and morphological properties were evaluated. On the basis of the experimental results, the optimum choice for the filler type and its percentage was determined. In addition, the chemical resistance of the samples against solvents such as xylene and MEK were determined from weight loss measurements of the samples. Finally, SEM images showed the extent of filler dispersion in the polyurethane matrices.

Materials and methods

Materials

Polyurethane prepolymer (TB 636) containing poly(glycol adipate) and toluene diisocyanate (with 3·6% free isocyanate), chain extender [a mixture of three methyl propane and three isopropanol amine (TMP/TIPA)] and the plasticiser (trade name, V03) were all polyurethane purchased from Baule Co. (France). The polyurethane prepolymer had a viscosity of 3·2 Pa s at the process temperature of 80°C and a solid state at 20°C. In addition, TMP/TIPA was solid at room temperature and had a viscosity of 0·075 Pa s at the process temperature of 80°C. The inorganic fillers BaSO₄, CaCO₃ and kaolin were supplied by Soft Powder Sepahan Co. (Iran). Quartz filler was provided from Iranian Mineral Production and Supplying Co. (Iran). The physical characteristics of these mineral fillers are given in Table 1.

Table 1 Technical data for different inorganic filler properties used in cast polyurethane samples

Brunauer–Emmett–Teller (BET)*/m ² g ⁻¹	Size/μm	pH	Type and shape	SiO ₂ /%	Filler
30	20	9	Crystalline, granular	6·13	BaSO ₄
60	25	9·5	Crystalline, layered	0·15	CaCO ₃
14	5	5	Amorphous, planar	68·8	Kaolin
2·5	40	7·5	Crystalline, spherical	98·7	Quartz

*Specific surface area.

Samples preparation

The above fillers were dried at 100°C for 24 h in an oven. A mixture of 10–40 phr filler and 15 phr plasticiser (V03) was added to 100 phr polyurethane prepolymer (TB 636). The mixture was then agitated in a mixer for 3 h at 50 rev min⁻¹. After vacuum evacuation of the gases from the mixture, 3·9 phr chain extender (TMP/TIPA) was added. After the mixing process was complete, the mixture was heated at 70°C for 12 h. It was then poured into a mould and heated at 110°C for 6 h. Finally, the moulded polyurethane samples were cured at 110°C for 16 h.

Samples characterisation

Mechanical tests

The TS of the samples was determined using a universal tensile tester (model 4505, Instron Co.) according to the standard test method ASTM D412. Furthermore, tear resistance was measured according to the standard test method ASTM D624 using die (C) (CCSi UltraLife specimen cutting dies, Ohio, USA), and the hardness (shore A) was evaluated according to ASTM D2240 using a durometer hardness tester (Zwick Co., Germany). The abrasion resistance of the samples was determined using a Hampden Northampton abrasion tester (UK) according to the standard test method DIN 53516. Cylindrical samples of 8 mm thickness and 16 mm diameter were prepared, and their weight loss on the volume basis (mm³) was recorded. In all these measurements, the results had a standard deviation <5%.

Chemical resistance tests

Solvent resistance of the polyurethane samples was evaluated according to standard test method ASTM D474, in xylene and MEK at room temperature for 72 h. Using equation (1), the weight loss was determined

$$\Delta W = [(W_2 - W_1)/W_1] \cdot 100 \quad (1)$$

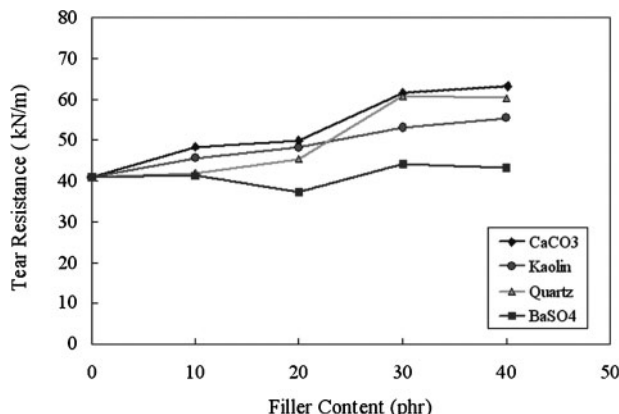
where W_1 and W_2 were the weight of the samples before and after solvent immersion respectively.

Scanning electron microscopy

Cast polyurethane samples were cut into small pieces, and after 10 min, their gold sputtering operation was carried out using a Bio-Rad automatic sputter coater (model E-5200, UK). Then, SEM images of the specimens obtained using CamScan (model MV-2300, Cambridge, UK), with 25 kV high voltage and 500× magnification.

Results and discussion

The reinforced mechanical properties of cast polyurethane samples, such as tear and abrasion resistances, TS and chemical resistance, are important factors for the



1 Variations of tear resistance against different amounts of fillers (0–40 phr) BaSO₄, CaCO₃, kaolin and quartz in cast polyurethane samples

selection of the most suitable filler in cast polyurethane samples.

Mechanical properties of samples

Tear resistance

Figure 1 shows the tear resistance variations of cast polyurethane samples containing 0–40 phr BaSO₄, CaCO₃, kaolin and quartz. The tear resistance is increased by an increase in filler content. For samples containing CaCO₃ and quartz, the increase in tear resistance was more than that in the other two fillers. For 30 phr filler content, the samples have similar tear resistance ~61 kN m⁻¹. One of the most important factors in the reinforcement of the tear resistance and toughness of the samples are the type and shape of the filler particles and also the value of Brunauer–Emmett–Teller (BET), which is directly related to the specific surface area of the filler particles.²⁷

Previous studies show that CaCO₃, as a neutral filler, is very effective in reinforcing toughness property of polymers.²⁸ The micromechanism consists of three stages:

- (i) stress concentration: the modifier particles act as concentrator because they have different elastic properties compared with the matrix polymer
- (ii) debonding: stress concentration gives rise to build-up of triaxial stress around the filler particles, and this leads to debonding at the particle/polymer interface
- (iii) shear yielding: the voids caused by debonding alter the stress state in the host matrix polymer surrounding the voids, which reduces the sensitivity towards crazing since the volume strain is released.

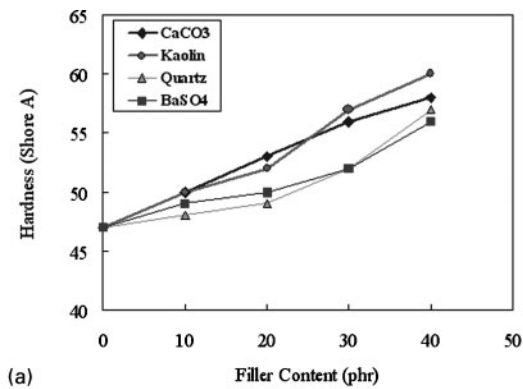
The experimental results also show that the highest tear resistance of the samples belongs to those containing CaCO₃ filler.

On the other hand, for semireinforcing fillers such as silica (quartz) and silica clay (kaolin) for lower values of BET, the surface area of the filler particles is smoother, and the interactions between filler particles and polymer chains increase.²⁹ Therefore, the highest values of tear resistance for these samples belong to CaCO₃, quartz, kaolin and BaSO₄ for an optimum 30 phr filler content respectively.

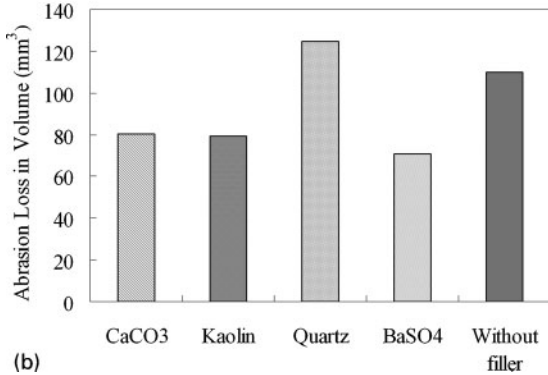
Usually, low particle size and high surface activity of a filler increases the viscosity of polyurethane, which

Table 2 Tensile strength, elongation at break and modulus at 300% elongation for samples containing 0–40 phr fillers BaSO₄, CaCO₃, kaolin and quartz

Filler/phr	BaSO ₄				CaCO ₃				Kaolin				Quartz			
	0	10	20	30	40	0	10	20	30	40	Property	Filler/phr	0	10	20	30
Tensile strength/ MPa	6.6	8.94	13.51	15.21	16.4	6.6	8.86	14.11	15.6	16.03	Tensile strength/ MPa	6.6	8.45	10	13.06	14.16
Elongation at break/%	963.4	1180.1	1113.5	1043.3	1008.3	963.4	1042.8	1058.2	1093.4	995.9	Elongation at break/%	963.4	1203.27	999.13	951.65	947.83
Modulus at 300%/MPa	1.83	2	2.82	3.47	3.76	1.83	2.07	2.86	3.18	3.4	Modulus at 300%/MPa	1.83	2	2.26	2.73	3.33



(a)



(b)

2 a variations of hardness (shore A) and **b** abrasion resistance against different amounts of fillers (0–40 phr) BaSO₄, CaCO₃, kaolin and quartz in cast polyurethane samples

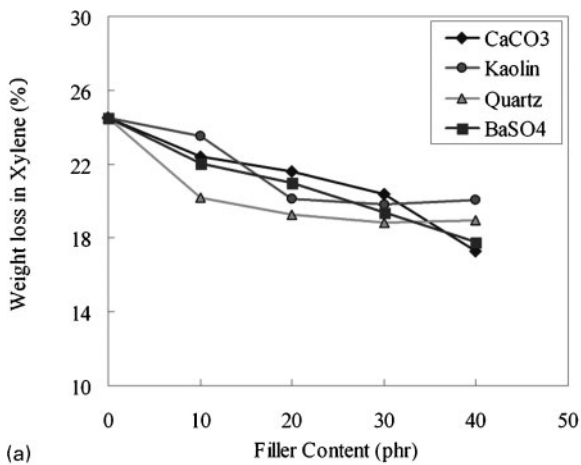
makes mixing and processing difficult. In this work, filler particles with similar dimensions were used.

Tensile strength, elongation at break and modulus

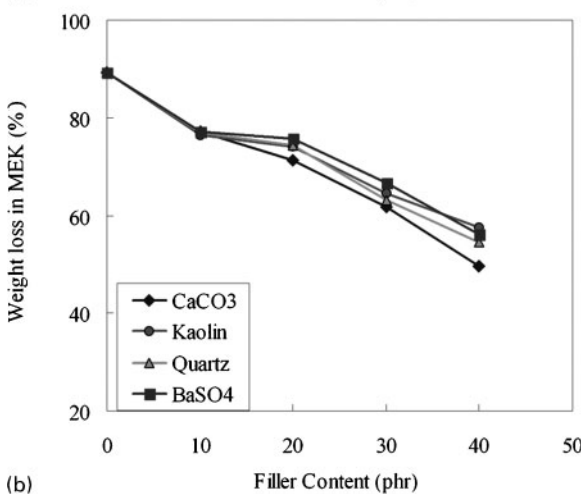
Table 2 shows TS, elongation at break (EB) and Young's modulus for 300% elongation. Our previous work²⁷ shows that SiO₂ has a suitable compatibility with polymer structures containing Si such as silicone rubber. However, in this study, the TS measurements for polyurethane samples show completely different results. Samples with quartz, kaolin, BaSO₄ and CaCO₃ fillers containing SiO₂ percentages 98·7, 68·8, 6·13 and 0·15% respectively, have an increase in their TS values. For instance, at 30 phr filler content, the extent of TS increases for these fillers is ~29%. On the other hand, when CaCO₃ content in the samples varies from 0 to 40 phr in the formulations, the TS increases ~142%. The tear resistance increase for samples from 30 to 40 phr CaCO₃ is not remarkable.

According to physical and mechanical properties of polymers,³⁰ when TS increases, EB is reduced. It was observed that by the addition of a filler to polyurethane samples, the EB relative to pure samples is increased. This behaviour can be explained in terms of increases in elastic property and the formation of junctions in polymeric chains. In polyurethane polymer chains, an increase in the degree of cross-linking leads to an increase in EB. As the amount of filler is increased in the samples, they become harder, and a reduction in EB is observed. Usually, the main purpose from the addition of a filler to a polymer is twofold:

- (i) an increase in modulus
- (ii) cost reduction in the final products.



(a)



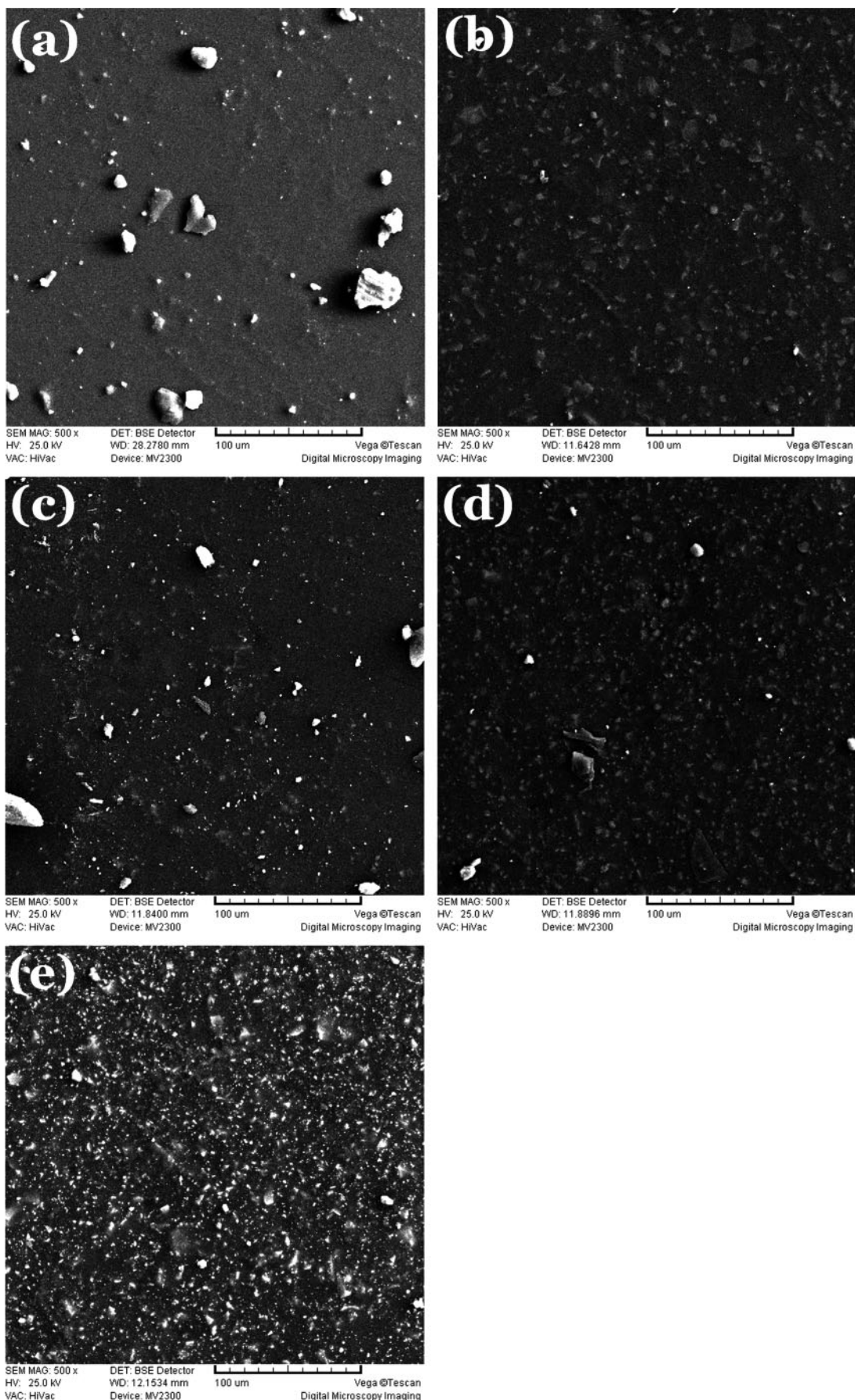
(b)

a xylene; **b** methyl ethyl ketone (MEK)
3 Chemical resistance of cast polyurethane samples versus filler content (0–40 phr) BaSO₄, CaCO₃, kaolin and quartz in two solvents

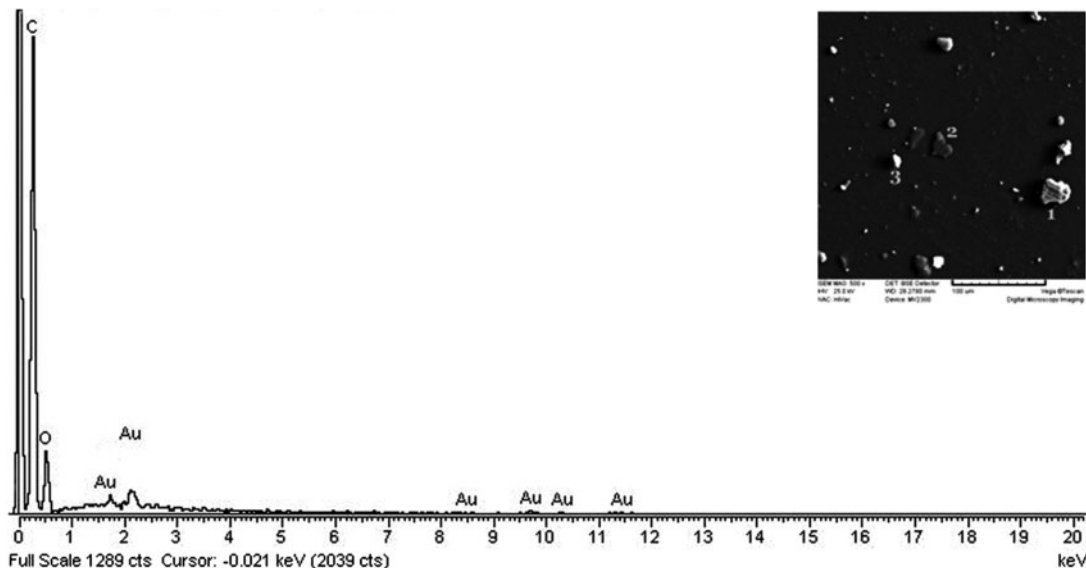
Therefore, an increase in filler content results to an increase in modulus, which leads to higher values of hardness in the samples. The role of CaCO₃ and BaSO₄ compared with the other two fillers is more significant for increases in the modulus.

Hardness and abrasion resistance evaluations of samples

The results from hardness (shore A) and abrasion resistance measurements are important for coating the surface of two-roll mill by cast polyurethane samples. Therefore, high values of hardness and abrasion resistance are considered as advantages of adding a suitable filler in the samples. Figure 2a shows the highest values of hardness for the samples containing kaolin, CaCO₃, BaSO₄ and quartz respectively. For lower values of SiO₂ in a filler, the surface of filler particles has higher interactions with elastic polyurethane chains, and therefore, the modulus and hardness of the samples are increased for higher values of the filler. On the other hand, the abrasion resistance of the samples is related to their hardness. Therefore, an increase in the hardness of the samples corresponds to a reduction in their abrasion volume loss. As can be seen in Fig. 2b, polyurethane cast sample containing quartz (30 phr) has the highest volume loss ~130 mm³, and samples containing BaSO₄, kaolin and CaCO₃ have the lowest abrasion values.



4 Images (SEM) of cast polyurethane samples surface *a* without filler and with 30 phr different fillers *b* BaSO₄, *c* kaolin, *d* CaCO₃ and *e* quartz



5 Energy dispersive X-ray spectrum and mapping of cast polyurethane samples in absence of filler

Chemical resistance evaluations of samples

Figure 3 shows weight reduction values of cast polyurethane samples containing CaCO_3 , kaolin, quartz and BaSO_4 for 10–40 phr. The effects of xylene and MEK solvents in the weight losses of the samples have a direct relation to the solubility parameter of solvent and polymer. As the solubility parameters of the solvent and polymer get closer together, the solubility of the polymer in the solvent increases.³¹ From the literature,^{31,32} solubility parameters are 18 and 19.3 MPa^{1/2} for xylene and MEK respectively and are 18.3–19.3 MPa^{1/2} for polyurethane samples, which are dependent on polyol and diisocyanate and their molecular weights. Considering the samples without a filler (Fig. 3) in xylene and MEK solvents, weight reduction values were ~25 and 90% respectively. It can be concluded that the solubility parameter for the samples without a filler is very close to the solubility parameter of MEK. The solubility parameters for the fillers used in the samples exist in the literature,³ which has a direct relation on the lowering of weight reduction of the samples and their resistance against xylene and MEK. Considering this characteristic, Fig. 3 shows an increase in chemical resistance of the samples by the addition of a filler and increasing its content. This behaviour for CaCO_3 and quartz is more than the other two fillers, which show the higher solubility differences between the filler and the solvent.

Morphology analysis of samples

From the previous results, especially tear resistance, hardness, abrasion and chemical resistance of the samples, CaCO_3 is the preferred filler compared with the other three selected fillers, and its most suitable percentage was 30 phr. Figure 4 shows SEM images of the samples without fillers (Fig. 4a) and containing 30 phr BaSO_4 , kaolin, CaCO_3 and quartz (Fig. 4b–e respectively). Furthermore, in mechanical property improvements such as tear and abrasion resistances, parameters such as suitable mixing properties of the filler in the polymer matrix, filler distribution and also the extent of filler migration to the surface of the polyurethane samples play a key role. As can be seen in Fig. 4, samples containing quartz (Fig. 4e), CaCO_3 (Fig. 4d), BaSO_4 (Fig. 4b) and kaolin (Fig. 4c) have the

best distribution of filler particles on the surface of the polymer matrix respectively. However, considering the high percentage of SiO_2 in quartz and kaolin fillers and because of incompatibility of the surface of the filler particle with rubbery chains, the filler migration to the surface is observed in the images as brighter points in Fig. 4e and c. Therefore, the surface of the samples becomes rougher and also results to a reduction of the abrasion resistance. Consequently, the samples containing 30 phr CaCO_3 were selected as the best ones.

For samples without a filler, in order to recognise bright points, numbered 1, 2 and 3 in Fig. 5, energy dispersive X-ray (EDX) images were taken from the surface of the sample. It was found that these points were holes containing carbon and oxygen elements which exist in the backbone of polyurethane chains. They may also be possibly due to Au from gold coating which has been gathered on the surface of the samples. Therefore, the results obtained from SEM images show darker and brighter points which represent the filler used in the samples, and EDX images also confirm these observations.

Conclusions

In this study, cast polyurethane samples containing BaSO_4 , CaCO_3 , quartz and kaolin fillers in the range of 0–40 phr were prepared, and their mechanical, chemical and morphological properties were investigated. The tear resistance examinations of these samples showed that the shape and topology of the fillers and also their specific surface area (BET) are the most effective parameters in reinforcing these properties, and 30 phr CaCO_3 samples showed the best results. In addition, mechanical test results including TS, EB and modulus indicate that different percentages of SiO_2 can be an important parameter in the variation of these properties. On the other hand, the evaluation of the samples' hardness and their abrasion resistance showed that a relative increase in hardness and abrasion resistance is observed. Finally, SEM and EDX images of the samples containing 30 phr CaCO_3 can be the best choice for coating the stainless steel surfaces of the two-roll mills.

References

1. K. C. Frisch and S. W. Wong: *Cell. Polym.*, 1989, **86**, 433–470.
2. X. Wang, Z. J. Du, C. Zhang, C. J. Li, X. P. Yang and H. Q. Li: *J. Polym. Sci. A*, 2008, **46A**, 4857–4865.
3. M. Szycher: ‘Szycher’s handbook of polyurethanes’, Chap. 18·5; 1999, Boca Raton, FL, CRC Press.
4. R. Kunic, M. Kozelj, B. Orel, A. S. Vuk, A. Vilcnik, L. S. Perse, D. Merlini and S. Brunold: *Sol. Energy Mater. Sol. Cells*, 2009, **93**, 630–640.
5. J. W. Hu, X. G. Li, J. Gao and Q. L. Zhao: *Prog. Org. Coat.*, 2009, **65**, 504–509.
6. B. Czuprynski, J. Paciorek-Sadowska and J. Lisz Kowska: *J. Appl. Polym. Sci.*, 2010, **115**, 2460–2469.
7. M. Liu, Z. S. Petrovic and Y. J. Xu: Proc. Conf. on ‘Architected multifunctional materials’, San Francisco, CA, USA, April 2009, MRS, 36–46.
8. B. Glasmacherseiler, H. Reul and G. Rau: *J. Long-Term Eff. Med. Implants*, 1992, **2**, 113–126.
9. M. C. Suen and C. C. Chen: *J. Appl. Polym. Sci.*, 2006, **100**, 191–197.
10. V. Mishra, C. J. Murphy and L. H. Sperling: *Macromolecules*, 1979, **12**, 360–369.
11. H. Kumar, S. R. Somashekhar and S. S. Mahesh: *Eur. Polym. J.*, 2007, **43**, (2), 611–619.
12. T. A. Walker, Y. B. Melnichenko, G. D. Wignall, J. S. Lin and R. J. Spontak: *Macromol. Chem. Phys.*, 2003, **104**, 2064–2077.
13. M. Y. Gelfer, H. H. Song, L. Liu, B. S. Hsiao, B. Chu, M. Rafailovich, M. Si and V. Zaitsev: *J. Polym. Sci. B*, 2003, **41B**, 44–54.
14. G. M. Jordhamo, J. A. Manson and L. H. Sperling: *Polym. Eng. Sci.*, 1986, **26**, 525–530.
15. I. R. Clemiston: ‘Castable polyurethane elastomers’, 5; 2008, Boca Raton, FL, CRC Press.
16. Z. Bartczak, A. S. Argon, R. E. Cohen and M. Weinberg: *Polymer*, 1999, **40**, 2347–2365.
17. L. Domka: *Colloid Polym. Sci.*, 1993, **271**, 1091–1099.
18. M. Furukawa and T. Yokoyama: *J. Appl. Polym. Sci.*, 1994, **53**, 1723–1729.
19. S. K. Dolui: *J. Appl. Polym. Sci.*, 1994, **53**, 463–465.
20. D. Feldman and M. A. Lacasse: *J. Appl. Polym. Sci.*, 1994, **51**, 701–709.
21. O. E. Otterstedt, E. A. Otterstedt, J. Ekdaal and J. Backman: *J. Appl. Polym. Sci.*, 1987, **34**, 2575–2582.
22. E. N. Sotnikova and N. S. Pesochinskaya: *Int. Polym. Sci. Technol.*, 1987, **14**, 22–28.
23. J. L. Caillaud, S. Deguillavme, M. Vincent and J. C. Giannotta: *Polym. Int.*, 1996, **40**, 1–7.
24. S. Roopa and Siddaramaiah: *J. Reinf. Plast. Comp.*, 2007, **26**, 681–686.
25. X. Gao, B. Zhou, Y. Guo, Y. Zhu, X. Chen, Y. Zheng, W. Gao, X. Ma and Z. Wang: *Colloids Surf. A*, 2010, **371A**, 1–7.
26. X. Gao, S. Zhou, Y. Zhu, W. Gao, Z. Wang and B. Zhou: *Colloids Surf. A*, 2010, **377A**, 312–317.
27. I. Rezaeian, P. Zahedi, M. S. Loghmani and M. Shahzamani: *Plast. Rubber Compos.*, 2009, **38**, 257–263.
28. W. C. J. Zuiderduin, C. Westzaan, J. Huetink and R. J. Gaymans: *Polymer*, 2003, **44**, 261–275.
29. H. Barthel, F. Achenbach and H. Maginot: Proc. Conf. on ‘93rd Mineral and Organic Functional Fillers in Polymer International Symposium (MOFFIS)’, Namur, Belgium, April 1993, 301–317.
30. L. E. Nielsen and R. F. Landel: ‘Mechanical properties of polymers and composites’, 377; 1994, New York, Marcel Dekker.
31. L. H. Sperling: ‘Introduction to physical polymer science’, 75; 2006, New York, John Wiley & Sons Inc.
32. K. C. Frisch and D. Klempner: ‘Advances in urethane science and technology’, 218; 1996, Lancaster, PA, Technomic Publishing Company Inc.

Novel Technology to Influence Hardness of Flexible Polyurethane Foams

MICHAEL KREBS

JENS SASSENHAGEN

ROLAND HUBEL

Evonik Industries AG

Goldschmidtstr. 100

45127 Essen

Germany

ABSTRACT

Easy, user friendly control of hardness is of high interest for the production of flexible polyurethane foam. There are several ways to influence the hardness. Reduction of hardness and obtaining a softening effect usually has only limited impact on other foam physical properties. However, an increase in hardness is not readily possible without undesirable changes of other foam physical properties in flexible polyurethane foams. There are different ways to increase hardness in flexible polyurethane foams. For example it is possible to strengthen the three dimensional network of the polyurethane foam. Usually a better cross-linking leads to an increased hardness. But normally this also gives rise to a more closed cell structure of the foam. This change in porosity is responsible for an undesired loss of breathability and a different long-term behavior of the polyurethane foam. In order to create a foam hardener which does not affect other foam physical properties, Evonik has put a lot of effort into understanding the hardening effect of foams. This has led to the development of a tailor-made, highly sophisticated foam hardener additive for flexible foam. Therefore we have synthesized a new ORTEGOL® product to combine low use level with a significant increase in hardness without impact on other foam physical properties.

INTRODUCTION

Polyurethane products have many uses. The majority of the global consumption of polyurethane products is in the form of foams, with flexible and rigid types being roughly equal in market size. The major markets of flexible polyurethane foam are in the furnishing, packaging and automotive industries [1]. These applications require the foam to have well controlled mechanical properties. Hardness, for instance, is one of the properties which is crucial for these applications. Polyurethanes are formed by the reaction of di- or polyisocyanates with active hydrogen-containing compounds. In water blown systems two hydrogen-containing compounds are used: water and polyols [2]. The cross-linking reaction between isocyanate and polyol leads to urethane groups and is called the gelling reaction (equation 1, figure 1), whereas the reaction between isocyanate and water is called the blowing reaction (equation 2, figure 1). During this reaction instable carbamic acid is generated which afterwards decomposes to the parent amine and carbon dioxide. More than 95% of the volume of the foam is created by the CO₂ built during this reaction [1]. Besides CO₂ the blowing reaction results in the formation of functionalized urea groups. Further reaction of the functionalized urea results in chain extension and incorporation of the resulting urea hard segments into the growing network. A block-segmented copolymer is built up in which the polyol is the soft segment and the urea forms the hard segment [3]. These hard segments contribute to the increase of the hardness of slabstock polyurethane foam.

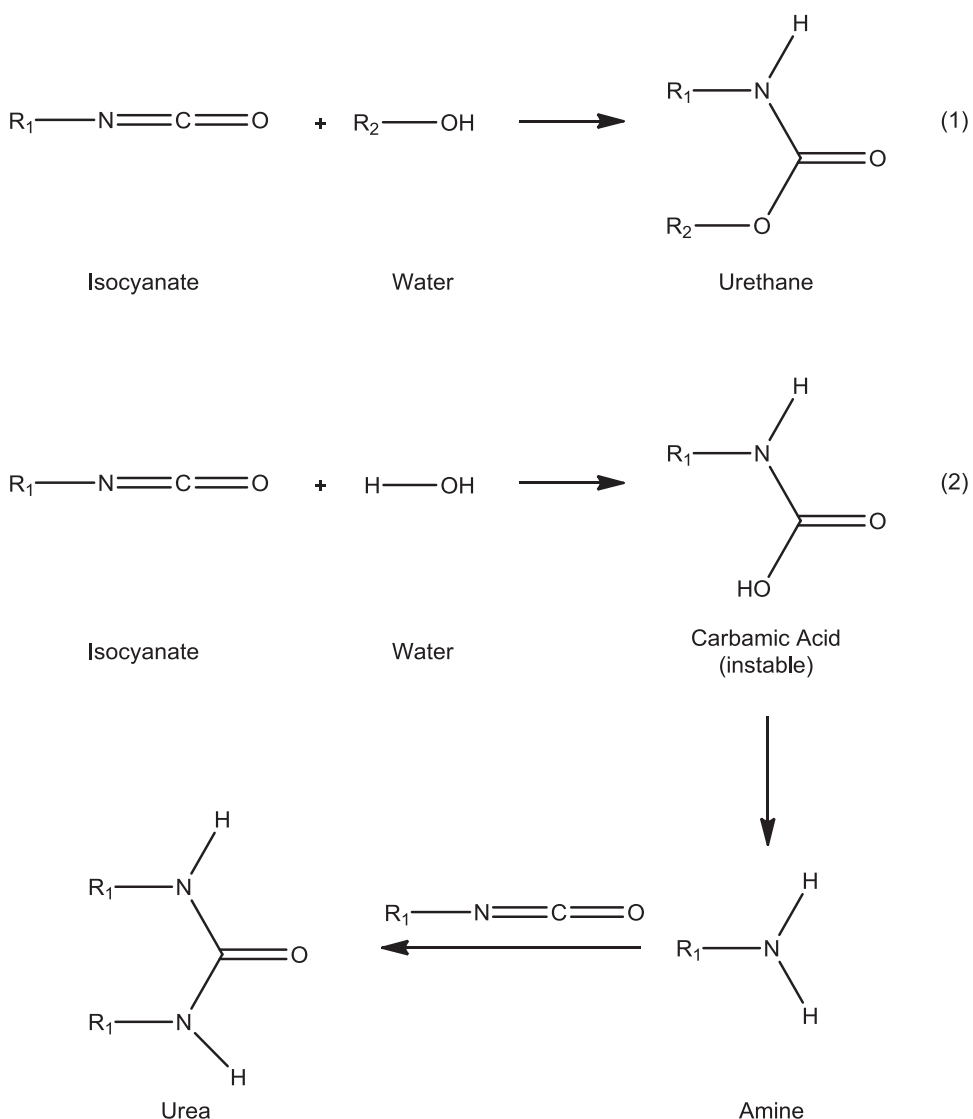


Figure 1. Gelling (1) and blowing (2) reaction during the polyurethane formation.

Control of hardness is one major issue in the production of flexible polyurethane foam. Flexible PU foam must meet diverse requirements depending on various applications. Therefore within the spectrum of flexible polyurethane foams there is a broad range of different grades with different degrees of hardness. Several ways exist in order to influence foam hardness. Reduction of hardness usually is a minor problem. It can either be achieved by the addition of softening additives while keeping the TDI index constant or by reducing the TDI index in combination with an addition of cross-linking additives in order to avoid splits. Generally only limited impact on other foam physical properties is observed. On the other hand an increase of hardness is not readily possible without undesirable changes of other foam physical properties such as air permeability. As already described in former publications [e.g. 1] there are different strategies in order to harden conventional slabstock foam (displayed in table 1). Most of them show serious disadvantages such as an unfavorable influence on the porosity, higher foam costs, an undesirable impact on the emanations of volatile organic compounds (VOCs) or a non-lasting foam hardness which leads to a bad durability of the resulting foam.

Table 1. Different ways to increase flexible foam hardness.

Method	Influence on porosity	Influence on foam costs	Influence on VOCs	Real or "fake" hardness	Remarks
Use of fillers	0	0	0	real	1) Density adjustment needed 2) Safety issues 3) Foam physical properties suffer
Use of polymeric polyol	0	+++	depending	real	
Increase of index	++	+	0	both	Safety issues
Increase of tin level	++	+	depending	both	
Use of cross-linkers	++	+	0	both	

Generally it can be observed that higher density foams show higher hardness. For water blown foams an increase of hardness of 0.1 kPa can be obtained when raising the density by 1 kg/m³ or 0.06 pcf (figure 2, left). That is why the addition of fillers also leads to harder foams. This is exemplified in figure 2 (right) with use of CaCO₃ and BaSO₄. However with an increasing amount of filler physical properties like tensile strength and elongation at break suffer which is one major disadvantage. Additionally more cross-linking is needed when using fillers in order to prevent splits.

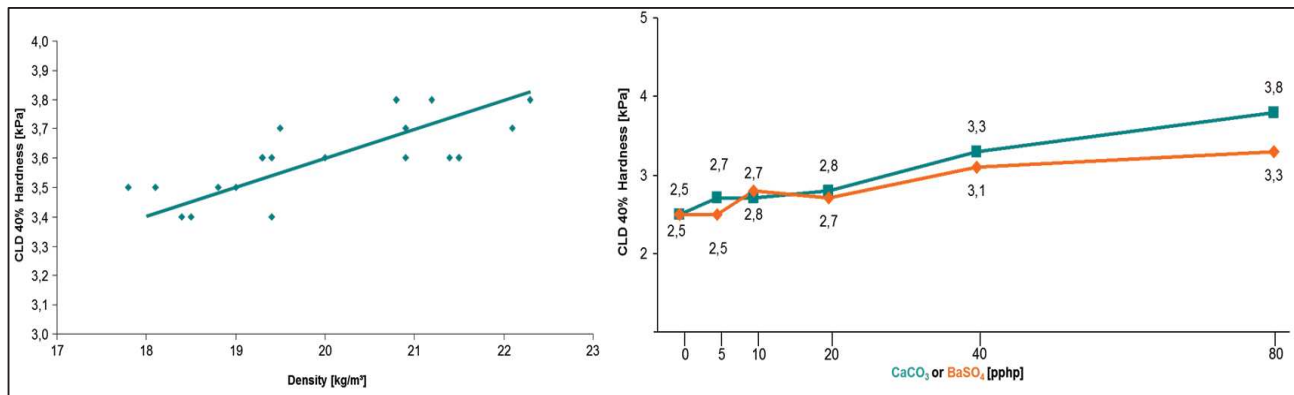


Figure 2. Increase of foam hardness with an increasing density (left) and variation of hardness generated by the addition of mineral fillers without density adjustment (right).

It will be necessary to compensate the density increase if foams of the same density shall be compared. This is either possible by the addition of water or by the addition of methylene chloride. With an increasing amount of water the quantity of aggregated hard segments is enhanced which leads to a harder foam. In contrast a higher methylene chloride loading leads to softer foams because methylene chloride disturbs the aggregation of hard segments. This is also illustrated in figure 3. It has to be noted that an increasing amount of water leads to a higher dosage of TDI (when an identical index is applied). This in turn results in a higher core temperature of the foam and an elevated risk of self-ignition results when the recommended maximum dosage of TDI of 55 pphp is exceeded.

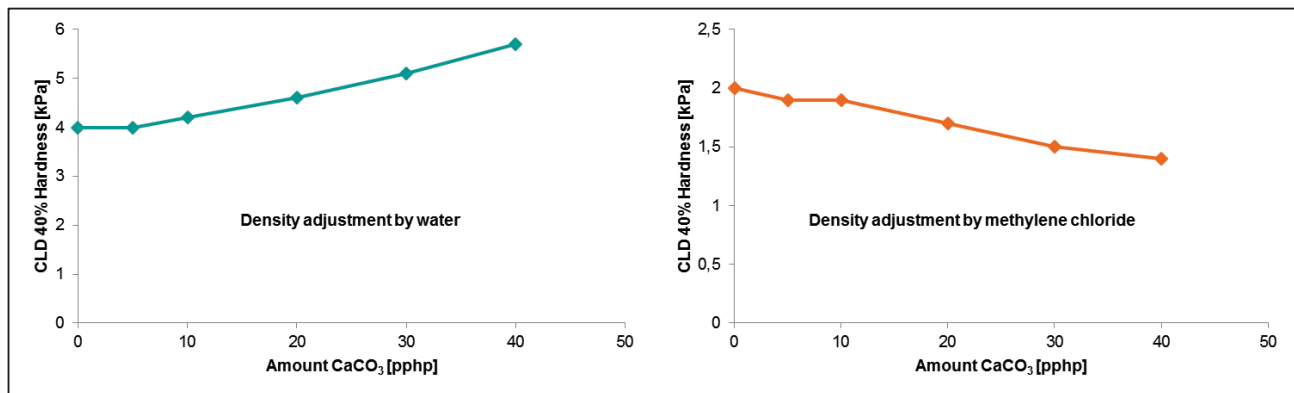


Figure 3. Variation of hardness generated by the addition of mineral filler with density adjustment by water (left) and by methylene chloride (right).

The most widely used method in order to increase the hardness of flexible polyurethane foams is the use of polymeric polyols also known as graft copolymer polyols. Most commonly utilized polymeric polyols are styrene/acrylonitrile (SAN) copolymers and polyurea modified polyols (PHD polyols) which are dispersions of polyurea particles, formed by the reaction between TDI and diamines in a conventional polyol. SAN polyols are obtained through free radical grafting of styrene and acrylonitrile polyether polyols in the presence of a radical initiator like for example AIBN. Polyurethane foams made with a copolymer polyol will have higher hardness than those made with a regular polyol due to the effect of hard organic fillers. However due to the extra step in copolymer polyol manufacturing, the cost of the foam product increases significantly. Additionally, SAN polyols will have a major contribution to the VOC content of flexible foams because rests of styrene and decomposition products of the radical initiator will be present owing to the production method. Another way to increase the hardness of flexible slabstock foams for a given density is to strengthen the polymer network. This can be achieved by several measures: Firstly the variation of the index in a foam has a pronounced effect on the hardness of the final foam. This increase in hardness has been shown to be directly related to increased covalent cross-linking resulting from more complete consumption of isocyanate reactive sites caused by the presence of excess isocyanate groups. However beside the desired increase of hardness there can be diverse severe disadvantages. Usually an increased index also leads to a bad air permeability of the foam due to the strong network and the hindered cell opening. Increased index also means higher TDI loading, resulting in a raised core temperature of the foam as well as increased foam costs. This higher core temperature might lead to scorch or, in worst case scenarios, spontaneous self-ignition of the foam block. A second method to strengthen the polymeric network is to accelerate the gelling reaction which means using an increased amount of tin catalyst. This results in higher foam costs and may also lead to a tighter foam structure. A third way is the use of cross-linking additives. Cross-linking additives are highly functionalized hydrogen-containing compounds reacting with isocyanates. However according to experience a usage of cross-linking additives also leads to very tight foam structures. Tight foams also show a certain increase in hardness when compared to the same foam grade with open cell structure. Nevertheless for most flexible foam applications tight foam structures are not desired. Besides the bad breathability which is especially undesired for mattresses, tight foams tend to have a declined durability. Closed foam cells will be crushed when the foam is frequently compressed and the so-called "fake" hardness will be lost. Additionally tight foams show a bad resiliency which lowers the comfort of the cushion.

OBJECTIVE

A multitude of applications require the foam to have well controlled mechanical properties. Hardness is especially a quality characteristic in many parts of the world. Since an increase in hardness is not readily possible without major impact on other foam physical properties and various disadvantages arise when applying the common ways to gain hardness of flexible foams, there appears to be a significant demand in the market for strategies to generate permanent hardness of flexible PU foams without tightening the foam. This paper presents a new ORTEGOL® product to combine low use level with a significant increase in hardness without major impact on the porosity of the foam and other foam physical properties. Foamers are able to save costs by reducing the amount of polymeric polyol, the tin catalyst or the TDI loading. Due to the potential reduction of TDI borderline formulations may be processed more safely and scorch issues might be reduced.

EXPERIMENTAL

Foams produced for this study were made either by hand pouring in the laboratory or by discontinuous box foam machine trials. In order to evaluate the hardening potency of the new product and its influence on the porosity, Evonik has developed two critical base formulations resulting in foams with different densities (table 2). The final foam density of formulation 1 is 16 kg/m³ (1.0 pcf), and formulation 2 leads to foams with a density of 25 kg/m³ (1.6 pcf). For the base trials, the index of the formulations 1 and 2 and the use level of tin catalyst were kept constant (as indicated in table 2). In further experiments the index and the dosage of KOSMOS® 29 were varied in order to analyze the potential savings of TDI or tin catalyst. Foams of formulation 1 were made using 200 g whereas foams of formulation 2 were made using 400 g of polyol with the other constituents of the formulation scaled accordingly. Here, for example, 1.0 part of a component means 1 g of this substance per 100 g of polyol. Water, catalysts and silicone surfactants were added to the polyol and mixed together by stirring at 1000 rpm for 60 s. After addition of the isocyanate, the mixture was stirred at 2500 rpm for 7 seconds. The liquid material was then poured into a paper-lined wooden box (base area: 30 cm x 30 cm). Foams were allowed to cure for 24 hours and cut afterwards. The following measurements were taken and recorded: rise time, height, settling after 3 min, foam density, air permeability of the foam, CLD or ILD hardness at 40% compression after 24 hours, cell size, ball rebound, compression set after 90% compression at 70°C for 22 hours, tensile strength and elongation at break. OH-numbers were determined according to Ph. Eur. 2.5.3 Method A and expressed as mg KOH/g.

Table 2. Base formulations for conventional flexible slabstock polyether foams. The amounts of raw materials and additives are given in parts per hundred parts (pphp).

Formulations	Formulation 1	Formulation 2
Density	16 kg/m ³ (1.0 pcf)	25 kg/m ³ (1.6 pcf)
Polyol OHN 48	100 – X	-
Polyol OHN 56	-	100 – X
Total Water	5.2	3.8
TEGOSTAB® B 8158	1.3	0.8
TEGOAMIN® 33	0.15	-
TEGOAMIN® B 75	-	0.15
KOSMOS® 29	0.25	0.18
Methylene Chloride	7.5	-
ORTEGOL® HA1 (OHN 193)	X	X
TDI Index	<110>	<110>

The possibility to reduce scorch in borderline formulations was evaluated with formulation 3 (table 3). For that foams produced with formulation 3 were stressed thermally in a microwave oven in order to simulate the thermal stress of production blocks. The index was reduced in comparison to a reference and in order to maintain hardness three parts of the hardening additive were added. Two reference foams were produced. First one with index <105>, the other one with index <110>. Three minutes after pouring the risen foam was placed in the microwave oven and irradiated for 80 s at 1000 W. In the following the foams were cut vertically and discoloration was evaluated by means of visual inspection.

Table 3. Borderline formulation for the evaluation of scorch of conventional flexible slabstock polyether foams. The amounts of raw materials and additives are given in parts per hundred parts (pphp).

Formulations	Formulation 3
Density	21 kg/m ³ (1.3 pcf)
Polyol OHN 48	100 – X
Total Water	4.8
TEGOSTAB® B 8232	1.0
TEGOAMIN® 33	0.20
KOSMOS® 29	0.22
TDCPP Flame Retardant	10
ORTEGOL® HA1 (OHN 193)	X
TDI Index	<variable>

Since one possible application of the hardening additive is the (partial) replacement of polymeric polyol, Formulation 4 was developed (table 4). The capability of the new ORTEGOL® to harden the foam was compared with the foam hardness obtained by using polymeric polyol. Formulation 4 is based on 400 g polyol.

Table 4. Formulation for polymer polyol containing conventional flexible slabstock polyether foams. The amounts of raw materials and additives are given in parts per hundred parts (pphp).

Formulations	Formulation 4
Density	24 kg/m ³ (1.5 pcf)
Polyol OHN 48	100 – Y – X
Polyol OHN 28, SAN 42%	Y
Total Water	4.0
TEGOSTAB® B 8002	1.0
TEGOAMIN® DMEA	0.25
KOSMOS® 29	0.20
ORTEGOL® HA1 (OHN 193)	X
TDI Index	<105>

In order to get an idea of the quality of hardness (real vs. “fake” hardness) and therefore of the durability of the resulting foams we produced some test foams in a discontinuous box foam machine (vol. 1 m³) according to formulation 5 (based on 9 kg of polyol), given in table 5 and performed a fatigue test. This fatigue was realized on the basis of the international standard 3385-1975 (E) [4]. The thickness and hardness measurements obtained before the test are compared to measurements after fatigue. The percentage loss is used to describe the fatigue durability performance. Hardness is measured as ILD 40% hardness before and after 80.000 times of 70% compression.

Table 5. Base formulation for conventional flexible slabstock polyether foams being used for a fatigue test according to ISO 3385-1975 (E). The amounts of raw materials and additives are given in parts per hundred parts (pphp).

Formulations	Formulation 5
Density	16 kg/m ³ (1.0 pcf)
Polyol OHN 56	100 – X
Total Water	5
Methylene Chloride	7.84
TEGOSTAB® B 8228	1.68
TEGOAMIN® 33	0.13
KOSMOS® 29	variable
ORTEGOL® HA1 (OHN 193)	X
TDI Index	<115>

In all formulations the amount of polyol in pphp is offset against the amount of ORTEGOL® HA1 and the amount of TDI is adjusted. Mechanical analysis (CLD 40% hardness as well as ILD 40% hardness, tensile strength and elongation at break) has been done by using a Zwick 1445 Test Machine. Hardness is either measured as CLD 40% hardness (expressed as kPa) or ILD 40% hardness (expressed as N) after 24 h. Resiliency was determined by the ball rebound test. Rise measurement was made by using Dr. Wehrhahn Ultrasonic Foam Rise Detection equipment. Cell structure analysis has been made by a flatbed scanner and image analysis software (a4i from Soft Imaging Systems). Porosity measurements were made by using the back pressure method. A constant air stream of 480 l/h is forced to flow through a 5 cm thick sheet of the foam, cut perpendicular to the rise direction. The resulting back pressure is measured in mm water column. High values indicate a very tight cell structure. The range is from 1 mm water column (very open) to > 300 mm water column (very tight).

RESULTS AND DISCUSSION

Investigation of the hardening potential of ORTEGOL® HA1 and its influence on the air permeability

Table 6. Foam physical properties of foams based on formulation 1 containing 3 pphp and 5 pphp of ORTEGOL® HA1 compared to a reference containing no hardening additive.

Entry	[pphp]	1	2	3
		Reference	3 pphp HA1	5 pphp HA1
Polyol OHN 48	[pphp]	100	97	95
TDI Index		<110>	<110>	<110>
Rise time	[s]	85	99	107
Height	[cm]	24.6	24.4	24.3
Settling	[cm]	0.2	0.2	0.3
Density	[kg/m ³]	15.9	16.0	16.0
Porosity	[mm]	23	30	74
CLD Hardness 40% (24 h)	[kPa]	2.5	3.1	3.4
Increase in Hardness	[%]	-	25	35
Cells	[cm ⁻¹]	12	12	12
Ball Rebound	[%]	30	29	24
Compression Set (90%/70°C/22 h)	[%]	3.1	6.7	7.3
Tensile Strength	[kPa]	74.6	80.3	80.0
Elongation at Break	[kPa]	83.4	89.4	87.0

In order to investigate the hardening potential of ORTEGOL® HA1 and its impact on the porosity of the obtained foams the new foam hardening additive was used in two different formulations, resulting in foams of different densities (formulations 1 and 2, table 2). In a first study the use level of the hardener was chosen to be 3 and 5 pphp and foams were compared to a reference containing no foam hardening additive. The results based on formulation 1 are shown in table 6 and figure 4.

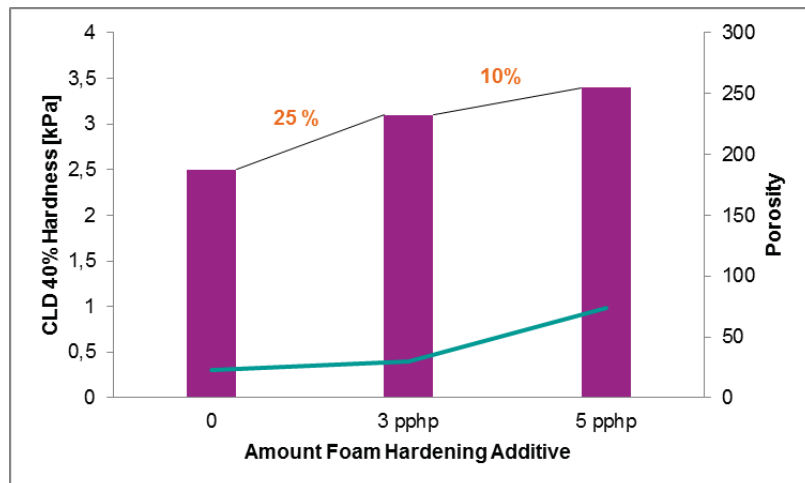


Figure 4. Hardness and porosity of foams based on formulation 1 containing 0, 3 and 5 pphp of ORTEGOL® HA1.

When using three parts of ORTEGOL® HA1 a CLD 40% hardness of 3.1 kPa could be obtained (entry 2, table 6) which corresponds to an increase of 25% compared to the reference (CLD 40 hardness 2.5 kPa, entry 1, table 6). When adding five parts of hardening additive hardness could even be enhanced up to 3.4 kPa (35% increase, entry 3, table 6). With a backpressure porosity of 30 mm the foam containing three parts of hardener is almost as open as the reference (23 mm backpressure H₂O). With five parts of ORTEGOL® HA1 a slight decrease in air permeability to 72 mm H₂O was observed.

Table 7 shows the foam physical properties of foams based on formulation 2. The results are illustrated in figure 5. Again a reference foam without hardening additive was compared to foams containing three and five parts of hardener, respectively. An increase of hardness of 25% was obtained when adding three parts of ORTEGOL® HA1 (3.6 kPa to 4.5 kPa) whereas porosity nearly stayed constant (15 mm H₂O compared to 21 mm H₂O, entries 4 and 5, table 7). A further enhancement of CLD 40% hardness to 4.8 kPa could be observed when adding five parts of hardener. Here again a slightly tighter foam with 52 mm backpressure porosity resulted (entry 6, table 7).

Table 7. Foam physical properties of foams based on formulation 2 containing 3 pphp and 5 pphp of ORTEGOL® HA1 compared to a reference containing no hardening additive.

Entry		4	5	6
		Reference	3 pphp HA1	5 pphp HA1
Polyol OHN 56	[pphp]	100	97	95
TDI Index		<110>	<110>	<110>
Rise time	[s]	107	106	104
Height	[cm]	32.4	32.7	32.7
Settling	[cm]	0.5	0.6	0.3
Density	[kg/m ³]	24.2	24.6	24.6
Porosity	[mm]	15	21	52
CLD Hardness 40% (24 h)	[kPa]	3.6	4.5	4.8
Increase in Hardness	[%]	-	25	34
Cells	[cm ⁻¹]	12	12	12
Ball Rebound	[%]	35	32	21
Compression Set (90%/70°C/22 h)	[%]	3.8	5.5	4.5
Tensile Strength	[kPa]	82.0	88.8	84.6
Elongation at Break	[kPa]	88.3	80.7	69.6

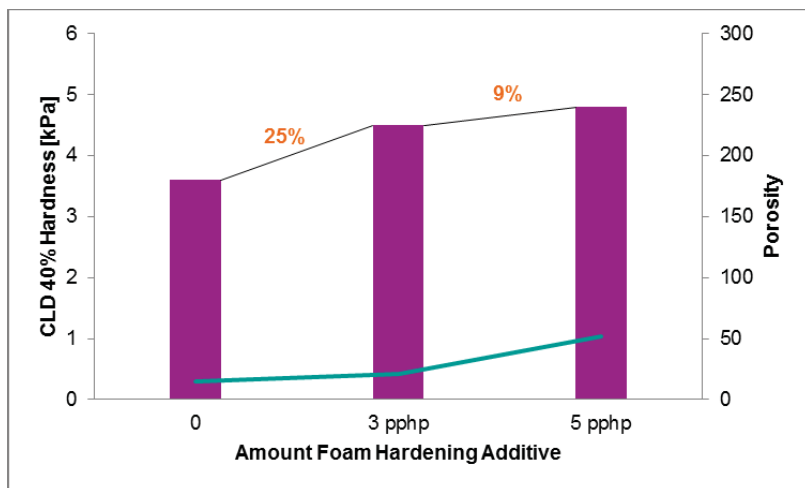


Figure 5. Hardness and porosity of foams based on formulation 2 containing 0, 3 and 5 pphp of ORTEGOL® HA1.

Investigation of the potential savings of TDI and tin catalyst by use of ORTEGOL® HA1

In the following, formulation 1 was used again producing foams based on different indices (thus with different TDI loadings). Foams were prepared using 3 pphp of ORTEGOL® HA1 and compared to reference foams containing no hardening additive. The results are shown in table 8 and figure 6. Starting with <103> we increased the index up to <118>. Obviously an increase of the index led to an increase of hardness of the resulting foams (2.2 kPa to 3.3 kPa for the reference foams without ORTEGOL® HA1 (entry 7 and 19, table 8) and 2.4 kPa to 3.9 kPa in the case of the use of 3 pphp foam hardening additive (entry 8 and 20, table 8)). Also a trend to tighter foam structures was clearly obtained (10 to 49 mm H₂O and 17 to 128 mm H₂O, respectively). We obtained same hardness and very similar porosity for the following foams:

1a) Index <110>, 0 pphp ORTEGOL® HA1 (CLD 40% hardness 2.5 kPa, porosity 25 mm H₂O, entry 13, table 8) *and*
1b) Index <105>, 3 pphp ORTEGOL® HA1 (CLD 40% hardness 2.5 kPa, porosity 30 mm H₂O, entry 10, table 8)

2a) Index <115>, 0 pphp ORTEGOL® HA1 (CLD 40% hardness 3.1 kPa, porosity 29 mm H₂O, entry 17, table 8) *and*
2b) Index <110>, 3 pphp ORTEGOL® HA1 (CLD 40% hardness 3.0 kPa, porosity 32 mm H₂O, entry 14, table 8)

For this formulation it was possible to reduce the index by at least 5 points which corresponds to a reduction of the TDI loading of at least 4% when adding three parts of ORTEGOL® HA1 without a major impact on hardness or porosity of the resulting foams.

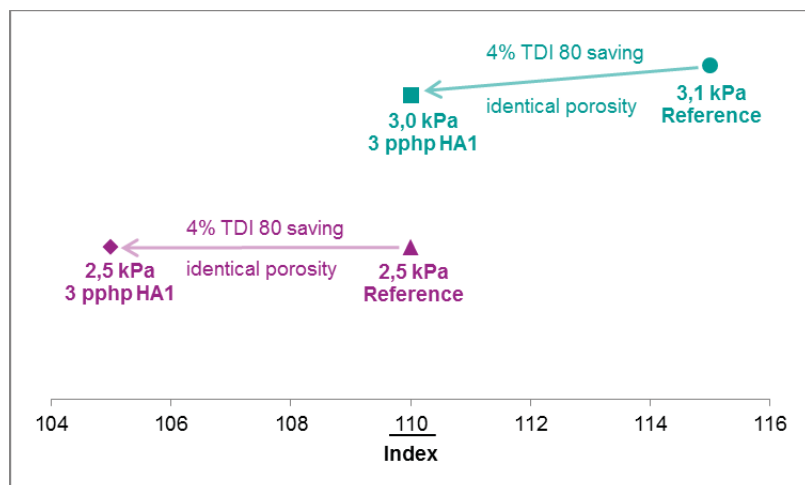


Figure 6. Variation of hardness of foams based on formulation 1 with reduction of the index and addition of 3 pphp of ORTEGOL® HA1.

Table 8. Foam physical properties of foams based on formulation 1. Reference foams were produced without hardening additive and compared to foams containing 3 pphp of ORTEGOL® HA1. The index was varied from <103> to <118>.

Entry		7	8	9	10	11	12	13	14	15	16	17	18	19	20
		Ref.	3 pphp HA1												
Polyol OHN 48	[pphp]	100	97	100	97	100	97	100	97	100	97	100	97	100	97
TDI Index		<103>		<105>		<108>		<110>		<113>		<115>		<118>	
KOSMOS® 29	[pphp]	0.25		0.25		0.25		0.25		0.25		0.25		0.25	
Rise time	[s]	96	104	93	101	90	103	89	102	85	100	85	94	84	92
Height	[cm]	22.5	22.2	23.0	23.8	23.8	24.1	23.8	23.2	24.8	23.9	25.0	24.7	26.1	26.0
Settling	[cm]	0.0	0.0	0.0	0.0	0.0	0.0	0.0	0.0	0.0	0.0	0.0	0.0	0.0	0.0
Density	[kg/m³]	16.7	17.0	16.5	16.6	16.6	16.6	16.5	16.9	16.4	16.5	16.3	16.2	16.2	16.2
Porosity	[mm]	10	17	13	30	16	28	25	32	20	38	29	42	49	128
CLD 40% (24 h)	[kPa]	2.2	2.4	2.2	2.5	2.4	2.8	2.5	3.0	2.9	3.1	3.1	3.6	3.3	3.9
Cells	[cm⁻¹]	12	12	12	12	12	12	12	12	12	12	12	12	12	12

Table 9. Foam physical properties of foams based on formulation 1. Reference foams were produced without hardening additive and compared to foams containing 3 pphp of ORTEGOL® HA1. The tin level was varied from 0.20 to 0.30 pphp KOSMOS® 29.

Entry		21	22	23	24	25	26	27	28	29	30
		Ref.	3 pphp HA1								
Polyol OHN 48	[pphp]	100	97	100	97	100	97	100	97	100	97
TDI Index		<110>		<110>		<110>		<110>		<110>	
KOSMOS® 29	[pphp]	0.20		0.22		0.25		0.28		0.28	
Rise time	[s]	104	106	98	101	91	96	83	92	83	83
Height	[cm]	22.3	22.0	23.0	23.7	22.6	23.2	23.6	23.8	23.7	24.0
Settling	[cm]	0.0	-0.2	0.0	0.0	-0.1	-0.2	0.0	-0.2	0.3	-0.2
Density	[kg/m³]	16.2	16.2	16.0	16.0	16.3	15.9	15.8	16.0	15.5	15.8
Porosity	[mm]	12	16	12	22	13	23	16	54	19	60
CLD 40% (24 h)	[kPa]	2.9	3.5	3	3.8	3.2	3.9	3.2	3.9	3.3	4.1
Cells	[cm⁻¹]	12	12	12	12	12	12	12	12	12	12

Table 9 shows the results when foams based on formulation 1 were prepared with different levels of tin catalyst. Again foams were produced using 3 pphp of ORTEGOL® HA1 and compared to reference foams containing no hardening additive. The loading of KOSMOS® 29 was varied from 0.20 parts to 0.30 parts. The effects on hardness and porosity are also illustrated in figure 7. A loading of tin catalyst of 0.20 parts led to a CLD 40% hardness of 2.9 kPa when no hardening additive was in use (entry 21, table 9) and to a hardness of 3.5 kPa when three parts of hardener were added (entry 22, table 9). In the case of 0.25 parts of KOSMOS® 29 a hardness of 3.2 kPa and 3.9 kPa was obtained, respectively (entries 25 and 26, table 9). With use level of 0.30 parts of tin we observed a hardness of 3.3 kPa and 4.1 kPa, respectively (entries 29 and 30, table 9). Porosity varied from 12 to 19 mm H₂O without hardening additive and from 16 to 60 mm backpressure when three parts of ORTEGOL® HA1 were added. In the graph of figure 7 two foams are compared:

- a) 0.25 pphp KOSMOS® 29, 0 pphp ORTEGOL® HA1 (entry 25, table 9) and**
- b) 0.20 parts KOSMOS® 29, 3 pphp ORTEGOL® HA1 (entry 22, table 9).**

Even with a reduction of the loading of tin catalyst from 0.25 parts to 0.20 parts (saving of 20% tin) the hardness of the foam could be increased by 10% (3.2 kPa without hardening additive and 3.5 kPa when three parts of ORTEGOL® HA1 were used) without negative impact on the porosity (13 mm backpressure porosity of the reference foam compared to 16 mm H₂O in the case of use of 3 pphp hardener) when three parts of hardening additive was used.

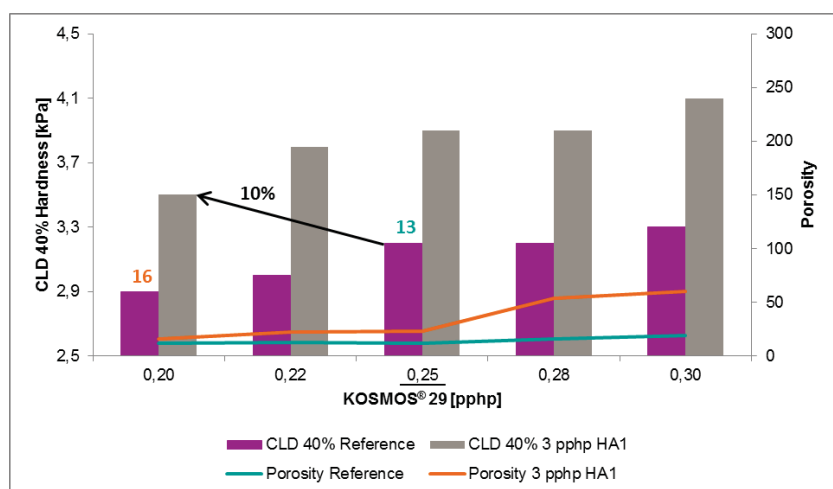


Figure 7. Variation of hardness and porosity of foams based on formulation 1 with reduction of the use level of KOSMOS® 29 and the addition of 3 pphp of hardening additive.

As before also index and tin level were varied in formulation 2. The outcomes are summarized in the tables 10 and 11 and figures 8 and 9. The index was again varied from <103> to <118> whereas the tin level was changed from 0.12 part to 0.23 parts. When varying the index again two couples of foams with similar porosity and hardness were compared:

- 1a) Index <110>, 0 pphp ORTEGOL® HA1 (CLD 40% hardness 3.6 kPa, porosity 13 mm H₂O, entry 37, table 10) and**
- 1b) Index <103>, 3 pphp ORTEGOL® HA1 (CLD 40% hardness 3.5 kPa, porosity 21 mm H₂O, entry 32, table 10)**

- 2a) Index <118>, 0 pphp ORTEGOL® HA1 (CLD 40% hardness 4.4 kPa, porosity 26 mm H₂O, entry 43, table 10) and**
- 2b) Index <110>, 3 pphp ORTEGOL® HA1 (CLD 40% hardness 4.5 kPa, porosity 22 mm H₂O, entry 38, table 10)**

For this formulation a reduction of 7 – 8 index points was possible without major changes to porosity and hardness when three parts of the new hardening additive were used. This corresponds to a TDI saving of at least 5%.

Table 10. Foam physical properties of foams based on formulation 2. Reference foams were produced without hardening additive and compared to foams containing 3 pphp of ORTEGOL® HA1. The index was varied from <103> to <118>.

Entry	31	32	33	34	35	36	37	38	39	40	41	42	43	44
	Ref.	3 pphp HA1												
Polyol OHN 56 [pphp]	100	97	100	97	100	97	100	97	100	97	100	97	100	97
TDI Index	<103>		<105>		<108>		<110>		<113>		<115>		<118>	
KOSMOS® 29 [pphp]	0.18		0.18		0.18		0.18		0.18		0.18		0.18	
Rise time [s]	117	117	116	114	112	110	113	110	104	104	104	104	100	101
Height [cm]	30.5	31.1	31.4	31.5	32.6	32.5	32.0	32.7	33.2	33.8	33.5	33.6	34.5	34.9
Settling [cm]	0.7	0.4	0.6	0.5	0.6	0.4	0.6	0.3	0.6	0.2	0.7	0.3	0.6	0.2
Density [kg/m³]	24.4	24.5	24.4	24.7	24.2	24.4	24.4	24.8	24.9	24.2	23.8	24.2	23.8	24.0
Porosity [mm]	13	21	14	29	13	22	13	22	26	49	20	74	26	117
CLD 40% (24 h) [kPa]	3	3.5	3.3	3.8	3.5	4.3	3.6	4.5	3.8	5.1	3.8	4.8	4.4	5.8
Cells [cm⁻¹]	12	12	12	12	12	12	12	12	12	12	12	12	12	12

Table 11. Foam physical properties of foams based on formulation 2. Reference foams were produced without hardening additive and compared to foams containing 3 pphp of ORTEGOL® HA1. The tin level was varied from 0.12 to 0.23 pphp KOSMOS® 29.

Entry	45	46	47	48	49	50	51	52	53	54
	Ref.	3 pphp HA1								
Polyol OHN 56 [pphp]	100	97	100	97	100	97	100	97	100	97
TDI Index	<110>		<110>		<110>		<110>		<110>	
KOSMOS® 29 [pphp]	0.12		0.15		0.18		0.20		0.20	
Rise time [s]	140	141	124	122	113	112	105	104	96	97
Height [cm]	30.3	30.7	31.6	32.0	31.4	31.6	32.6	33.2	33.2	33.7
Settling [cm]	0.2	0.7	0.6	0.7	0.5	0.4	0.6	0.2	0.3	0.0
Density [kg/m³]	25.1	25.0	24.4	24.6	24.6	24.9	24.1	24.2	24.3	24.1
Porosity [mm]	13	19	15	21	15	22	19	48	37	230
CLD 40% (24 h) [kPa]	3.3	3.9	3.4	4.3	3.7	4.6	3.8	4.8	3.9	5.5
Cells [cm⁻¹]	12	12	12	12	12	12	12	12	12	12

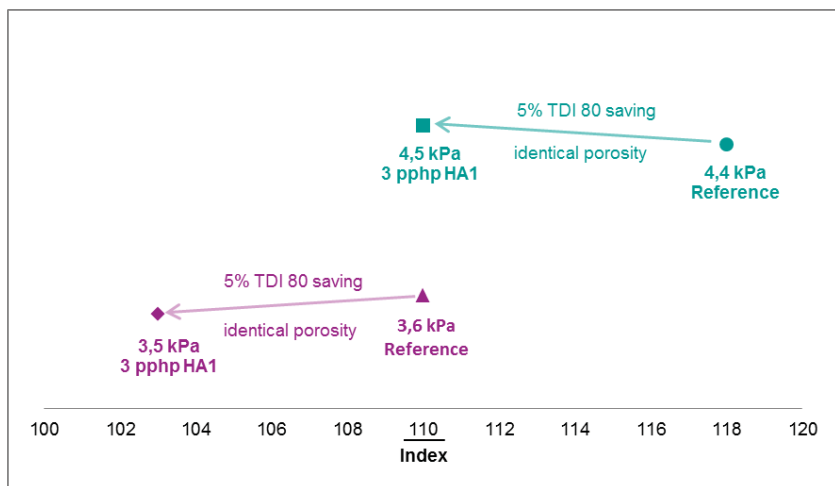


Figure 8. Variation of hardness of foams based on formulation 2 with reduction of the index and addition of 3 pphp of ORTEGOL® HA1.

When the tin level of formulation 2 was varied (constant index of <110>) from 0.12 pphp to 0.23 pphp a CLD 40% hardness of 3.3 kPa to 3.9 kPa was obtained when no hardening additive was used (entries 45 and 53, table 11) whereas hardness could be increased to 3.9 kPa to 5.5 kPa in the case of hardener usage (entries 46 and 54, table 11). Again two foams with similar porosity were compared in the graph of figure 9:

- a) 0.18 pphp KOSMOS® 29, 0 pphp ORTEGOL® HA1 (entry 49, table 11) and
- b) 0.12 pphp KOSMOS® 29, 3 pphp ORTEGOL® HA1 (entry 46, table 11).

With the reduction of tin catalyst from 0.18 pphp to 0.12 pphp (saving of 33% tin) and the addition of three parts of ORTEGOL® HA1 even a slightly harder foam (+ 5% hardness, 3.7 kPa CLD 40% hardness) was obtained compared to the reference foam without hardening additive (3.9 kPa CLD 40% hardness). Additionally only little impact on the porosity was observed (reference 15 mm H₂O compared to 22 mm H₂O in the case of hardener usage).

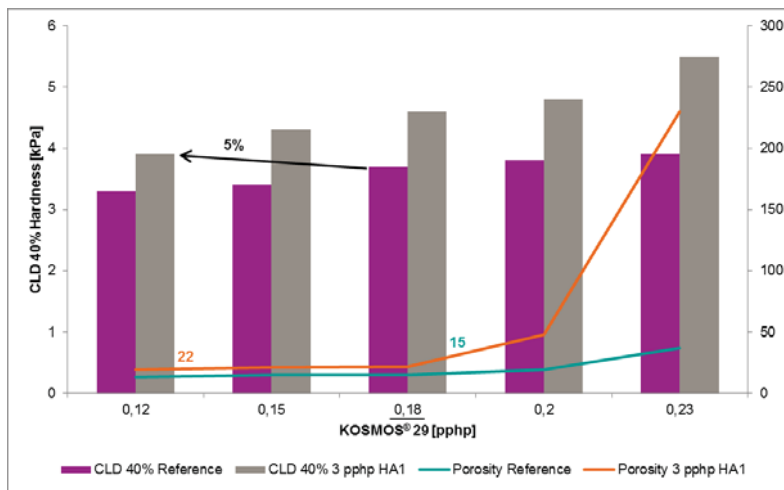


Figure 9. Variation of hardness and porosity of foams based on formulation 2 with reduction of the use level of KOSMOS® 29 and the addition of 3 pphp of hardening additive.

Reducing of scorch in borderline formulations by usage of ORTEGOL® HA1 and reducing the TDI loading

As already mentioned above it is possible to save TDI by the usage of ORTEGOL® HA1. One application of that could be the reduction of the core temperature of foam blocks in order to reduce scorch or to minimize the risk of self-ignition. For that the possibility to reduce scorch in borderline formulations was evaluated with formulation 3. Two pairs of foams were prepared

with reference foams of index <105> and <110>, respectively. Afterwards the index was reduced in comparison to the reference and in order to maintain hardness three parts of the hardening additive were added. Foaming results are shown in table 12. The first pair of foams (entry 55, table 12, index <105> & entry 56, table 12, index <100>, 3 pphp HA1) showed nearly identical physical properties. Very similar values for CLD 40% hardness (3.6 kPa vs. 3.5 kPa) and air permeability (9 mm H₂O vs. 12 mm H₂O) were obtained. The same trend was obtained with regard to the second couple of foams (entry 57, table 12, index <110> & entry 58, table 12, index <105>, 3 pphp HA1). Again very similar hardness (4.0 kPa vs. 4.1 kPa) and porosity (9 mm H₂O vs. 12 mm H₂O) of the resulting foams were obtained.

Table 12. Foam physical properties of two couples of foams based on formulation 3 containing 3 pphp ORTEGOL® HA1 compared to a reference with increased index containing no hardening additive.

Entry	55	56	57	58	
	Reference	3 pphp HA1	Reference	3 pphp HA1	
Polyol OHN 48	[pphp]	100	97	100	97
TDI Index		<105>	<100>	<110>	<105>
Rise time	[s]	84	88	80	85
Height	[cm]	22.7	22.4	22.3	23.2
Settling	[cm]	0.3	0.2	0.2	0.2
Porosity	[mm]	9	12	9	12
CLD Hardness 40% (24 h)	[kPa]	3.6	3.5	4.0	4.1
Cells	[cm ⁻¹]	12	12	12	12

In the following the risen foams were placed in the microwave oven and stressed thermally (irradiation for 80 s at 1000 W). The foams were cut vertically and discoloration was evaluated by means of visual inspection (figure 10). For both couples of foams a significant reduction of scorch and therefore a significant reduction of the core temperature of the foam was observed when the index was reduced by 5 points whereas only negligible effects on the foam physical properties were obtained.



Figure 10. Scorching test of two pairs of foams made according to formulation 3. Reduction of the index and an addition of ORTEGOL® HA1 to maintain hardness led to a significant reduction of scorch (microwave irradiation: 80 s, 1000 W).

Investigation of the potential savings of polymeric polyol by use of ORTEGOL® HA1

Hard foams often are obtained by using polymer solids containing polyol. In order to save costs it is often desired to reduce the amount of such polymeric polyol in hard foam formulations. In the following, formulation 4 was used to compare the hardening potential of the new ORTEGOL® to the hardness increase as a result of the usage of polymeric polyol. For that a polymeric polyol with an OH number of 28 mg KOH/g and a polymer solid content (SAN) of 42% was chosen. Five pairs of foams were prepared, in each case one without and one with three parts of hardening additive: Firstly two foams were made containing no polymeric polyol but only conventional polyol. Without the use of hardening additive a CLD 40% hardness of 3.8 kPa was obtained (entry 59, table 13) and by using three parts of the new ORTEGOL® an increase of hardness to 4.8 kPa could be achieved (entry 60, table 13). Next two foams which consisted of 100% polymeric polyol were produced (entry 61 and 62, table 13). Logically very hard foams were generated. Without hardening additive a hardness of 10.5 kPa whereas with three parts of ORTEGOL® HA1 a hardness of 12.3 kPa could be obtained. In the following three pairs of foams were made out of a mixture of conventional and polymeric polyol, ratios were 50 : 50, 70 : 30 and 90 : 10. In the cases where ORTEGOL® HA1 was in use, the amount of *conventional* polyol in pphp was offset against the amount of foam hardening additive. Foams consisting of 50% of conventional and 50% of polymeric polyol showed a hardness of 6.6 kPa and 7.9 kPa, respectively (entry 63 and 64, table 13). Foams containing 70% of conventional and 30% of SAN polyol showed an interesting behavior: Without

hardening additive a CLD 40% hardness of 4.8 kPa was obtained (entry 65, table 13), just as much as the hardness of the foam without polymeric polyol containing three parts of ORTEGOL® HA1 (entry 60, table 13). Accordingly it was possible to replace 30 pphp of SAN polyol by three parts of the new hardening additive ORTGEOL® HA1 in this formulation. By adding 3 pphp of hardener to that 30% polymeric polyol containing foam formulation hardness even could be increased to 5.6 kPa (entry 66, table 13). Another remarkable situation is observed when foams were made with 90% of conventional and 10% of SAN polyol: Without hardening additive nearly no increase in hardness was noted (3.9 kPa, entry 67, table 13) compared to the foam containing no polymeric polyol and no foam hardener (3.8 kPa, entry 59, table 13). The same could be seen when three parts of ORTEGOL® HA1 were added. A foam with a CLD 40% hardness of 4.8 kPa was obtained (entry 68, table 13), just the identical hardness as in the case of a foam without SAN polyol containing 3 pphp hardener (entry 60, table 13). Therefore with respect to CLD 40% hardness no benefit in using 10 pphp of polymeric polyol was observed in this formulation. In all cases the resulting foams had a very open cell structure. Air permeability varied from 1 mm H₂O (entry 61, table 13) to 15 mm backpressure (entry 68, table 13).

Table 13. Comparison of the hardening potential of polymeric polyol and ORTEGOL® HA1 according to formulation 4.

Entry		59	60	61	62	63	64	65	66	67	68
		Ref.	3 pphp HA1	Ref.	3 pphp HA1	Ref.	3 pphp HA1	Ref.	3 pphp HA1	Ref.	3 pphp HA1
Polyol OHN 48	[pphp]	100	97	0	0	50	47	70	67	90	87
Polyol OHN 28, SAN 42%	[pphp]	0	0	100	97	50	50	30	30	10	10
ORTEGOL® HA1	[pphp]	0	3	0	3	0	3	0	3	0	3
Rise time	[s]	93	98	76	78	77	80	83	87	89	91
Height	[cm]	28.2	28.6	28.2	28.2	28.5	29.4	28.3	29.4	28.8	28.4
Settling	[cm]	1.1	0.9	0.9	0.5	0.5	0.6	0.7	0.7	0.9	1.0
Density	[kg/m ³]	25.5	26.0	25.3	25.0	25.4	25.3	25.5	25.4	25.3	25.3
Porosity	[mm]	9	12	1	4	1	9	4	4	6	15
CLD 40% (24 h)	[kPa]	3.8	4.8	10.5	12.3	6.6	7.9	4.8	5.6	3.9	4.8
Cells	[cm ⁻¹]	12	12	12	12	12	12	12	12	12	12

Investigation of the durability of foams being prepared by the use of ORTEGOL® HA1

Generally, tight cell structure leads to some hardness increase as well. This hardness however is not a stable hardness when the foam is permanently loaded. In order to differentiate the so-called "fake" hardness from the real long-lasting hardness which is obtained with ORTEGOL® HA1 and thus to evaluate the quality of hardness, we prepared two foams with equivalent porosity and hardness based on formulation 5. In order to be able to work with the same index and to obtain a similar hardness the tin catalyst level had to be slightly adjusted. Both foams were produced at an index of <115>, the reference containing no ORTEGOL® HA1 was made using 0.28 pphp KOSMOS® 29 whereas the foam containing three parts of hardening additive was made using 0.22 pphp KOSMOS® 29. In the following a fatigue test was performed on the basis of ISO 3385-1975 (E). In the test, a 380 mm x 380 mm x 50 mm foam sample was repeatedly intended to 70% of its original thickness at a rate of 70 cycles per minute for 80,000 cycles. The thickness and hardness measurements obtained before and after fatigue were recorded and expressed as *percentage loss of thickness and hardness*, respectively.

Table 14. Fatigue test of two foams based on formulation 5, comparing a reference to one foam containing 3 pphp ORTEGOL® HA1

Entry		69	70
	Reference	3 pphp HA1	
Polyol OHN 56	[pphp]	100	97
KOSMOS® 29	[pphp]	0.28	0.22
Porosity	[mm]	49	43
ILD Hardness 40% (24 h)	[N]	110	113
Fatigue (Thickness)	[%]	2.0	2.0
Fatigue (ILD 40%)	[%]	24.6	16.2

As shown in table 14 there was no significant loss of thickness observed when performing the fatigue test. However a major impact could be seen in the change of ILD 40% hardness. When using three parts of hardening additive the loss in ILD 40% hardness could be reduced from 24.6% (entry 69, table 14) to 16.2% (entry 70, table 14). This is a very interesting outcome as many countries have regulations stating a maximum hardness loss at a specific density.

SUMMARY

Many applications require flexible polyurethane foam to have well controlled mechanical properties. Hardness was identified to be one of the properties which are crucial for a multitude of applications. Whereas the reduction of hardness and obtaining a softening effect usually has only limited impact on other foam physical properties, the increase of hardness is often not readily possible without undesirable changes of other foam physical properties. Different ways to increase hardness were discussed, however most of them showing severe disadvantages as for instance an unfavorable influence on the porosity, higher foam costs, an undesirable impact on the emanations of volatile organic compounds (VOCs) or a non-lasting foam hardness which leads to a bad durability of the resulting foam. The new versatile hardening additive ORTEGOL® HA1 was developed in order to meet the requirements for a broad range of different PU foam grades. ORTEGOL® HA1 combines low use level with a significant increase in hardness with minor impact on other foam physical properties. It was possible to increase the hardness of foams of different densities up to 35% whereas porosity nearly stayed constant. In terms of cost saving it was possible to reduce the TDI loading up to 10% and the tin catalyst amount up to more than 30% when using three parts of the new ORTEGOL® additive. A replacement of 30 parts of SAN polymeric polyol was achieved by the use of three parts of hardening additive without changes in other physical properties. This might lead to a significant reduction of costs when high priced polymeric polyol can be reduced. It was further possible to minimize scorch in a borderline formulation by decreasing the TDI index and adjusting hardness by usage of ORTEGOL® HA1. The high quality hardness which can be obtained by using ORTEGOL® HA1 could be proved with the little loss in ILD 40% hardness after a fatigue test performed according to the international standard 3385-1975 (E). These exceptional properties make the new ORTEGOL® Hardening Additive an ideal candidate for the production of hard flexible slabstock foams.

ACKNOWLEDGEMENT

The authors would like to thank the many colleagues who played an important role in the development of this novel ORTEGOL® Hardening Additive and in generating the data for this presentation, in particular Mrs. Funk.

REFERENCES

1. X. D. Zhang, L. M. Bertsch, C. W. Macosko, R. B. Turner, D. W. House, R. V. Scott. 1998. "Effect of Amine Additives on Flexible, Molded Foam Properties", *Cellular Polymers*, 17 (5): 327-349.
2. J. H. Saunders, K. C. Frisch. 1962. *Polyurethanes: Chemistry and Technology*. Applied Science Publishers. London.
3. R. Herrington, K. Hock. 1991. *Flexible Polyurethane Foams*. DOW Chemical Co, Midland, MI, pp. 68-125.
4. International Standard 3385, "Flexible Cellular Materials – Test for Dynamic Fatigue by Constant Load Pounding", 1975.
5. DIN 16000-9, "Determination of the emission of volatile organic compounds from building products and furnishing - Emission test chamber method", 2006.

BIOGRAPHIES

Michael Krebs



Dr. Michael Krebs studied chemistry at the University of Stuttgart, Germany and the University Louis Pasteur of Strasbourg, France in a Franco-German double degree course. After completing his studies in France he received his PhD in organic chemistry in the field of natural product synthesis in 2013. In April 2013 he joined the application technology team of the business line Comfort and Insulation of Evonik Industries as a Technical Manager for Flexible Foam. Among others his tasks include the development of new foam stabilizers and performance additives. He is in charge of the quality control of Flexible Slabstock Polyurethane Stabilizers and he is technically responsible for Flexible Polyurethane Additives in Africa.

Roland Hubel



Dr. Roland Hubel, born in 1972, studied Chemistry at the Ludwig-Maximilians-University of Munich. He received his PhD in Coordination- and Metal organic Chemistry. After working for one year in the field of genetic engineering as civil servant he joined Degussa Goldschmidt Polyurethane Additives as a research scientist in 2000. After that he was responsible for R&D of polyethers and development and application technology of additives for microcellular foams. Today he is globally responsible for development and application technology for Flexible Slabstock Polyurethane Additives.

Jens Sassenhagen



Jens Sassenhagen started his education as a chemical technician in 1991. From 1994 - 2011 he worked in the production plant for silicone stabilizers at the Th. Goldschmidt AG (later Degussa/Evonik Industries AG). In 2011 he moved to the application technology department for flexible foam additives as a lab technician and was promoted to a Technical Service Manager afterwards. Today he is responsible for technical service for Flexible Slabstock Polyurethane Additives in South East Asia and Africa.

See discussions, stats, and author profiles for this publication at: <https://www.researchgate.net/publication/267944286>

Optimum Calcium Carbonate Filler Concentration for Flexible Polyurethane Foam Composite

Article in *Journal of Minerals and Materials Characterization and Engineering* · January 2012

DOI: 10.4236/jmmce.2012.113023

CITATIONS

19

READS

18,335

3 authors, including:



Moe Usman

King's College London

20 PUBLICATIONS 381 CITATIONS

[SEE PROFILE](#)



Samson Adeosun

University of Lagos

65 PUBLICATIONS 288 CITATIONS

[SEE PROFILE](#)

Some of the authors of this publication are also working on these related projects:



Characterizing Chitin from Dendrobranchiata and Caridea Decapod Crustaceans [View project](#)



research [View project](#)

Optimum Calcium Carbonate Filler Concentration for Flexible Polyurethane Foam Composite

*M. A. Usman¹, S. O. Adeosun² and G. O. Osifeso¹

¹Department of Chemical Engineering, ²Department of Metallurgical and Materials Engineering,
University of Lagos, Akoka –Yaba, Lagos, Nigeria.

*Corresponding Author: mawwal04@yahoo.com

ABSTRACT

The production cost of flexible polyurethane foam is significantly dependent on the cost of polyol, which constitute the largest percentage of materials used in foam production with the characteristics to induce superior mechanical properties. Suitable fillers that are relatively cheap can be introduced in the foam matrix as replacement for polyol. However, certain compositions of filler have deleterious effect on some relevant mechanical properties of the foam. This paper investigates the effect of CaCO₃ filler in flexible polyurethane foam matrix for the dual purposes of achieving sustained mechanical properties and reduction in production cost. The optimum CaCO₃ composition was found to be 20 wt % representing a concomitant 18.54% reduction in cost of production.

Key words: polyurethane, CaCO₃, tensile strength, elongation at break, indentation hardness.

1. INTRODUCTION

Flexible polyurethane foams are one of the most important classes of cellular plastic used in the manufacture of such materials as foam mattresses, pillows, furniture, cushioning materials for automobiles, packing, recreation, shoes, etc [1]. The global consumption of flexible polyurethane foam was estimated to be above 7 million metric tons in 2007 and the average annual growth rate is about 5% [2]. In general, industries that produce flexible polyurethane foams use fillers to modify the material's properties in some way to achieve dimensional stability ease of retraction from the mold and service density [3-4]. When adding a filler to a polymer to form a conjugated biphasic material, the tension applied to the polymeric matrix will be transferred in part to the

disperse filler phase since it presents properties superior to the pure polymer [5]. The use of several fillers to achieve improved properties in foam has been widely studied [6]. Some notable ones include inorganic materials such as calcium carbonate, dolomite, aluminum silica, titanium dioxide, and talc [6] while some of the organic materials used as filler are carbon black and natural fibers [7-8].

In flexible polyurethane foams, the fillers promote an increase in density and resistance to compression. However, they reduce the resilience and contribute to the increase in permanent deformation. In addition, properties such as tear strength are significantly affected by the introduction of filler [9]. Accordingly, it is necessary to determine the correct concentration of the filler in the polymer matrix, so as to obtain a product of reliable quality [10].

Usage of flexible polyurethane foam in Sub- Sahara Africa has been mainly for mattresses and furniture and recently, there has been a growing demand for durable and high hardness characteristic (i.e. high compression resistant) foam at low cost [11]. Foams with these qualities are of interest to many sectors of the economy, and therefore their preparation, characteristics, and applications are subject interest [12]. However, the cost of petro-chemical based polyol, which constitute the largest percentage of materials used in foam production and which possess the characteristics to induce superior mechanical properties in foam currently commands a high value due to the rising costs of the petro-chemical feed stocks [13].

Several studies have been conducted on the suitability of calcium carbonate as filler in flexible polyurethane foam composite. Notable ones are the works of Sabina et. al[14] and Latinwo et.al.[12,15]. Sabina et. al.[14] investigated the physico-chemical properties of flexible polyurethane foam containing commercial CaCO_3 and observed that the excess of commercial CaCO_3 utilized in industry causes the increase of hysteresis, possibly causing permanent deformations and damaging the quality of the final product. Latinwo et. al. [12] studied the effect of CaCO_3 of different compositions and particle size distributions on the mechanical properties of flexible polyurethane foam. The study reported that finely divided filler material increased the hardness characteristics of the foam to compositions of up to 35wt%, while coarse filler did not show any appreciable improvement in the property. For all particle sizes, the tensile strength and elongation at break decreased while increasing filler content.

It is evident from previous works that foam properties are optimized at specific filler composition and particle size distribution. However, cost implication was not given prime consideration in these works.

For example, the cost benefit of nano-size filler particle is doubtful considering the cost of nanotechnology. Therefore, this paper presents the results of the effect of various composition of

CaCO_3 as replacement for polyol in the range 0-30 wt % on the mechanical properties of flexible polyurethane foam with the view to determining the optimum properties and cost implication.

2. EXPERIMENTAL METHODOLOGY

The flexible foam production method employed is a continuous one known as the **Slab Stock Foaming** process. In this process, the raw materials are weighed, measured and/or metered continuously from separate lines into an in-line mixer while the mixed reactants still in liquid form are poured into a continuous mould with paper covering on a mould conveyor. In the mould, the foaming proper takes place to form a solid continuous block of foam.

The slab stock foaming process usually commences with the preparation, treatment and conditioning of the chemicals. The polyol and toluene di-isocyanate to be used must be cooled to a temperature between 22 – 25°C and 20 – 22°C respectively. This is important as the density, viscosity and chemical reactivity of the two chemicals vary with temperature. This *chilling* operation is accomplished using Chiller units with a Shell and Tube heat exchanger connected to the storage tanks containing the chemicals. Also, the stannous octoate to be used is pre mixed with polyol in the ratio 1:11. Likewise, amine is also pre mixed with polyol in the ratio 2:3.

Thereafter the Foam **Formulation Sheet** is prepared. This *polyol – based* formulation sheet contain a list of the chemicals needed for the production and their various calculated proportions usually based on parts per 100 parts of polyol. This formulation is then used to calibrate the various meters, gauges and flow lines in the plant. The raw materials are pumped to the mixer head in their correct proportions.

Metering accuracy and continuous uniform flow is maintained as any error will lead to the production of poor quality foam. In order to ensure the metering accuracy, each production line is calibrated to determine the efficiency of the machine before production commenced.

Before the production process proper is carried out a **Laboratory Mix (box foam)** or laboratory analysis is done. Experience has shown that efficiency of production is greatly enhanced when the laboratory analysis is integrated into the production programme. Laboratory analysis is a process by which a little quantity of foam is made in the laboratory under controlled conditions. The essence of this is to:

- Evaluate the suitability of the raw materials in a proposed formulation;
- Determine the actual levels of activators and silicone required for efficient production;
- Check for the presence of contaminants in any of the chemicals; and
- Determine appropriate *cream* and *rise* times of a proposed formulation.

Samples from foam produced are cut into various sizes suitable for their respective test equipment. For this work, varying concentration of CaCO_3 ranging from 0 to 30 wt % were introduced into the formulation as shown in Table 1 and the following properties measured: density, tensile strength, elongation, compression set, indentation and hardness characteristics.

Table 1. Formulation Table for Experiment.

CHEMICALS	SAMPLES AND CONCENTRATIONS						
	A	B	C	D	E	F	G
Polyol (g)	1000	950	900	850	800	750	700
CaCO_3 (g)	0.0	50.0	100.0	150.0	200.0	250.0	300.0
TDI (g)	516.00	490.20	464.40	438.60	392.80	387.00	361.20
Water (g)	42.00	39.90	37.80	35.70	33.60	31.50	29.40
Amine (g)	0.80	0.76	0.72	0.68	0.64	0.60	0.56
Stannous (g)	2.00	1.90	1.80	1.70	1.60	1.50	1.40
Silicone (g)	10.00	9.50	9.00	8.50	8.00	7.50	7.00

3. RESULTS AND DISCUSSION

The percentage (%) composition of calcium carbonate (CaCO_3) in each sample varies from 0% in Sample A to 30% in sample G at 5% interval. The foam properties studied and their corresponding results are as shown in Figures 1 – 6.

Figure 1 illustrates the rise time variation and it shows a uniform decrement in rise time as calcium carbonate (CaCO_3) concentration increases. This implies that the foam rises faster when the filler composition increases indicating that the blowing / gas production reaction between toluene-di-isocyanate and water occurs faster. It could therefore be inferred that the introduction of fillers in foam formulation greatly influences the reaction time which is a positive development.

The density of the foam is improved as CaCO_3 content increases to 30% as shown in Figure 2. There is a gradual increase in density value until 20% filler concentration before a sharp rise in density occurred afterwards. This clearly indicate that the filler concentration could be as high as 20% and still produce the same density foam (22.6kg/m^3)as when not introduced at all (21.1kg/m^3).

It is however worthy of note that it is possible to still maintain the density while increasing filler concentration further, if so desired. This could be done by making adjustments in the other chemical compositions. The 20% filler concentration obtained as optimum in this study is just the most convenient to determine the effect of fillers on foam manufacture.

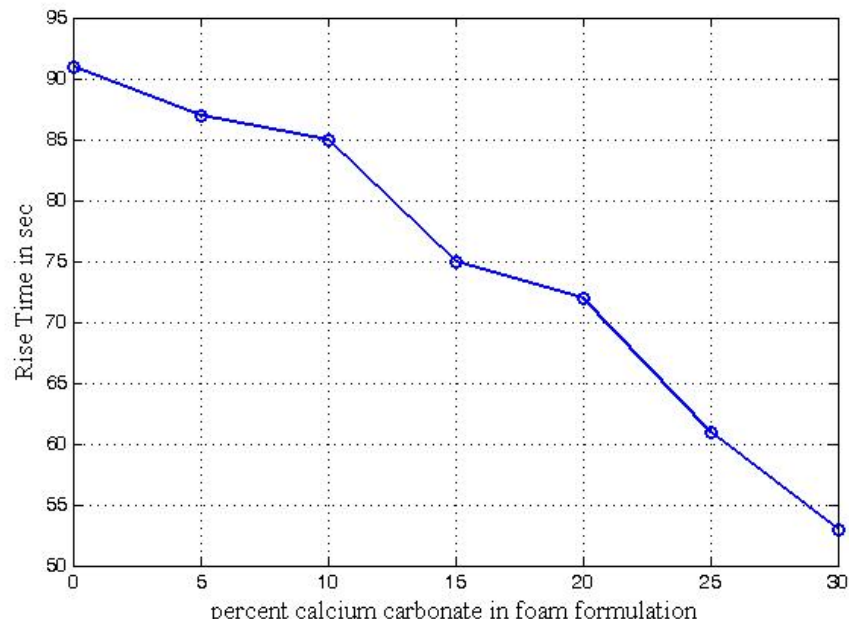


Figure 1 Rise Time with concentration of calcium carbonate

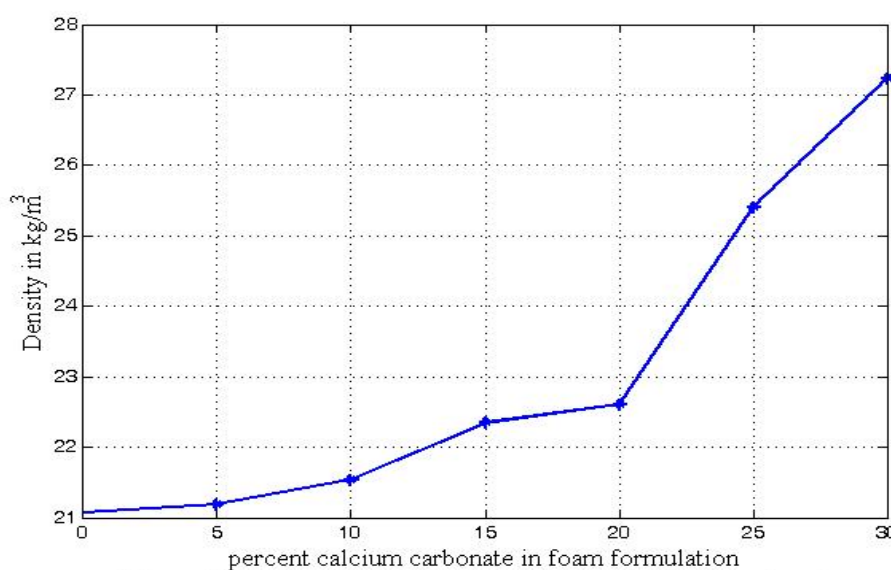


Figure 2 Density of foam with concentration of calcium carbonate

Also, one of the properties of foam that distinguishes good foam from a bad one is its percentage elongation which describes its elastic properties. Figure 3 shows that the elastic property of the foam was maintained between the normal ranges of $90\text{--}110\text{ kN/m}^2$ up till the point where the filler concentration is about 20%. Thereafter, a sharp drop in the elastic property was experienced. This depicts also that the elastic property of foam can be maintained while introducing fillers into the concentration.

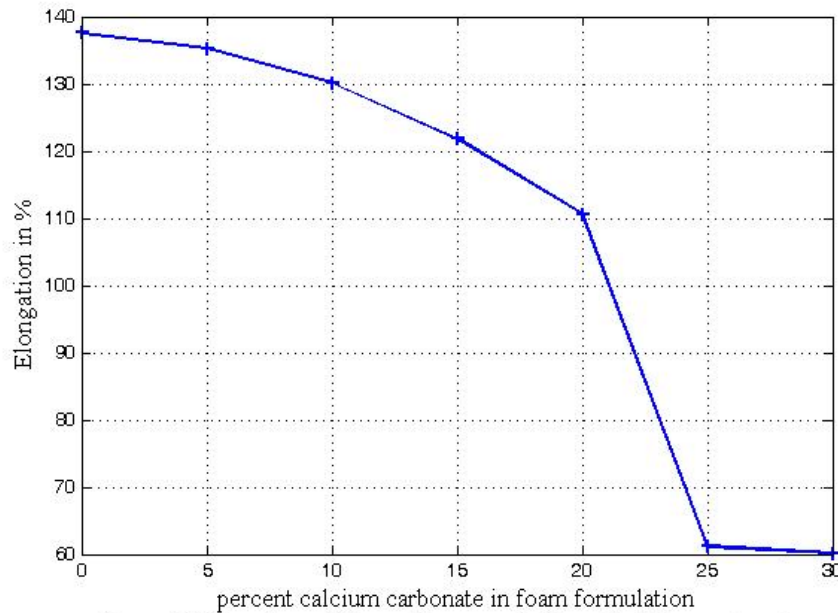


Figure 3 Elongation of foam with concentration of calcium carbonate

Furthermore, in Figure 4 the tensile strength of the foam was maintained until 20% filler content (145-120 kPa) after which there was a sharp and sudden decrease in tensile strength. The compression and load bearing ability of the foam was uniform (3.5%) between 0-10% CaCO₃ despite the introduction of the filler until 20% filler addition with an exception at 15% CaCO₃ (5.5%) (see Figure 5). When there was no filler in the formulation the foam resilience steadily increased to 148 (see Figure 6) as the filler was being introduced.

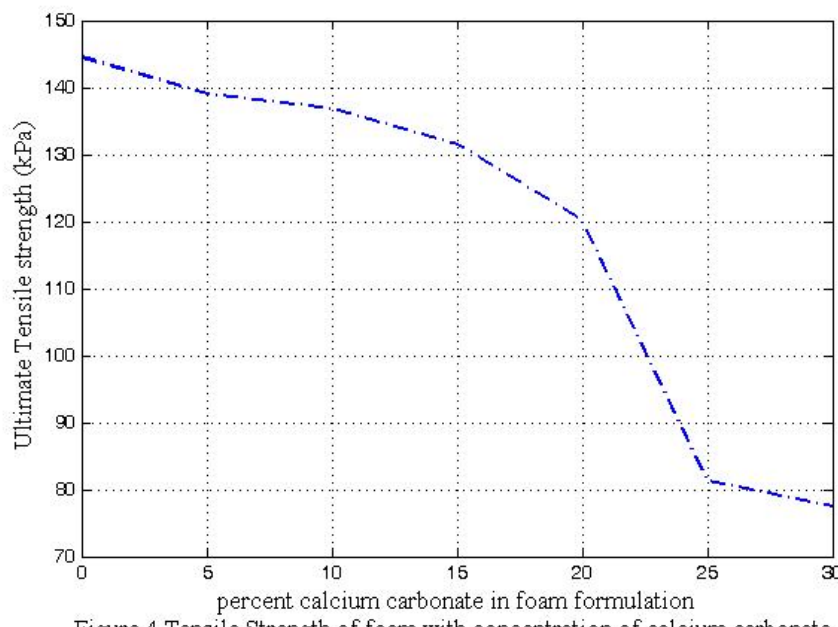


Figure 4 Tensile Strength of foam with concentration of calcium carbonate

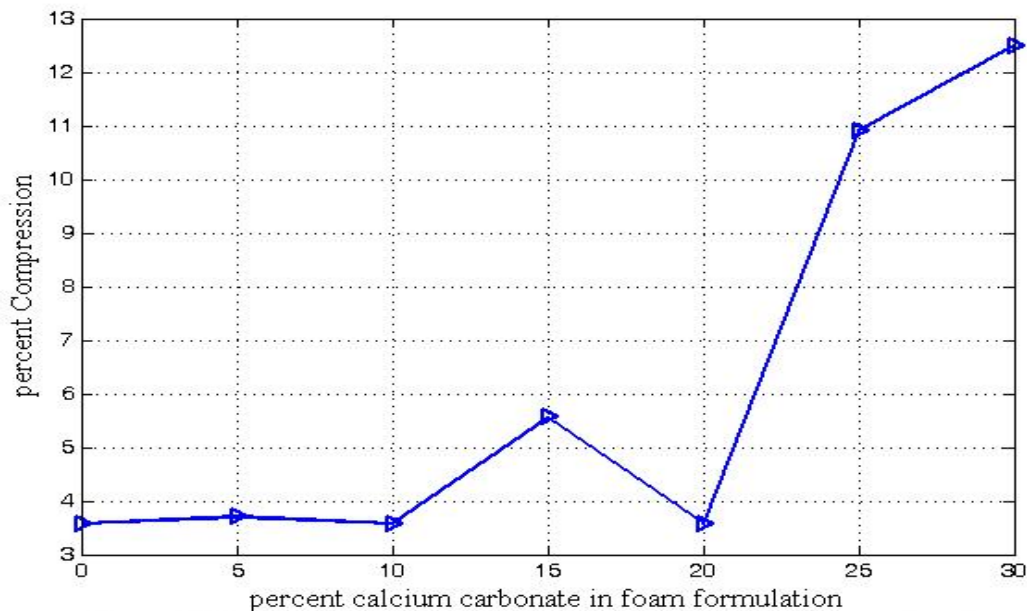


Figure 5 Compression of foam with concentration of calcium carbonate

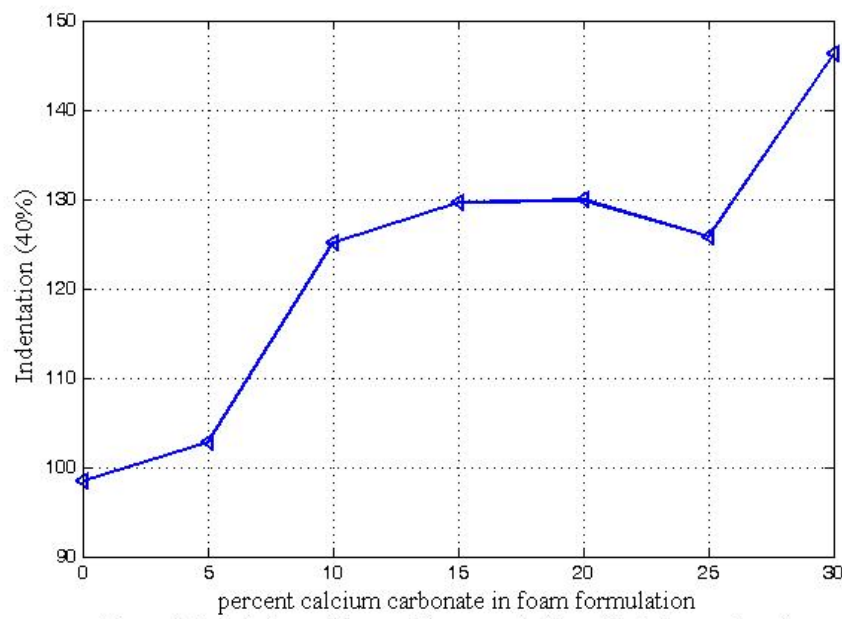


Figure 6 Indentation of foam with concentration of calcium carbonate

Cost effectiveness of this foam formulation is another significant aspect of this study. The result of this research has shown that CaCO_3 filler can be introduced into the foam formulation up to 20% optimum content with enhanced foam qualities as when no filler was used. Cost analysis of the cost of production for formulation without filler (sample A) and formulation with 20% filler

concentration (sample E) is presented below after carrying out a market survey. The current market prices per kilogram of each chemical used and the foam formulations for samples A and E are shown in Tables 2 and 3 respectively based on their requirements for production.

Table 2. Cost Per kg of Each Chemical in Foam Formulation

CHEMICALS	COSTS OF 1 KG (#)
Polyol	273.00
CaCO₃	70.00
TDI	356.00
Water	50.00
Amine	608.00
Stannous	1000.00
Silicone	800.00

Table 3. Total Cost of Production per kg of Each Chemical in Foam Formulation

CHEMICALS	SAMPLES AND COST ESTIMATES			
	Sample A (0%)	COST ESTIMATE (#)	Sample E (20%)	COST ESTIMATE (#)
Polyol (g)	1000	273.00	800	218.40
CaCO₃ (g)	0.0	0.00	200.0	14.00
TDI (g)	516.00	183.70	392.80	139.84
Water (g)	42.00	2.10	33.60	1.68
Amine (g)	0.80	0.49	0.64	0.39
Stannous (g)	2.00	2.00	1.60	1.60
Silicone (g)	10.00	8.00	8.00	6.4
Total Costs		<u>#469.29</u>		<u>#382.31</u>

To estimate the percentage reduction in cost of production given the total costs in Table 3, equation 1

$$\% \text{ Reduction} = \frac{\text{sampleA} \text{total cost} - \text{sampleE} \text{total cost}}{\text{sampleA} \text{total cost}} \times 100 \quad 1$$

⇒

$$\% \text{ Reduction} = \frac{469.29 - 382.31}{469.29} \times 100 = 18.54\%$$

Hence, the cost of production was reduced by about 18.54% while the foam qualities and properties were either maintained or improved upon as the CaCO_3 filler was introduced into the foam formulation to an optimum 20% content. Thus CaCO_3 can effectively replace polyol in flexible foam manufacture. Therefore the introduction of CaCO_3 into foam formulation will not only help reduce the cost of production but also help to maintain/or improve the foam qualities and its physical properties thereby making this an attractive venture.

4. CONCLUSION

This study has shown that calcium carbonate addition in foam formulation increase the rate of the blowing / gas production reaction between toluene-di-isocyanate and water with reduction in the rise time. However the elastic and tensile strength characteristics of foam are not affected by the presence of the filler. If calcium carbonate filler is properly introduced into the foam formulation, the desired tensile strength and elastic qualities of the foam can be achieved, and in effect significantly improves the foam resilience ability as the desired load bearing ability is enhanced.

REFERENCES

1. Woods G. *The ICI Polyurethanes Book*. 2 ed. New York: Wiley; 1990.
2. Avar G. *Polyurethanes (PU)*. *Kunststoffe International*. 2008; (10): 123-127.
3. Saliba CC, Oréfice RL, Carneiro JRG, Duarte AK, Schneider WT, Fernandes MRF. Effect of the incorporation of a novel natural inorganic I3 438 Sant'Anna et al. *Materials Research short fiber on the properties of polyurethane composites*. *Polym. Test.* 2005; 24(7): 819-824.
4. Bartczak Z, Argon AS, Cohen RE, Weinberg M. Toughness mechanism in semi-crystalline polymer blends: II. High-density polyethylene toughened with calcium carbonate filler particles. *Polymer* 1999; 40(9): 2347-2365.
5. Callister WD. *Materials Science and Engineering: An Introduction*. 5 ed. New York: John Wiley & Sons; 2000.
6. Nunes RCR, Fonseca JLC, Pereira MR. Polymer-filler interactions and mechanical properties of a polyurethane elastomer. *Polym. Test.* 2000; 19(1): 93-103.
7. Mothé CG, Araújo CR, Oliveira MA, Yoshida MI. Thermal decomposition kinetics of polyurethane-composites with bagasse of sugar cane. *J. Therm. Anal. Calorim.* 2002; 67(2): 305-312.
8. Mothé CG, Araújo CR. Properties of polyurethane elastomers and composites by thermal analysis. *Thermochim. Acta*. 2000; 357-358(14): 321-325.
9. Vilar W. *Química e Tecnologia de Poliuretanos*. 2 ed. Rio de Janeiro: Vilar Consultoria; 1998.
10. International Organization for Standardization. ISO document 3386-1. *Polymeric materials,*

- cellular flexible: Determination of stress-strain characteristics in compression. Part 1, Low-density materials. Geneva; 1986.
11. Latinwo G.K. The Predictive Effects of Filler Materials on the Mechanical Properties of Flexible Polyurethane Foam. Ph.D Thesis, University of Lagos, Nigeria, 2009.
 12. Latinwo, G.K., Aribike, D.S., Oyekunle, L.O., Susu, A. A., Kareem, S.A, Effects of Calcium Carbonate of Different Compositions and Particle Size Distribution on the Mechanical Properties of Flexible Polyurethane Foam, Nature and Science, 2010, 8(9), 92-101.
 13. Niemeyer T., Patel M., and Geiger E. A Further Examination of Soy-Based Polyols in Polyurethane Systems. Alliance for the Polyurethane Industry Technical Conference. Salt Lake City, UT, 2006
 14. Sabrina Sá e Sant'Annaa, Denilson Arlindo de Souzaa, Danielle Marques de Araujoa, Cornélio de Freitas Carvalhob, Maria Irene Yoshidaa, Physico-chemical Analysis of Flexible Polyurethane Foams Containing Commercial Calcium Carbonate, Material Research, 2008, 11(4), 433 – 438.
 15. Ganiyu Kayode Latinwo, David Stan Aribike, Alfred Akpoveta Susu, Semiu Adebayo Kareem, Effects of Different Filler Treatments on the Morphology and Mechanical Properties of Flexible Polyurethane Foam Composites, Nature and Science, 2010, 8(6), 23-31.